To the Graduate Council:

I am submitting herewith a thesis written by Daniel Inman entitled "Relative Efficacies of GPR and EM-31 Compared to Traditional Soil Investigation Techniques on Loess / Alluvium / Tertiary Deposits in Southwest Tennessee" . I have examined the final copy and recommend that it be accepted in partial fulfillment of the requirements for the degree of Master of Sciences, with a major in Plant and Soil Sciences.

John T. Ammons, Major Professor

We have read this thesis
and recommend its acceptance:

Ronald E. Yoder

Robert S. Freeland

Accepted for the Council:

Associate Vice Chancellor and
Dean of the Graduate School

RELATIVE EFFICACIES OF GPR AND EM-31 COMPARED TO TRADITIONAL SOIL INVESTIGATION TECHNIQUES ON A LOESS / TERTIARY DEPOSITS IN SOUTHWEST TENNESSEE

A Thesis

Presented for the

Master of Science

Degree

The University of Tennessee, Knoxville

Daniel Joseph Inman II
August, 2000

AG-VET-MED.
Thesis
2000
.I55

Acknowledgments

The author would like express gratitude to the Tennessee Agricultural Experiment Station, the Ames Plantation, and the Department of Plant and Soil Sciences for providing financial assistance and the facilities to pursue this research. Thanks is also given to Dr. John T. Ammons, who's guidance and insight were integral to the completion of this project. My appreciation is given to my committee members, Dr. Ronald Yoder, and Dr. Robert Freeland, for assistance in collecting and analyzing data as well as comments and suggestions. Thanks to Dr. Janice Branson for editorial advice. I would also like to acknowledge the following people for their assistance: Vanessa Stevens, Leroy Leonard, Tommy Cook, Andy Hartman, David Walker, Zack Parham and Ryan Noble. Finally, I would like to give sincere thanks to Dr. Carl Sams, under his tutelage I was given the encouragement to further my education.

Dedication

This work is dedicated to my mother, Sandra Gupton, who's support made this work possible.

Abstract

Remote sensing technology such as ground penetrating radar (GPR) and electromagnetic induction (EMI) have great promise as soil investigation tools. For certain applications, using tools such as these can potentially provide a more complete picture of the sub-surface than traditional soil investigation techniques. In order to evaluate the efficacy of such tools, GPR and EMI data were compared to traditional soil investigation data on loess / alluvium / Tertiary deposits in southwest Tennessee. The objectives of this study were to i) conduct a complete soil morphological, chemical, and physical characterization of a landscape at the Ames Plantation; ii) classify the soils to the family level of soil taxonomy; iii) conduct non-intrusive soil investigation using both GPR and EMI; and iv) compare remote sensing data to the traditional soils data.

A total of nine pedons were sampled on field #75 at the Ames Plantation. Sites were sampled on a 30.5-m X 30.5-m grid. Each site was spaced 15.25 m apart. Sampling depths ranged from 2.5 m to 3.0 m. Standard soil survey laboratory methods were performed on all sites for particle size, cation exchange capacity, exchangeable bases, free iron oxides, easily reducible manganese, KCl extractable aluminum, pH, total elemental analysis, total carbon, organic carbon, and $BaCl_2$-TEA extractable acidity. Bulk density was determined using the Varsol method. Saturated hydraulic conductivity was measured *in situ* using an Amoozemeter. Soil physical data were analyzed and grouped using Ward's Minimum Variance Clustering Analysis. Non-intrusive mapping was completed using a Trimble Ag. GPS™ 132, a Geonics EM-31™ , and an SIR system 10-A™ GPR

unit. Maps of bulk soil conductivity to the 3-m and 6-m depths as well as GPR images were produced. Sites were clustered based upon similarities seen in the remote sensing data. Final groupings from both techniques were analyzed for agreement using SAS.

All sites were located on an upland position with loess over alluvium over Tertiary sand parent material sequence. Loess thickness ranged from 90 cm to 144 cm. Alluvium thickness ranged from 82 cm to 151 cm. Pedons sampled at sites four and seven did not reach the Tertiary sand. Carbon distribution was somewhat irregular throughout the alluvium at all sites except site six. A fining upward sequence was seen throughout the alluvium at all sites. Data were insufficient to distinguish different loess depositions. All soils were classified as Ultic Hapludalfs.

Statistical analysis of soil morphological and physical data yielded the following groups: 1) 1, 3, 4, 7; 2) 5, 6, 8; 3) 2, 7; site 9 was not grouped. GPR and EM-31 data produced the following groups: 1) 1, 3, 4, 7; 2) 6, 8, 9; 3) 2, 5. Agreement between the groupings was strong, $K = .8 \pm 0.34$. The GPR and EM-31 were effective for detecting slight variations in physical properties and grouping soils based on these differences in soils formed in loess/alluvium/Tertiary sands.

Table of Contents

Chapter Page

1. Introduction....1

2. Complete Soil Morphological, Chemical, and Physical Characterization of a Landscape at the Ames Plantation....5

Introduction....5

Review of Literature....5

Geology....5

Loess....12

Lower Mississippi River Loess....14

Regional Geomorphology....21

History of Pedology....23

Soil Forming Factors....27

Physical Properties and Water Movement....31

Materials and Methods....34

Site Selection....34

Field Methods....35

Laboratory Methods....35

Results and Discussion....39

Site 1....39

Site 2....48

Site 3....55

Site 4.....61
Site 5.....69
Site 6.....78
Site 7.....85
Site 8.....91
Site 9.....98
Conclusions.....107
3. Non-Intrusive Soil Investigation of a Landscape at the Ames Plantation.....109
Introduction.....109
Remote Sensing.....109
Ground Penetrating Radar.....110
EMI.....115
Materials and Methods.....117
Field Methods.....117
Statistical Analysis.....117
Results and Discussion.....118
Conclusions.....121
References.....122
Appendices.....136
Appendix A. Morphology and Laboratory Data for Site One.....137
Appendix B. Morphology and Laboratory Data for Site Two.....147
Appendix C. Morphology and Laboratory Data for Site Three.....157

Appendix D. Morphology and Laboratory Data for Site Four.....167

Appendix E. Morphology and Laboratory Data for Site Five.....177

Appendix F. Morphology and Laboratory Data for Site Six.....187

Appendix G. Morphology and Laboratory Data for Site Seven.....197

Appendix H. Morphology and Laboratory Data for Site Eight.....207

Appendix I. Morphology and Laboratory Data for Site Nine.....217

Appendix J. EM-31 Maps of Field 75.....227

Appendix K. GPR Scans of Field 75.....230

Vita.....232

List of Figures

Figures		Page
1.	Location map for the Ames Plantation	2
2.	Geologic time	6
3.	Generalized loess sequence of the Lower Mississippi River Valley	17
4.	West Tennessee terraces as interpreted by Saucier, 1987	22
5.	Field 75 site location map	36
6.	Cumulative particle size plot for site 1	40
7.	Bulk densities for sites one, two, and three	41
8.	Plots of fine clay, total clay, free iron, and total iron for site 1	42
9.	Plot of total and organic carbon for site 1	43
10.	Plots of fine sand and titanium to zirconium for site 1	45
11.	Graph of hydraulic conductivity values at 102-cm and 129-cm for site 1	47
12.	Cumulative particle size plot for site 2	49
13.	Plots of fine clay, total clay, free iron, and total iron for site 2	50
14.	Plot of total and organic carbon for site 2	51
15.	Plots of fine sand and titanium to zirconium for site 2	52
16.	Graph of hydraulic conductivity values at 113-cm and 129-cm for site 2	54
17.	Cumulative particle size plot for site 3	56
18.	Plots of fine clay, total clay, free iron, and total iron for site 3	57
19.	Plot of total and organic carbon for site 3	59
20.	Plots of fine sand and titanium to zirconium for site 3	60

21. Graph of hydraulic conductivity values at 102-cm and 135-cm for site 3.....62

22. Cumulative particle size plot for site 4.....64

23. Bulk densities for sites four, five, and six.....65

24. Plots of fine clay, total clay, free iron, and total iron for site 4.....66

25. Plot of total and organic carbon for site 4.....67

26. Plots of fine sand and titanium to zirconium for site 4.....68

27. Graph of hydraulic conductivity values at 101-cm and 116-cm for site 4.....70

28. Cumulative particle size plot for site 5.....71

29. Plots of fine clay, total clay, free iron, and total iron for site 5.....73

30. Plot of total and organic carbon for site 5.....74

31. Plots of fine sand and titanium to zirconium for site 5.....75

32. Graph of hydraulic conductivity values at 104-cm and 122-cm for site 5.....77

33. Cumulative particle size plot for site 6 79

34. Plots of fine clay, total clay, free iron, and total iron for site 6.....80

35. Plot of total and organic carbon for site 6.....81

36. Plot of fine sand and titanium to zirconium for site 6.....82

37. Graph of hydraulic conductivity values at 116-cm and 142-cm for site 6.....84

38. Cumulative particle size plot for site 7.....86

39. Bulk densities for sites seven, eight, and nine.....87

40. Plots of fine clay, total clay, free iron, and total iron for site 7.....88

41. Plot of total and organic carbon for site 7.....89

42. Plots of fine sand and titanium to zirconium for site 7.....90

43. Graph of hydraulic conductivity values at 101-cm and 127-cm for site 7.....92

44. Cumulative particle size plot for site 8.....94

45. Plots of fine clay, total clay, free iron, and total iron for site 8.....95

46. Plot of total and organic carbon for site 8.....96

47. Plots of fine sand and titanium to zirconium for site 8.....97

48. Graph of hydraulic conductivity values at 102-cm and 122-cm for site 8.....99

49. Cumulative particle size plot for site 9.....101

50. Plots of fine clay, total clay, free iron, and total iron for site 9.....102

51. Plot of total and organic carbon for site 9.....103

52. Plots of fine sand and titanium to zirconium for site 9.....104

53. Graph of hydraulic conductivity values at 111-cm and 125-cm for site 9.....106

List of Tables

Table		Page
1.	Relative success of GPR surveys in different media	112
2.	Dielectric constants of ubiquitous materials	113
3.	Table of cluster by site for horizon = Ap	118
4.	Table of cluster by site for horizon = Bt1	118
5.	Table of cluster by site for horizon = Bt2	119
6.	Table of cluster by site for horizon = BC1	119
7.	Table of cluster by site for horizon = BC2	119
8.	Frequency of clustering from horizon = Ap, Bt1, Bt2, and BC1	119
9.	Groups based upon frequency of 3 or more	120
10.	GPR/EM-31 Groups	120
11.	Groups (by site) of soil data compared to GPR/EM-31 data	120
12.	Frequency statistics of final groupings	120

Chapter I.

Introduction

The Ames Plantation is located near Grand Junction, Tennessee. It straddles the border of Fayette and Hardeman counties in southwestern Tennessee (Fig.1). The largest experiment station in The University of Tennessee System, the Ames Plantation is in fact one of the largest agricultural research facilities in the U.S. It has 18,460 acres of land dedicated to agricultural research (Campbell, 1996). It is the large amount of acreage that allows a great diversity of research to be conducted at Ames.

The land that is now the Ames Plantation was first settled around 1820 by John T. Patterson, who built a house on the banks of the North Fork of the Wolf River. Over the next two decades settlement escalated, with settlers coming from all over the southeast to live and farm in the area. Cotton was the primary crop in this area until the beginning of the civil war. From the Civil War until the end of the Nineteenth Century the plantation was divided into a share cropping arrangement.

In 1901 a wealthy industrialist from North Easton, Maine, Hobart Ames, purchased the plantation from John W. Jones. His penchant for bird dogs and quail hunting led him to this purchase. In addition to hunting, he used the plantation for raising livestock and for cotton production. In 1915, the bird dog National Championship was first held at the Ames Plantation, a tradition that continues to this day. Hobart Ames died in 1945 and left the plantation to his widow, Julia Colony Ames.

Julia Ames decided to immortalize her late husband by creating the Hobart Ames Foundation. Upon her own death, Julia Ames left the plantation under the control of the



Figure 1. Location map for the Ames Plantation.

trustees of the Hobart Ames Foundation. In her will, Mrs. Ames directed that the plantation be preserved to provide a grounds on which to hold the National Championship for bird dogs and to provide resources for The University of Tennessee's College of Agriculture. Today, the Ames Plantation, unlike the other experiment stations in the The University System, operates for the most part without the help of state tax dollars.

The fate of agricultural chemicals in our water supply is of great concern to us all as a society. It was this issue that prompted the funding in 1990 of a long-term water quality project by The University of Tennessee Agricultural Experiment Station. The large area of land available makes Ames a perfect site for this project.

Researchers chose sites based on similarities in soil types and geomorphic position within a 970-ha watershed. Since the inception of this study many experiments have been conducted using monitoring systems to collect water from the surface, vadose zone, and aquifer. The herbicides metribuzin, metachlor, and fluometuron as well as the tracer potassium bromide have been monitored in the samples taken from various wells. From the data collected since 1990, three observations have become noticeable: 1) a small volume of soil carries a large volume of water flow in the vadose zone; 2) these flow paths appear to be relatively well defined, but have not yet been identified; and 3) while bromide tracer moved rapidly off site and is still found in some off-site locations, none of the herbicides have ever been found in any of the off-site subsurface locations (Yoder et al., 1998).

The objectives of this study were to 1) to conduct a soil investigation of a transect including complete soil morphological, chemical, and physical characterization, 2) classify soils to the family level of soil taxonomy, 3) use remote sensing to conduct a soil investigation, and 4) compare the data obtained objective 1 and 2 to data obtained in objective 3 to assess the efficacy of both the EM-31 and the GPR as a non-intrusive soil investigation tool.

Chapter 2.

Complete Soil Morphological, Chemical, and Physical Characterization of a Landscape at the Ames Plantation

Introduction

Soils can have great linear variability with in a short distance. Before inferences can be made about the subsurface, "truth" data must be obtained regarding the physical and chemical make-up of the soil and/or soils present on a landscape. The objectives of this chapter were to provide a complete physical and chemical characterization of the soil present on field 75 and to classify these soils to the family level of soil taxonomy.

Review of Literature

Geology

Geologic structures in West Tennessee began forming during the Silurian Time period of the Paleozoic Era, (430 million years B.P.) (Fig.2). During the Silurian period the area now known as West Tennessee was covered by shallow seas (Miller, 1974). These seas abounded with life, therefore, rocks of this age have many fossils, such as brachiopods, cephalopods, corals, crinoids, gastropods, sponges, and trilobites (Miller, 1974). Many of the Silurian and Devonian aged rocks are composed of limestone interbedded with shales, indicating the capricious sea levels.

Deposition in West Tennessee resumed during the Cretaceous time period of the Mesozoic Era (Fig.2). Time periods of the Mesozoic Era consist of from oldest to

Era	Period	Epoch	Age in millions of years before present
Cenezoic	Quaternary	Holocene	0.01
		Pleistocene	1.6
	Tertiary	Pliocene	5.3
		Miocene	23.7
		Oligocene	36.6
		Eocene	57.8
		Paleocene	66.4
Mesozoic	Cretaceous		144
	Jurassic		208
	Triassic		245
Paleozoic	Permian		286
	Pennsylvanian		320
	Mississippian		360
	Devonian		408
	Silurian		438
	Ordivician		505
	Cambrian		570

Figure 2. Geologic Time.

youngest, the Triassic; the Jurassic; and the Cretaceous (Fig.2). In the late Triassic, Pennsylvanian sandstones that capped the Nashville dome began to be weathered, exposing less resistant Mississippian aged limestones to erosion. By the beginning of the Cretaceous time period, a low relief coastal plain surface had been developed by the prodigious erosion and deposition episodes (Miller, 1974). This period is represented by (from oldest to youngest): the Tuscaloosa, Eutaw, Coffee Sand, Sardis, Demopolis, Coon Creek, McNairy Sand, and Owl Creek Formations.

The Tuscaloosa Formation is composed of chalky white pebbles and gravels of chert in a clayey matrix (Russell, 1975). Much of the chert is Mississippian in age and is deposited in layers that are devoid of bedding. It is thought that the Tuscaloosa was deposited via colluviation (Russell, 1975). A continuous narrow belt of Tuscaloosa gravels stretches from McGlamerys Stand, TN northward to Waynesboro TN (Russell, 1975).

By the late Cretaceous time period, the land in West Tennessee underwent major topographic changes. The Ouachita orogeny caused synclinal warping of Paleozoic rocks and subsequent subsidence in the region (Saucier, 1994). This area was then inundated by a shallow sea called the Mississippi Embayment, the axis of which was the Mississippi River itself. It was estimated that by the end of the Late Cetaceous that the water depth in the Mississippi embayment approached 1,000 meters (Miller,1974). The Embayment continued to experience transgressive and regressive cycles through out the Tertiary and into the Early Quaternary periods.

Deposited during a transgressive phase, Eutaw sediments consist of near shore marine sands and clays, well sorted glauconitic sand, quartz sand and thin bedded to

laminated, montmorillonitic clays (Russell, 1975). A fine grained, massive, glauconitic member called the Tombigbee sand member is also contained within. The formation overlies Paleozoic aged rocks and the Tuscaloosa formation locally (Russell, 1975).

Overlying the Eutaw Formation is the Coffee Sand. It is composed of fine grained, glauconitic, micaceous, thinly bedded to cross bedded quartz sand (Russell, 1975). Coffee Sands are continuously distributed from Hardin County, TN northward to the border of Kentucky. It was deposited in a lagoonal, barrier bar depositional environment. The Coffee Sand is less glauconitic and less micaceous than the Eutaw Formation.

Situated on top of the Coffee Sand are, from oldest to youngest: The Sardis, Demopolis, and Coon Creek Formations as well as the McNairy Sand. They represent the transgressive - regressive depositional episodes of the Cretaceous Mississippi Embayment, with the Demopolis representing the transgressive maximum.

Geologists have described the Sardis Formation as having a very narrow outcrop belt, rarely more than a few kilometers wide (Miller,1974). The most distinguishing feature of the Sardis Formation is an abundance of dark green glauconitic sand reaching up to 10-m in thickness. In places, the Sardis Formation grades upward into the clayey marls of the younger Demopolis Formation. Locally the contact is abrupt and is marked by fossil oysters (Russell, 1975).

The transgressive maximum of the ancient West Tennessee seas is marked by the deposition of the Demopolis Formation. Deposited on a relatively deep shelf, the Demopolis was composed primarily of marls, chalks, and calcareous clays. A notable feature observed in the Demopolis Formation is the occurrence of euhedral biotite. Biotite is associated with igneous rocks of Cretaceous age in the Mississippi Embayment.

A shallow mixing zone between the deeper shelf sediments of the Demopolis Formation and the near shore/alluvial sediments of the McNairy Sand unit is represented by the Coon Creek Formation. Initially, the Coon Creek was mapped as part of the Ripley Formation. However, it was raised to formation status and the Ripley Formation was dropped from the nomenclature (Russell, 1974). It is composed of glauconitic marine sand and clay that tend to be dark grey. Average thickness of the Coon Creek Formation is approximately 140 feet across its outcrop belt (Russell, 1974).

The McNairy Sand is a thick wedge of non-marine and near shore sediments. Within the McNairy Sand are three lithologic sequences: a regressive, near shore, basal sand that contains copious amounts of heavy minerals and is generally fine grained. A middle wedge that is composed of coarser grained sediments and appears to be of fluvial deltaic origin. And an upper transgressive marine sand that outcrops locally. While each unit is distinctive, their boundaries are indistinct and transitional (Russell, 1975). Thickness of the McNairy Sand's is variable across the outcrop belt. A U.S. Geological Survey T-1-M test well in Madison County penetrated at least 345 feet of the McNairy Sand (Russell, 1975).

A very thin fossiliferous unit composed of marine sands, called the Owl Creek Formation, represents the northeastern most transgression of the youngest Cretaceous seas in West Tennessee (Russell, 1975). It is composed of glauconitic, fine-grained sands. In Tennessee the Owl Creek is approximately 35 feet thick, thinning northward, and becomes more sandy (Russell, 1975).

A major unconformity exists between the Mesozoic and Cenozoic sediments in West Tennessee (Miller, 1974). Sediment deposited in the Lower and Upper Eocene are

preserved, however, sediment deposited in the Middle Eocene are not present (Stearns, 1957). The Lower Eocene is represented by the Midway Group (Clayton and Porters Creek Formations); and the Wilcox Group (Holly Springs and Grenada Formations). The Upper Eocene is represented by the Jackson Formation.

Overlying the Owl Creek is the Clayton Formation. It is capricious in its lithology across its outcrop belt. Subdivided by geologists into five lithologic facies, the Clayton Formation consists of: 1) a lower limestone and glauconitic sand member, 2) a middle fossiliferous and clay member, 3) a micaceous sand facies, 4) a "McNairy like" sand and clay facies, and 5) and an upper glauconitc sand member (Russell, 1975). Thickness of the Clayton Formation averages eighty feet but has been found to be as much as one hundred feet locally (Russell, 1975).

Porters Creek Clay is composed of a thick clay body containing lenses of sand. Sand lenses occurring in the Porters Creek, range from less than a foot to more than twenty feet thick (Russell, 1975). According to Russell (1975), the Porters Creek is the most easily recognizable Tertiary unit in west Tennessee. This formation varies in thickness across its distribution from one hundred feet thick to more than one hundred and fifty feet.

Unconformably situated on top of the Porters Creek Clay, the Wilcox Formation is composed of a heterogeneous mixture of sand, silt, and clay (Russell, 1975). A distinctive lithologic feature of the Wilcox Formation is "saw-dust sand." Whitlatch was the first person to used the term "saw-dust sand" to describe the coarse grained appearance throughout the outcrops, although it is actually fine grained. Throughout the Wilcox Formation, clay breccias and clay balls are ubiquitous (Russell, 1975). Its thickness varies

greatly due to the fact that the upper and lower boundaries are erosional unconformities. Thickness ranges from zero to over two hundred feet. Maximum thickness occurs in the southern most portion of its outcrop belt (Russell, 1975).

Disconformably overlying the Wilcox Formation is the Claiborne Formation (also known as the Claiborne Sand). It consists primarily of a thick body of sand with subordinate lenses of clay through out. It is poorly sorted and cross-bedded with some cut and fill structures occurring locally. Geologists believe that the Claiborne was deposited via low gradient streams that cut across a low relief coastal area. In the basal portion of the Claiborne, contact with the Wilcox is marked by the presence of a thin layer of ironstone and in some locations ferriginous sandstone. This contact is variable over the out crop area due to the undulating erosional surface of the Wilcox Formation. The thickness of the Claiborne is not well documented. Correlations made by Moore and Brown in 1969 indicate the maximum thickness to be 1100 feet at a test well at Fort Pillow in Lauderdale County (Russell, 1975).

Deposition recommenced in the Quaternary time period. This period had a major influence on the present day landscape in West Tennessee. The Quaternary is divided into two epochs, the Pleistocene and the Holocene. During the Pleistocene, what is commonly called the "ice age" took place. The Pleistocene is further divided into four periods named after the respective glacial maximum. The four periods of the Pleistocene are as follows from oldest to youngest: the Nebraskan, Kansan, Illinoisan, and Wisconsin. In addition to the glacial periods, interglacial periods are recognized as follows from oldest to youngest, Aftonian, Yarmouthian, Sangamonian, Peorian (a.k.a. Farmdalian), and the Holocene. During these periods of warming, fine silts resulting from the glaciers scouring the

landscape to the north and north west were carried and deposited by the north westerly prevailing winds. This material is called loess.

Loess

"Few words have caused more debate in the realm of earth science than loess" (Follmer, 1996). Lyell (1834), was the first to describe loess on the banks of the Rhine river in Germany. Prior to the twentieth century, loess was generally thought of as a fluvial deposit (Follmer, 1996). The definitions of loess fluctuated from definitions that include origin as the determining factor to ones that concentrated on the mineralogy alone and considered the depositional process secondary. Compounding this debate was the heated controversies surrounding the origin and distribution of the loess in the Mississippi river valley. All of this contention caused a boom in loess research. Through the extensive research, today's understanding of what loess is, its origin, and its make up was attained.

Disagreement persists today among the international community of researchers on definitions of loess. The word loess is derived from the German word *löss,* which is strictly a textural term for loose, crumbly earth (Smalley, 1975). However, this definition was rejected because it did not include the unique properties that are inherent in loess. Flint (1957), defined loess as "a sediment, commonly nonstratified, and commonly unconsolidated, composed primarily of silt sized particles, ordinarily with accessory clay and sand, and deposited primarily by wind action" (Smalley, 1975). Flint's definition was very similar to that of Saucier, "loess is a homogeneous, seemingly non-stratified,

unconsolidated deposit consisting of well-sorted silt deposited via eolian action" (Sauicer, 1987). Alternatively, Russell (1944), defined loess as "unstratified, homogenous, porous, calcareous silt; it is characteristic that it is yellowish or buff, tends to split along vertical joints, maintains steep faces, and ordinarily contains concretions, and snail shells. From the qualitative standpoint at least 50% by weight must fall within the grain size fraction 0.01 - 0.05mm, and it must effervesce freely with dilute hydrochloric acid." Berg (1964) approached loess as a geologic unit, "the rock is indeed loose, porous, non-laminar, of straw-yellow color, rich in carbonates of calcium and of magnesium (the amount of which may reach 10 - 15% by weight, or more), and have a tendency to collapse and form vertical walls. As compared to sand, this rock is compact and as compared to clay it is loose and not plastic." Similarly, Pecsi (1990), defined loess as "a loose deposit with coarse silt predominating grain size, unstratified, porous, permeable, stable in steep walls, easily erodible by water, structured light loam of pale yellow color due to finely dispersed limonite (iron hydroxides), 40-80% quartz, subordinate amounts of feldspars, variable amounts of clay minerals (5-20%), and carbonates (1-20%)." The main point that differentiates these definitions and subsequently fuels the debate over the definition of loess is the mention of the sedimentary process. A strictly descriptive definition for loess such as those by Russell, Berg, and Pecsi is inadequate because the process of its deposition is critical to its eventual state. Smalley's definition of loess is as follows, "loess is a clastic deposit which consists predominantly of quartz particles with diameters of 20-50 microns and which occurs as wind lain sheets" (Smalley, 1975). It is this definition that this writer will consider appropriate for the purposes of this study.

Lower Mississippi River Loess

The loess present in West Tennessee is part of one of the most extensive loess deposits in the world (Rutledge, 1996). The loess of the lower Mississippi River Valley (LMV) was first described by Sir Charles Lyell in 1847. He wrote that "the bluffs bounded the valley and were 15-75 m high, contained deposits and resembled the loess of the Rhine River Valley" (Lyell, 1847). Lyell thought the deposit was alluvial in origin. E.W. Hilgard (1860), examined the loess of the LMV , he described the loess as yellow-brown and reddish-brown loam, he thought that the reddish brown loam to be a stratigraphic unit that was lain on top of the water lain loess (Hilgard, 1860). In agreement with Lyell, Hilgard felt the loess to be alluvium.

Call (1891) was the first scientists to digress from this paradigm. He felt that the deposits were a result of "double submergence." At Crowley's Ridge, Arkansas, Call identified two loess layers separated by a soil. He thought that the soil was evidence of "double submergence". He also felt the loess was correlative to the glacial periods in the Upper Mississippi River Valley.

Mabry (1898) conducted research on the loess that Hilgard researched in 1860. Mabry concluded the upper loam described by Hilgard and the loess to be one and the same. Mabry believed the loess to be alluvial and formed via subaereal exposure (Rutledge, 1996).

Leverett (1899) proposed a theory combining both eolian and fluvial processes. He proposed loess was a result of " glaciofluvial - eolian" processes. Leverett and many others recognized the silt that was present on many of the upland areas in the LMV. However, this was seen as merely circumstantial due to the lack of eolian land forms and

stratification (Follmer, 1996).

The first purely eolian hypothesis was presented by Shimek (1902). At Natchez, Mississippi, he identified one loess deposit. Studying the fossils present in the loess, Shimek examined over 50 exposures and 4600 fossil shells. All fossils were terrestrial in origin and found to be living in and around the study area. Later, Emerson (1918), pointed out that in addition to Shimek's evidence, the loess was present on both sides of the MRV which indicates variable winds. Emerson concluded the loess was wind blown alluvium from upstream.

Guy Smith (1942), a proponent of the eolian hypothesis, investigated the loess in Illinois. Through his observations, he created a mathematical model of loess deposition. Smith's model stated that the thickness of the deposit decreased with log (base 10) of the distance from the source, and that coarse silt content decreases and fine silt content increases with the log of the distance from the source.

The biggest controversy surrounding loess and more specifically the loess of the LMV came in 1944, when the theory of loessification was published by Russell. Russell was initially a supporter of the eolian theory until he conducted research on the loess himself. Russell based much of his theory on the work of other scientists who proposed an *in-situ* formation hypothesis (Russell, 1944). He concluded the loess formed via a process that he called "loessification." Russell felt the loess formed by the accumulation of calcareous terrace deposits in a back swamp environment (Russell, 1944). He believed the terrace deposits to have weathered into soils and in doing so the clay-sized particles were elluviated, leaving behind the silt-sized particles that are characteristic of the loess

deposits (Russell, 1944). Russell only delineated one loess deposit at the sites he studied.

Most of Russell's peers felt his conclusions were erroneous. However, his research was significant nonetheless. The loessification theory stimulated a surge in research on the loess in the LMV and ushered in the modern era of loess research (Rutledge, 1996). During this time, local loess stratigraphy was known on a state-by-state basis but no attempts to do a regional correlation had been made. Most scientists of the day considered it speculative to correlate across state lines (Follmer, 1996).

Wacsher et al. (1947), identified and correlated three eolian loess deposits in the LMV. They identified an uppermost loess deposit that they correlated with the Peoria loess of the Midwest (Wacsher et al., 1947). Wacsher et al.(1947), described the Peoria loess as being more than 4.5-m thick and containing well developed soils. The middle loess unit was described as being thinner than both the top (Peoria) and the basal loess unit. They called the middle loess "Late Sangamon" after the interglacial period they felt it was correlated with. The basal loess unit could not be correlated and was simply called the Third Loess. However, they suggested it was correlative to the Loveland Loess of the Missouri River Valley.

Four loess deposits were identified by Leighton and Willman (1950) (Fig. 3). Their research was conducted throughout the LMV. Four loess units were correlated with the loess of the Upper Mississippi River Valley (Leighton and Willman, 1950). The upper loess was designated as Peorian. It was described as 23-30 m thick at Vicksburg and Natchez Mississippi. Underlying the Peorian was the Farmdale loess, which is non-calcareous and chocolate brown . In most of their studies, Leighton and Willman saw only three loess deposits. The basal loess was called the Loveland Loess and was noted as

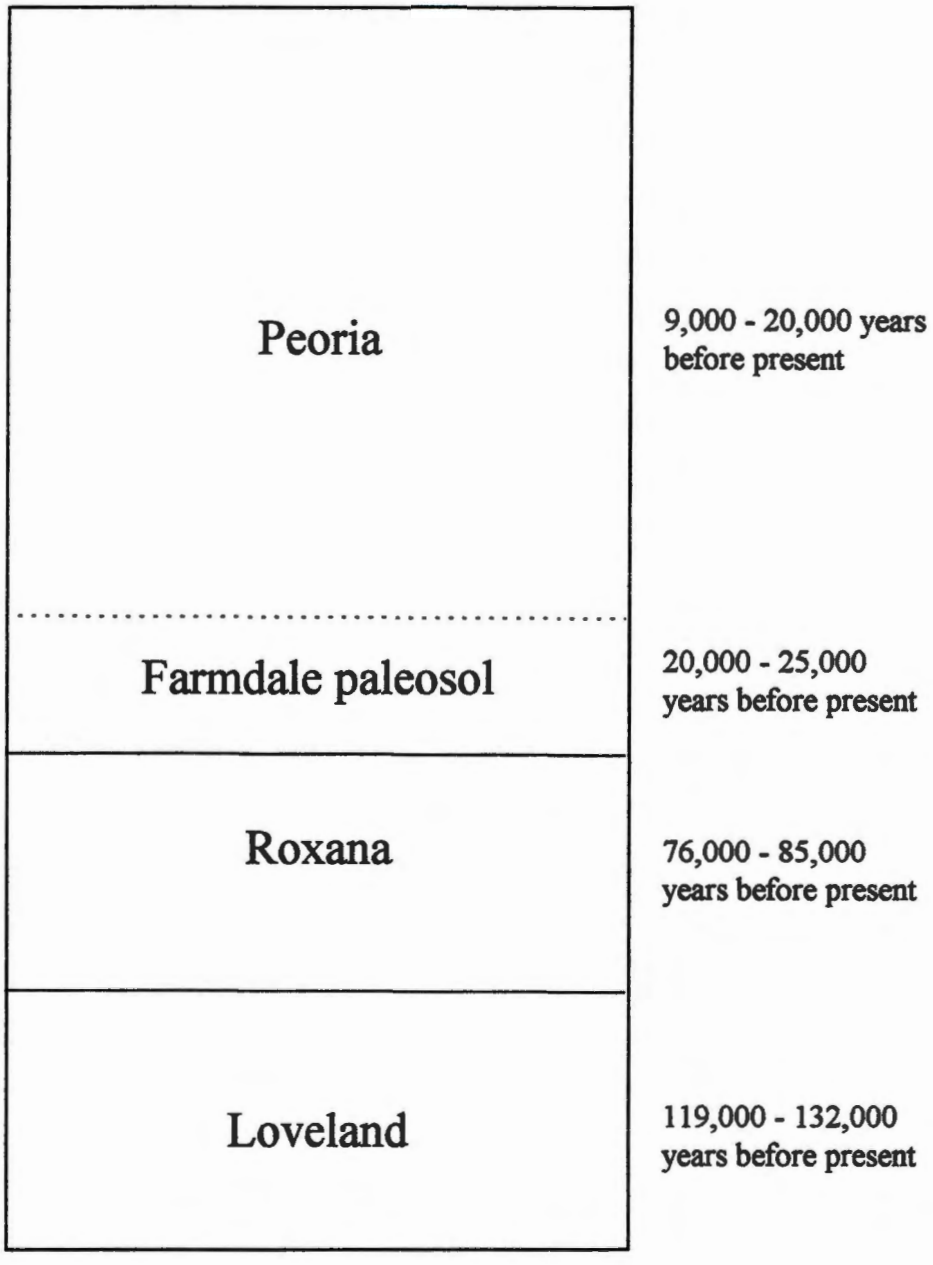


Figure 3. Generalized loess sequence of the
Lower Mississippi River Valley.

being leached of carbonates (Leighton and Willman, 1950). At Natchez, Mississippi, Crowley's Ridge Arkansas, and other sites in both Tennessee and Mississippi, a deposit that was termed Pre-Loveland was identified by Leighton and Willman (1950). They suggested that it was correlative with the pro-Kansan Loess of the Upper Mississippi Valley. This "Pre-Loveland" loess was described as being non-calcareous and containing a clay increase suggestive of a B horizon (Leighton and Willman, 1950).

The work done by Leighton and Willman was very controversial. At the time of its publication, it was considered unwise to correlate the loess in the Lower Mississippi River Valley to loess deposits in the Upper Mississippi River Valley until better techniques for correlation were developed and proven (Rutledge, 1996). It was felt that degree of weathering was a grossly inadequate method of correlation. Krinitzsky and Turnbull (1967) recognized three depositions of loess and a possible fourth. The youngest layer (Peorian) was called the Vicksburg, and was described as having a soil formed in it and being calcareous (Krinitzsky and Turnbull, 1967). The basal mixing zone in the Vicksburg was determined to be a separate loess, suggesting that it could be equivalent to the Roxana loess of Illinois. It was thought the "Pre-Vicksburg" loess was equivalent to the Loveland loess of Illinois.

Snowden and Priddy (1968), identified and correlated four LMV loess deposits with loess deposits of the Upper Mississippi River Valley. They separated the loess deposits based upon leached zones, the development of paleosols, and radio-carbon dating. They proposed that the Pre-Farmdale loess could be correlated with the Loveland loess and the Roxana Loess of the Midwest. According to their work, the Peoria contained the modern soil, the Farmdale contained a paleosol, and the two "pre-

Farmdalian" loess both contained paleosols. In addition to separating four loess sequences, Snowden and Priddy obtained the first radio-carbon dates on the Peoria and the Farmdale loess. Ages of the Peoria loess was determined to be less than 22,000 years B.P. and the Farmdale as greater than 22,000 years B.P.

West et al. (1980) conducted studies at Crowley's Ridge in Arkansas in order to determine source areas and direction of the winds that deposited the loess. Using clay free particle size data in conjunction with observations made by Guy Smith (1942), the researchers could determine the most plausible source area and prevailing wind data. Descriptions from West were in agreement with the descriptions of earlier researchers, therefore they accepted the previous terminology and correlated them with loess of the Upper Mississippi River Valley (Rutledge, 1996). Correlations by West were as follows: Peoria Loess having a modern soil, Roxana Silt with a weak paleosol, and a thick Loveland Silt with a developed paleosol. West et al.(1980), concluded that the Peoria and the Roxana had their source areas to the east of Crowley's Ridge deposited by east to west blowing winds. The Loveland Loess had its source both east and west of Crowley's Ridge (West et al., 1980).

Miller (1989) conducted extensive research in Louisiana, where he studied over 30 transects. In addition to the Louisiana studies, Miller conducted copious research at Crowley's Ridge in Arkansas and Vicksburg Mississippi (Miller, 1989). Results of Millers prodigious research were two fold; he mapped the loess distribution in Louisiana and proposed new correlations for the loess of the LMV and he correlated the youngest loess as the Peoria loess and determined it to be Late Wisconsin in age. The second loess was correlated as Roxana Loess, and was Middle Wisconsin in age. Miller found that the

Roxana Loess is present at the southern end of Crowley's Ridge but is also present at more southern locations (Autin, 1996). At locations south of Crowley's Ridge, Miller correlated the third loess. Called the Sicily Island Loess, it was Early Wisconsin in age. The fourth loess correlated by Miller was the Crowley's Ridge Loess. It was Illinoisan in age. Miller found the oldest loess to be the Marianna. Due to the fact that the Mairana has not been correlated to any other location, it is thought that it is a silty water deposit . The Marianna has only been observed at the Bledsoe section on Crowley's Ridge near Wynne, AR (Rutledge, 1996).

Markewich (1994) used both carbon 14 and thermoluminescence to determine relative ages of the Peoria Loess and soil contained in the Roxana Loess. For the Peoria, carbon 2014 ages were 21,070 ± 300 years B.P. and 24,450 ± 565 years B.P. and thermoluminescence ages were 24,700 ± 1,900 years B.P. and 23,200 ± 2,300 years B.P. Using Radiocarbon analysis, the Roxana was determined to be 26,460 ± 270 years B.P., 28,980 ± 800 years B.P. Using data obtained from thermoluminescence, ages for the Roxana ranged from 30,000 ± 6,000 to 33,900 ± 2,900 years B.P. In addition to the Peoria and Roxana, the Loveland Loess had thermoluminescence run on in, it was determined to be 122,000 ± 14,000 years B.P. to 189,000 ± 3,000 years B.P. (Markewich, 1994).

Overall, the researchers of today agree on the following: 1) the Peoria Loess is the youngest and Late Wisconsin in age, 2) the loess underlying the Peoria is the Roxana Silt the distribution of which is not agreed upon, and 3) the loess under the Roxana is still a source of controversy. According to Rutledge (1996) the data regarding the name and age of the loess often referred to as Loveland or Sicily Island is ambiguous. Some

researchers feel that the Loveland or Sicily Island Loess is composed of two separate depositions, one of Wisconsin age and one of Illinoisan age.

Regional Geomorphology

Saucier (1987), identified four terraces on the Obion, Forked Deer, Hatchie, Wolf, and Loosahatchie Rivers in West Tennessee (Fig. 4). Using 1:24,000 scale topographic maps as the primary source of data, he identified and delineated terraces on the basis of geomorphic expression alone. In an effort to reduce confusion, Saucier assigned proper names to the terrace levels. Terraces were from youngest to oldest: the Finley, Hatchie, Humboldt, and Henderson. Present on all five rivers investigated, the Finley terrace is the easiest to recognize. Elevations range from 3 to 5 meters above the recent (Holocene) flood plains. The second and best preserved terrace identified was the Hatchie, at 10 to 15 meters above the present flood plain. The third terrace level is named the Humboldt terrace, it is present on all but the Wolf and Loosahatchie rivers. It parallels the present day flood plain and is 10 to 20 meters above the flood plain. The oldest terrace is named the Henderson and is limited in its distribution to the upper levels of the three forks of the Forked Deer River.

Rivers of West Tennessee have been characterized as "under fit" by geologists. The law of uniformitarianism fails to account for their formation; under present conditions the streams are not large enough to create valleys that are as broad as the ones seen in West Tennessee. Two hypotheses have been presented in the literature, one fluvial and one tidal. Fluvial-based theories center on the fact that during interglacial periods great quantities of water drained from the waning glaciers. Due to this influx of water, streams

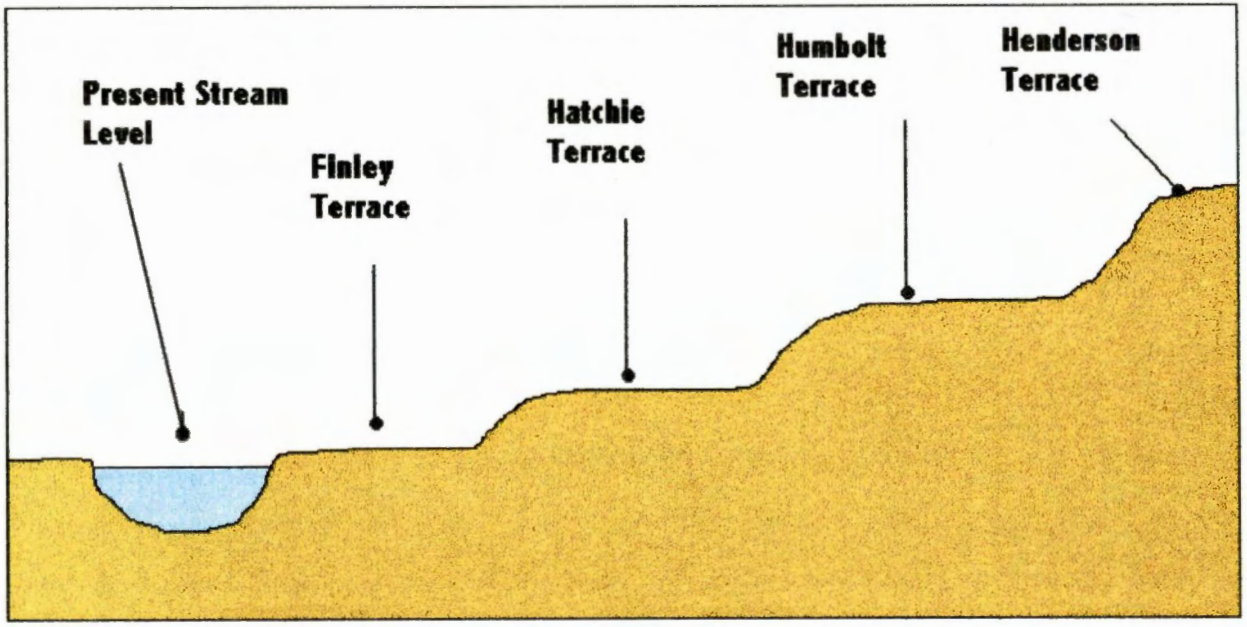


Figure 4. West Tennessee Terraces as interpreted by Saucier, 1987.

were much larger than seen today. Reduction in runoff and precipitation has left streams carrying only a fraction of what they once did, leaving behind the under fit appearance seen today.

An equally plausible alternative to the fluvial based theory was presented by Geyl (1996). Comparing numerous tidal streams in Australia, Europe, and the United States to fluvial streams, Geyl noticed some profound distinctions. Geyl looked primarily at discharge, stream width, meander wavelength, stream length, and catchment area. Plotting these parameters on regression line (a morphometric graph) he found the discharge of fluvial rivers are not as much as tidal streams, and become less as catchment area increases. For example, streams in the Wadden Sea have no catchment area to speak of yet have discharges ranging from 45,000 to 90,000 m^3/sec, whereas the Mississippi at bankfull at a point where the catchment area is 2,300,000 km^2, has a discharge of 28,600 m^3/sec (Geyl, 1996). Also he found that tidal rivers' widths increase much more rapidly in a seaward direction than fluvial rivers, especially below the tidal limit. Meander wavelengths of tidal versus fluvial rivers had the same trend as stream width. Looking at the West Tennessee landscape, Geyl saw "incontrovertible resemblance to the present land forms of the tidal Wadden Sea of the North Sea coast, visually and quantitatively they must be tidal paleomorphs, relict tidal land forms" (Geyl, 1968).

History of Pedology

Pedology is a collective term used to refer to the combination of two phases of soil science; soil genesis and soil classification. Soil genesis is defined as the science that studies the factors and processes of soil formation. It involves description,

characterization, and interpretation of soil profiles. Soil classification is the ordering of soil into groups based upon morphological properties (Boul et al., 1997).

The first known attempt to classify soils occurred in China during the Yung Dynasty (2357-2261 B.C.), the soils were assigned to one of nine classes according to their known productivity (Simonson, 1962). Despite this, it was not until the late nineteenth century that pedology as a scientific discipline gained acceptance. In 1883, V.V. Dokuchaev (1846-1903), the father of pedology, published a report on a field study of Chernozems. In his report, Dokuchaev applied soil morphology principles, described major soil groups, created the first classification system of soils, and developed soil mapping techniques. Additionally, in 1886 Dokuchaev proposed that the term *soil* be used to refer to "those horizons of rock which daily or nearly daily change their relationship under the joint influences of water, air, and various forms of organisms both living and dead." Dokuchaev later modified his definition of soil to "an independent natural evolutionary body formed under the influence of five factors" , of which he considered vegetation to be the most influential (Vilenskii, 1957). Dokuchaev's student K.D. Glinka (1867-1927) translated Dokuchaev's work into German which enabled Dokuchaev's work to gain wide recognition. In addition to this, K.D. Glinka and S.S. Neustuyev reemphasized the concept of soil as a surficial geologic entity, a weathered crust that exhibits specific properties correlated with climatic zones (Boul et al., 1997). Glinka stated that the primary factors in soil formation are climatic and geological conditions. Both Glinka and Neustuyev regarded soil as "the elluvium of rocks" (Vilenskii, 1957).

E.W. Hilgard (1833-1916) while employed as a geologist in California and

Mississippi, wrote about the relationship between soils and climate. Hilgard "saw the farmer's dirt as a richly embroidered mantle of earth, whose design and fabric were deserved of scientific zeal and quest." Hilgard later defined soil as "the more or less loose and friable material in which, by means of their roots, plants may or do find a foothold and nourishment, as well as other conditions of growth" (Hilgard, 1906). Hilgard, like many soil scientists of the day considered soil a means of plant production (Jenny, 1941). This paradigm not withstanding, G.W. Coffey while working with the U.S. Division of Soil Survey in 1912 produced a classification system inspired by the genesis principles of Dokuchaev and Glinka. In his report on soils of the United States, Coffey wrote that "soils are an independent, natural body, a bio-geological formation, differing from the underlying rock, but closely related to it." He proposed that soils be classified based upon the characteristics of the soils themselves (Simonson, 1962). Unfortunately Coffey's system was not widely accepted, the idea of soil as a surficial geologic material still dominated (Boul et al., 1997).

With the help of U.S. Soil Survey director C.F. Marbut (1863-1935) and his successor C.E. Kellogg (1902-1977), Dokuchaev and Glinka's work on soil genesis and classification was introduced to the U.S. system. In addition to Dokuchaev and Glinka's work, Marbut introduced his own emphasis on the soil profile and the "normal soil"(Boul et al., 1997). In 1941, Hans Jenny wrote a treatise entitled "Factors of Soil Formation" . Jenny explained soil formation with the formula S= F(cl, o, r, p, t...). This formula explained that soil formation is a function of climate, organisms, relief, parent material, and time. The significance of Jenny's work is that he divided the soil forming factors into independent variables that "define the status of a soil system." This allows the soil

properties to be expressed as functions of soil forming factors, thus enabling quantitative correlations between soil properties and soil forming factors (Jenny, 1941).

G.D. Smith (1907-1981) with the help of other soil scientists is responsible for a classification system above the level of the soil series. The final system was entitled "Soil Taxonomy" and published in 1975. In addition to this, Smith also made the point that "soil genesis is very important for soil taxonomy, but genesis alone cannot be used as a basis for classification because the genetic processes can rarely be quantified or actually observed" (Boul et al., 1997). G.D. Smith's classification, as of 1999, has undergone eight revisions and is still in use today.

Currently, the soil taxonomy system is based upon six divisions; the soil order, the suborder, the great group, the sub-group, the family, and the series. The soil order is the broadest level of taxonomy, it is differentiated on the presence and or absence of major diagnostic horizons. Currently there are twelve soil orders in the U.S. system of soil taxonomy. The sub-order differentiates the soil orders based on the homogeneity within the orders due to properties associated with soil wetness, soil moisture regimes, major parent material, and vegetal cover. There are currently 60 sub-orders in the U.S. taxonomy system. The great group divides the sub-order based upon the degree of horizonization, the arrangement of horizons, and the presence of specific diagnostic horizons such as fragipans and duripans. There are approximately 300 great groups in U.S. taxonomy. The sub-group divides the great group based upon the idea of the central concept of the soil expressed as "Typic", the sub-group includes intergradations and extragradations to other great groups, sub-orders, and orders. The family includes the textural class across the control section, the dominant mineralogy of the soil, clay activity

class and the temperature regime. The soil series is based on all the above criteria and is named locally (Boul et al., 1997).

Soil Forming Factors

Development of earthen material into a soil depends upon the influences and interactions of five factors; time, parent material, climate, relief, and organisms. The process of soil formation is a complex series of reactions that are catalyzed by the afore mentioned factors. The following discussion will focus upon the individual factors and their contribution to soil formation.

Time

Time as a concept is both infinite and continuous. However, as a soil forming factor it is not. With regards to soil, time has finite limits. Time is reset with every geomorphically catastrophic event, thus soils are perpetually starting over. Geomorphically catastrophic events include any event that alters the landscape to a degree that the soil is throughly disturbed such as a landslide, severe erosion, major changes in water, geologic disturbances, etc.

Time can be expressed as the horizonization of a soil body which is directly related to the maturity of the soil body. Although degree of horizonization is regarded as an indication of age, the ideas behind soil genesis as expressed by horizonization in the profile are only inferences (Jenny, 1941). The importance of time on soil formation has long been known to those who study the soil. Some of the early classification systems were based

upon the concept of a "mature" soil. Terms such as azonal (young), intrazonal (immature), and zonal (normal) were used to put soil into categories. Marbut thought of a mature soil as one that was constantly exposed to geologic erosion (Boul et al., 1997). Due to the variability between ideas of a central concept on soil maturity this classification scheme was replaced by less subjective means of classification.

Climate

Climate as a soil forming factor is exceedingly complex, therefore, it cannot be measured numerically. Climate can however be broken down into individual factors, two most important of which are temperature and moisture (Jenny, 1941).

Moisture is crucial to soil development. On a micro scale, the transport of clay, organic colloids, carbonates, and minerals through a soil profile is driven by soil moisture. On a macro scale, large scale precipitation events on sloping surfaces or on loosely held soils can continually redistribute soil material and impede soil horizon development. Freezing and thawing of water is a major factor in mass movement of soil and the mixing of horizons in Arctic regions. Soil moisture is determined to a large extent by the amount and pattern of precipitation at a location (Miller, 1990). For example, soils of humid regions tend to have higher clay content, greater acidity, higher CEC, and lower base saturation than soils formed in arid regions (Foth, 1984). Additionally, moisture effects biological activity and biomass production in a soil, therefore more humid soils will have greater amounts of humus (Foth, 1984).

Mean air and soil temperature is directly related to the climate of an area. In general the highest temperatures are recorded in the equatorial regions and decrease

towards the poles. This generalization does not take into account micro-climate influences such as elevation. Temperature of a soil is very important to the chemistry of the soil and thus to its genesis. With each 10 degree C increase in temperature the rate of chemical reactions will double (Foth, 1984). This affects the weathering of minerals and the decomposition of material in a soil profile. Soil temperature is affected by solar radiation, a soil that is tilled or is left bare will see more pronounced effects than those with vegetal cover (Livingston, 1993).

Parent Material

Parent material can be defined as the initial state of the soil system. In other words, the parent material of a soil is the depositional energy of the soil at time zero and not the underlying geology. To be sure, geology beneath a particular soil is very important, however, one cannot assume that the soil material has formed from the underlying bedrock (Jenny, 1941). Kellogg (1941), stated that "a great many entirely different soils can be derived from the same rock conversely many similar soils may be developed from very different rocks." There is a distinction between weathering processes and soil forming processes. According to Jenny (1941), weathering processes are geologic and involve solution, hydrolysis, oxidation, reduction, and clay formation. Soil forming processes are pedogenic and involve calcification, podsolization, laterization, salinization, de-saliniztion, alkanization, and de-alkanization. In practice one cannot draw such a clear line between pedogenic processes and geologic weathering because there is no point at which weathering ends and pedogenesis begins.

Organisms

Activity of soil organisms play a major role in the development of soils. According to many soil scientists such as Marbut view organisms and especially plants as the most important soil forming factor (Jenny, 1941). According to Kellogg (1941), "plants are the real makers of soil." This can be illustrated by observing soils under differing natural plant covers. For example, comparing soils that are developed under grasses versus those that are developed under dense tree cover. Soils developing under humid forests tend to have many horizons and are leached of organic matter in the upper horizons. In contrast, soils developing under grasslands often have decomposed organic matter well into the mineral soil (Miller, 1990).

Microorganisms have a profound influence on soil. Decomposition of organic matter is governed by the abundance of microorganisms. Microorganisms such as *nitrobacter,* fix mineral matter into plant available forms. Jenny (1941) stated that within a large region the microbiological component for soil is constant. His reasoning is based on the belief that through natural processes such as rain events, dust storms, etc., soils are continuously being re-inoculated with micro fauna.

Macroorganisms such as burrowing mammals, earthworms, ants, etc., have a major role in the organism component of soil formation. They provide pedoturbation, thus mixing the horizons and redistributing the minerals and hence nullifying the illuvial transport of colloids and clays (Miller, 1990). By burrowing through the soil, macroorganisms provide oxygen availability for the microorganisms, roots, and some chemical reactions.

Relief

Relief, sometimes referred to as topography, is defined as the contour of the earth's surface (Miller, 1990). According to Jenny (1941), relief as a soil forming factor has not had the attention it deserves. Relief of a particular soil will influence water and temperature relations (Miller, 1990). As a soil forming factor, relief essentially causes the redistribution of matter and energy with out any direct output. The most pronounced effects of relief on soil formation can be observed in mountainous areas (Joeff, 1949). In a mountainous area weathering products will be removed via erosion. Infiltration of water will be lower due to the more rapid runoff associated with steep slopes.

Topography also influences the temperature of a soil. Overall, slopes that face south, will be warmer and experience fluctuations in both the temperature and moisture. Alternatively, north facing slopes will have lower average temperatures and experience fewer fluctuations (Joeff, 1949).

Physical Properties and Water Movement

Soil is heterogeneous and is considered to be a three-phase system: the solid phase, the liquid phase, and the gaseous phase . The solid phase includes soil particles that vary greatly in composition, size, and arrangement. In addition to soil particles, the solid phase includes amorphous substances such as humus. The liquid phase includes water and any substances dissolved within. Finally, the gaseous phase is comprised of any gas trapped in the solid phase or the liquid phase (Hillel, 1982).

Measurements found to be useful in describing the relationship of the three phases of a soil are the following: mean particle density (ρ_s), dry bulk density (ρ_b), total porosity

(f), soil wetness (ω), and air filled porosity (f_a). The particle density of a soil is the density of the soil particles. It ranges from 2.5 and 2.7 g/cm^3, which is close to the density of quartz. Dry bulk density of a soil is a measure of the mass of the soil to its total volume, it includes the volume of the pores present, and tends to be lower than the particle density with average values ranging between 1.3 and 1.6 g/cm^3. Total soil porosity is a measure of the volume of pores present. It is expressed as a percentage of the total volume, with average values of 30 to 60%. Soil wetness measures water present in a soil, and is expressed both gravimetrically and volumetrically. Air filled porosity measures the relative amount of air in a soil (Hillel, 1982).

Movement of fluids through a medium can be described by Darcy's Law, named after French scientist Henri Darcy. In 1856, Darcy conducted experiments using a sand filled cylinder with water flowing through it and manometers at each end of the apparatus. He was interested in the relationships between the inflow (Q), cross-sectional area (A), rate at which water moved through the sand (K), the distance between the inflow and outflow (∂l), and the elevation of the water levels in both manometers (∂h). Darcy found that the relationship between these can be expressed as $v = -K \cdot \partial h/\partial l$; where v is equal to the specific discharge or *flux* and is defined as $v = Q/A$ or the rate of flow per unit area, K is the hydraulic conductivity which is a measure of how easily water flows through a material (often expressed as cm/sec), ∂h is the hydraulic head (cm), and $\partial h/\partial l$ is the hydraulic gradient (Freeze and Cherry, 1979).

Water movement through a soil profile is considered to be too complex to be described in microscopic detail. Instead, water movement is thought of in macroscopic terms and is treated as if it were a uniform medium (Freeze and Cherry, 1979). The

physical properties of a soil such as those discussed in the preceding paragraphs as well as others such as texture and soil structure will greatly influence the movement of water in a soil. Most of the time, soil water movement takes place under what is referred to as unsaturated flow and occurs in the vadose zone. In the vadose zone, the pressure head is < 0 and is referred to as tension head, suction head, or matric potential. This results from the pores being only partially filled with water. With regard to unsaturated flow, Darcy's Law is written as $v(x)=-K(\psi)dh/dl$; where $v(x)$ is flow in the x direction and (ψ) is suction head (Freeze and Cherry, 1979). As soil moisture is increased, the suction head (ψ) increases, i.e., approaches zero and the hydraulic conductivity is increased until the soil is saturated (Hillel, 1982). Hydraulic conductivity at the point of saturation is known as the saturated hydraulic conductivity.

The hydraulic conductivity of a soil will vary a great deal over a small area due to heterogeneity of physical properties in the soil. Luxmoore (1981) found that part of the variability obseved in hydraulic conductivity measurements was due to the occurrence of macropores. The saturated hydraulic conductivity of a soil is affected by soil properties such as structure, texture, bulk density, porosity, and clay mineralogy (Schoenberger et al., 1995). Of these factors, texture has the most pronounced influence on the hydraulic conductivity of a soil, with highest conductivity readings for coarse textured soils (Hillel, 1982).

Water in the soil profile is exposed to three forces that govern its movement. These forces are: gravitational potential (ϕ_g), matric potential (ϕ_p), and osmotic potential (ϕ_o). The sum of these forces is referred to as total soil water potential (ϕ_t) (Hillel, 1982). Gravitational potential at a specific point is determined by the elevation of that point

relative to an arbitrary datum. Gravitational potential energy of soil water is equal to $E_g = \rho_w * V_g * Z$; where E_g is gravitational potential, ρ_w is the density of water, V_g is acceleration due to gravity (9.81 m/s^2), and Z is height above the datum. Matric potential, also referred to as pressure potential, is the pressure acting upon soil water with regard to atmospheric pressure. In the unsaturated zone, the matric potential is negative due to capillary forces within the soil matrix. Matric potential of soil water is equal to $P_o - P_c = \Delta P = \gamma(1/R1 + 1/R2)$; where P_o is atmospheric pressure, taken as zero, P_c is soil water pressure, ΔP is the deficit of pressure, γ is the surface tension of water (73 dynes/cm), R1 and R2 are the radii of curvature of a point on the meniscus (Hillel, 1982). Osmotic potential is due to the presence of solutes in the soil water, which lower its potential energy. The pressure results from the tendency of pure water to travel across a semipermeable membrane into a reservoir of water with solute dissolved within it, and is actually a suction rather than a pressure, a phenomenon known as osmosis (Hillel, 1982).

Materials and Methods

Site Selection

The research site is located on Field 75 at the Ames Plantation, (N 35°08'4.1"; W 089°13'23.8"), Hickory Valley, TN quadrangle (USGS, 1980). This site was selected because it is similar in topography and adjacent to but not on the Ames Water Quality Monitoring site, located on the West Pasture and the Hancock tract experimental areas.

Field Methods

Nine pedons were sampled on field 75 at the Ames Plantation (Fig.5). The cores were sampled within a 30.5-m x 30.5-m grid and were spaced approximately 15.25 m apart. A Giddings GSRP-S-M hydraulic probe with a 7.62-cm sampling tube was used to extract the samples. Core samples were taken to a depth of 2.5 -3.0 meters.

Each pedon was described in the field according to the Soil Survey Manual (Soil Survey Staff, 1993). Cores were separated into horizons, depth, color, texture, structure, and consistence as well as other predominant soil properties were recorded. A representative sample was taken from each horizon and approximately 3 kg were placed in a plastic bag for use in laboratory analysis (Soil Survey Staff, 1996). Soils were classified to the family level of Taxonomy (Soil Survey Staff, 1999)

Laboratory Methods

Each sample was air dried and crushed in order to pass a 2-mm sieve. The weight of the > 2-mm portion was recorded as well as the portion that was < 2 mm. One fourth of the portion that was < 2 mm was ground to pass a 60-mesh sieve (Soil Survey Staff, 1996)

Soil Physical Analysis

Bulk density was determined using the Varsol method from Smith (1957). Particle density was determined for selected samples by the pycnometer method from Blake (1965) in order to verify bulk density values. Particle size analysis was determined for all samples using the pipette method from (Kilmer and Alexander, 1949). The amounts of clay, sand,

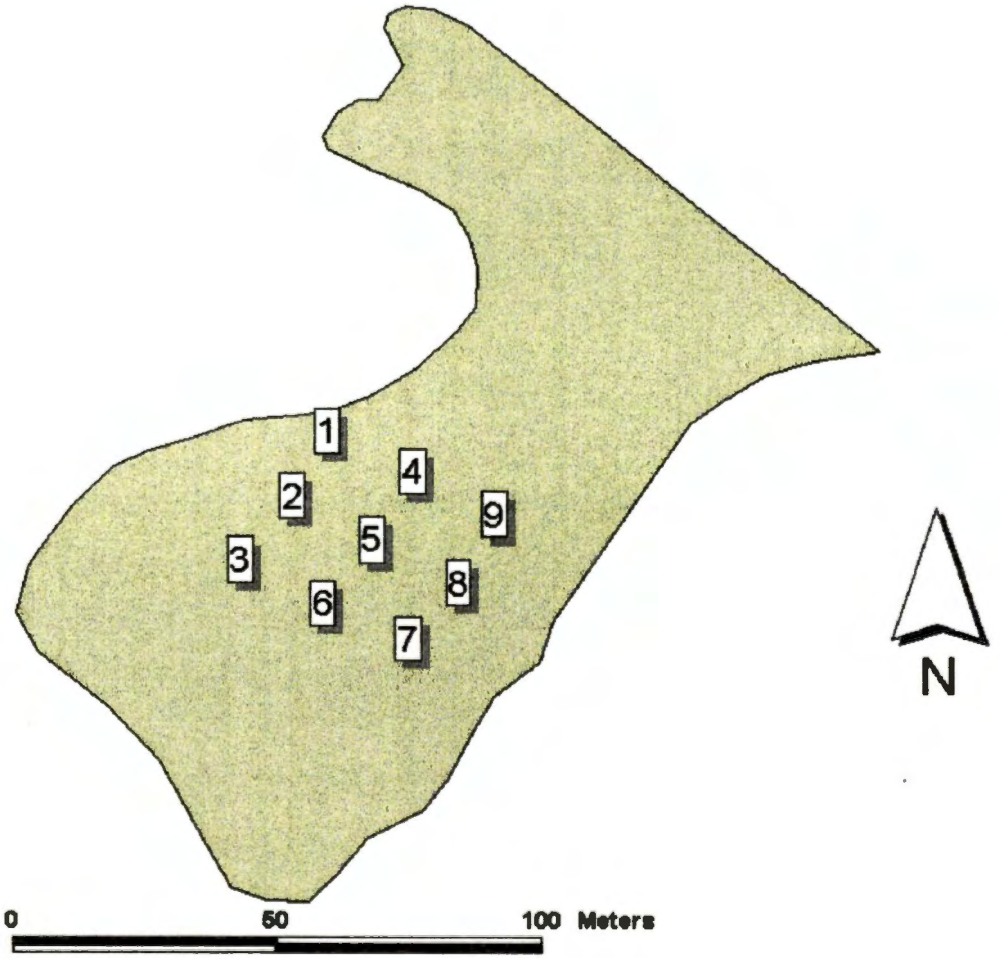


Figure 5 . Field 75 site location map.

and silt were determined in accordance with the USDA system of textural classification. The sand sized fraction was further differentiated into very coarse, coarse, medium, fine, and very fine sands using a series of sieves and a CSC™ mechanical sieve shaker that was set to shake for five minutes prior to weighing (Gee and Bauder, 1986).

Saturated hydraulic conductivity (Ksat) was determined in the field at selected sites using the compact constant-head well permeameter (CCHP) method, also known as an "Amoozemeter" (Amoozegar, 1989a). From the data obtained, the *in situ* saturated hydraulic conductivity was determined by using the Glover Solution; $Ksat = CQ/(2\pi H^2)$, where $C = \sinh^{-1}(H/r) - (r^2/H^2 + 1)^{1/2} + r/H$, (H) is equal to the height of water maintained in a cylindrical auger hole of radius (r), and (Q) is the steady-state rate of water flow into the soil (Amoozegar, 1989b). K_{sat} measurements were taken above and below the loess/alluvium interface for the nine sites.

Chemical Analysis

Soil pH was determined using a Orion Research Analog pH meter, model 301. Both a 1:1 (soil and water) mixture and a 1:2 (soil $CaCl_2$) mixture were run on each sample (McLean, 1982). Total carbon analysis was conducted on all samples (using soil that was ground to pass a 60-mesh sieve) using a Leco CR-12 Carbon System. Organic Carbon was determined using the Walkley-Black method (Jackson, 1958).

Iron oxides were extracted using the citrate-dithionite method (Olsen and Ellis, 1982). Manganese oxides were extracted using the hydroxylamine hydrochloride method (Gambrell and Patrick, 1982). Extracts were then analyzed using atomic adsorption spectroscopy on a Perkin-Elmer model 5000 spectrophotometer.

Total elemental analysis was determined using a modified aqua-regia, hydroflouric acid, microwave dissolution proceedure (Gallagher, 1993; Nadkarni, 1984). Extracts were analyzed by inductively coupled argon plasma emission spectroscopy on a Thermo Jarrell Ash ICAP 61.

Exchangeable bases were determined via the ammonium acetate pH-7 technique and were analyzed on a Perkin-Elmer 5000 Atomic Absorption Spectrophotometer (Jackson, 1958). The cation exchange capacity (pH 7) was determined by the ammonium acetate rapid distillation method (Chapman, 1965). Percent base saturation (direct measurement) and ECEC were determined mathematically (Soil Survey Staff, 1996). Exchangeable aluminum was determined by KCL extraction, extracts were analyzed by atomic absorption spectroscopy (Thomas, 1982). Extractable acidity was determined by the $BaCl_2$ - TEA procedure. Calculations for percent base saturation and CEC pH 8.2 were then made (Soil Survey Staff, 1996).

Results and Discussion

Site One

Site one was located at N 35° 8' 4.9", W 89° 13' 41", on an upland position under a forage cropping arrangement, at an elevation of 164 meters above mean sea level. Soil morphology was sampled and described to a depth of 290 cm below the soil surface. The parent material sequence was loess over alluvium over Tertiary aged sands.

Loess extended from the surface to a depth of 105 cm (Fig. 6). Soil color throughout the loess was 7.5YR 4/4, except for the uppermost horizon which was 10YR 3/4 due to organic matter inherent in Ap horizons. Bulk densities ranged from 1.64 g/cm^3 in the Bt1 horizon (4 - 18 cm) to 1.40 g/cm^3 in the Bt2 horizon (18 - 53 cm) (Fig. 7). One explanation for the unusually high bulk density in the Bt1 horizon is that it may have experienced some compaction from the field being used as a parking lot for field days over several years. Free iron oxide concentration and total iron increased with depth to the Bt2 horizon (18 - 53 cm) before dropping off in the BC1 horizon (53 - 105 cm), illustrating a typical weathering pattern (Fig. 8). Total silt percentage ranged from 72.5% in the uppermost horizon to 65.2 % in the BC1 horizon (53 - 105 cm) (Fig. 6). There was a fine clay bulge in the Bt2 horizon (18 - 53 cm), in the underlying BC1 horizon (53 - 105 cm) the fine clay percentage dropped off significantly, as one would expect (Fig. 8). Total and organic carbon had a regular decrease with depth to the BC1 horizon, 105 cm below the surface (Fig. 9). Fine sand percentage increased sharply below the BC1 horizon (53 - 105 cm), while the titanium to zirconium ratio increased slightly, indicating a lithologic

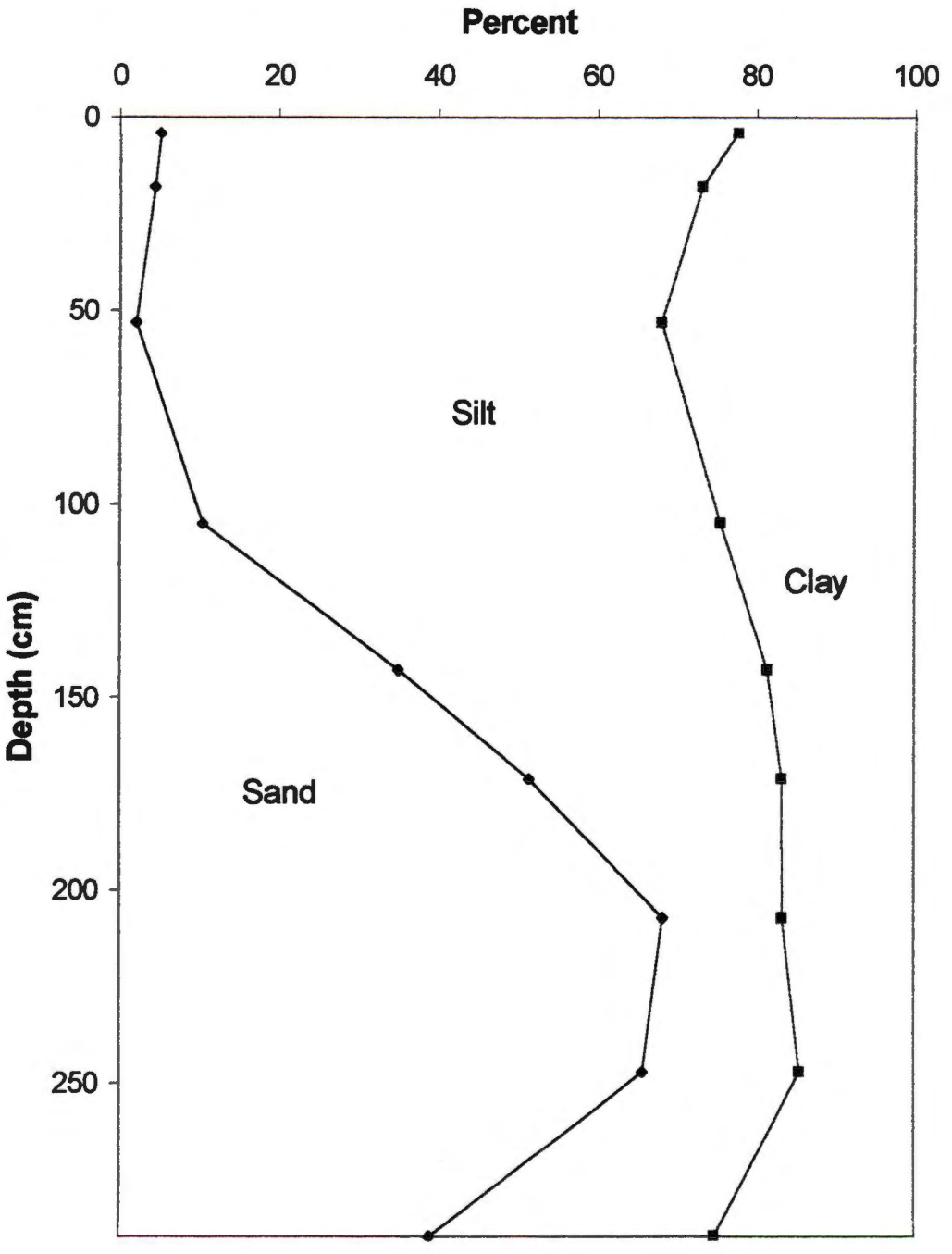


Figure 6. Cumulative particle size plot for site 1.

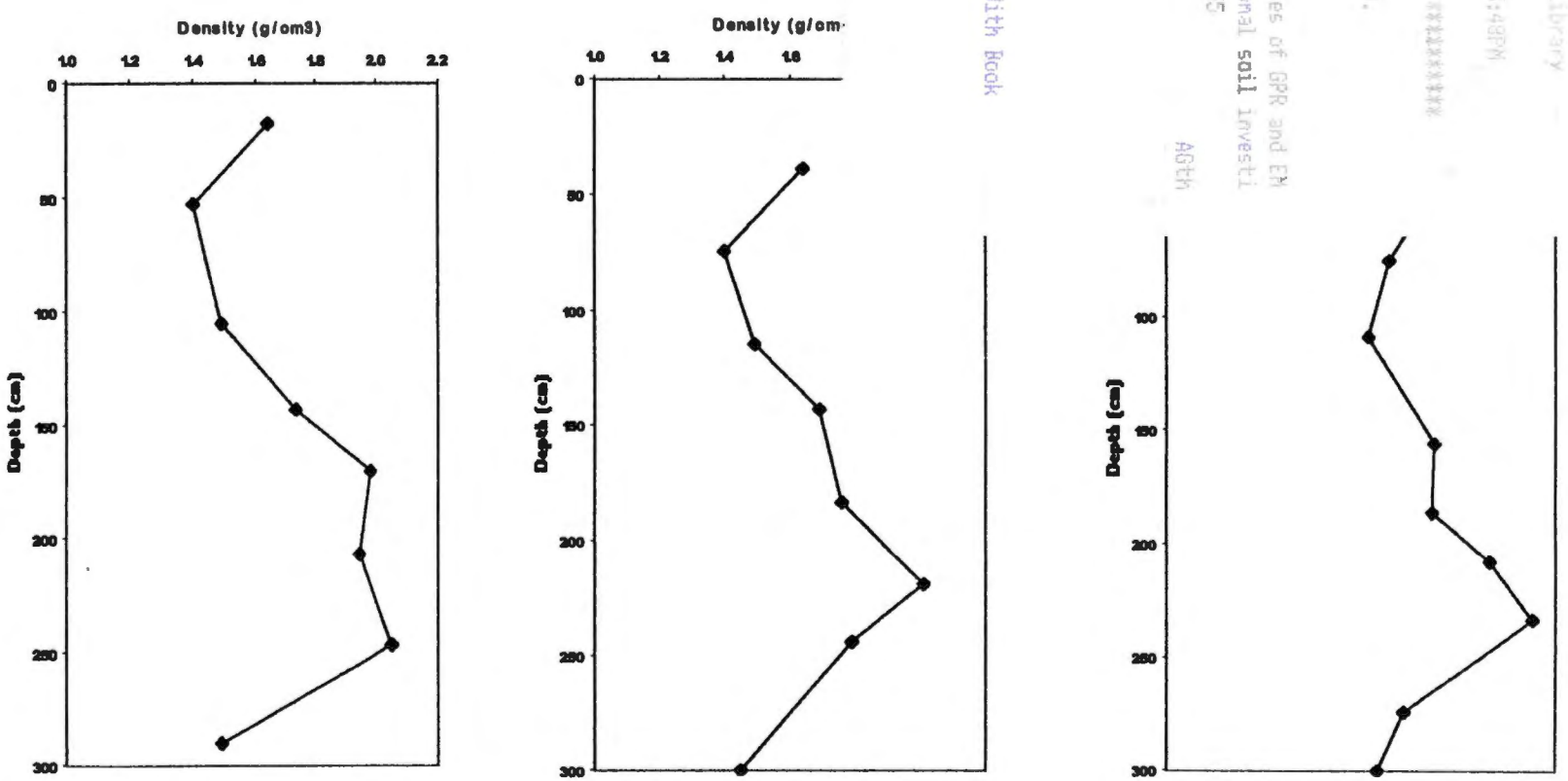


Figure 7. Bulk densities for sites one, two, and three.

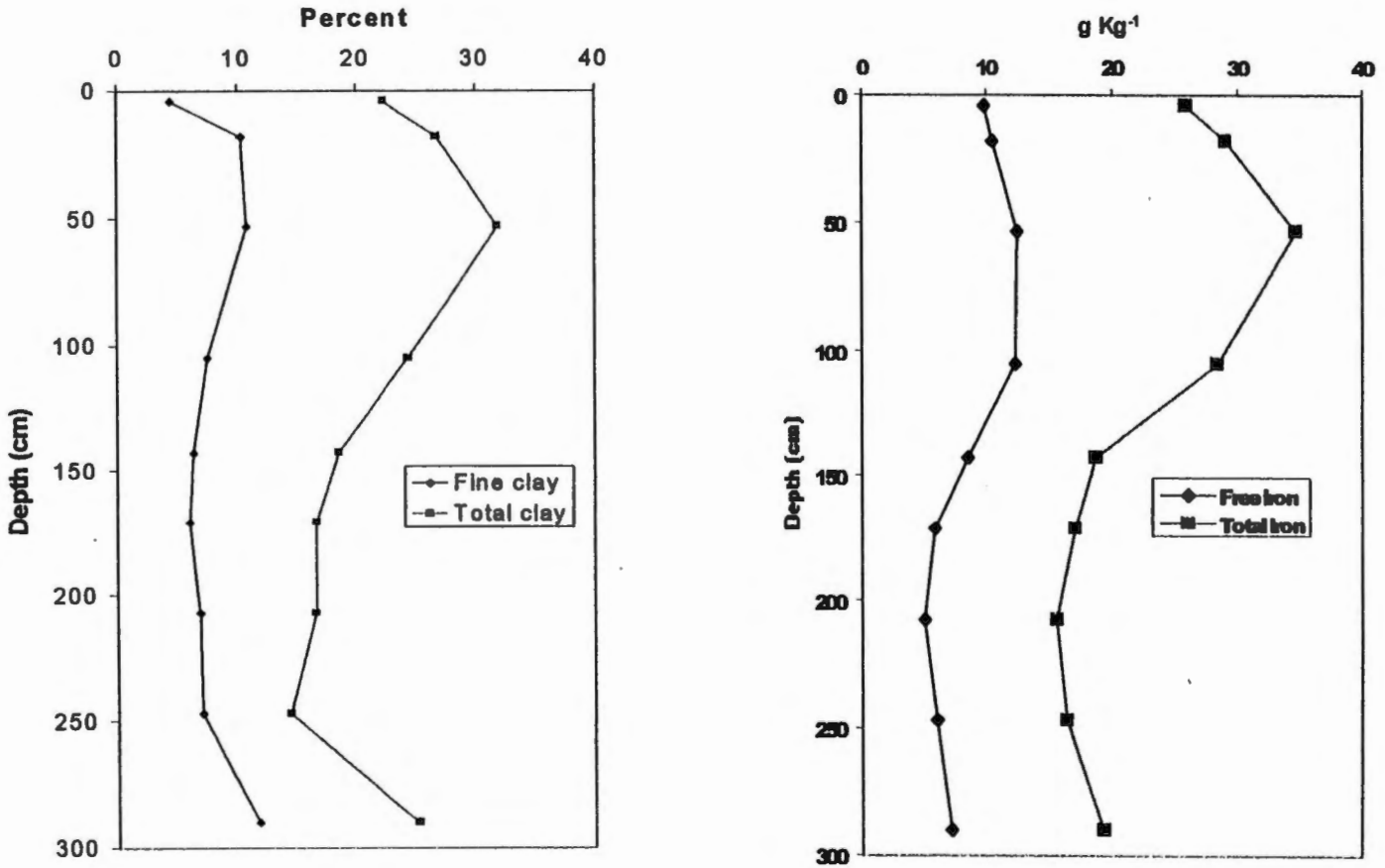


Figure 8. Plots of fine clay, total clay, free iron, and total iron for site 1.

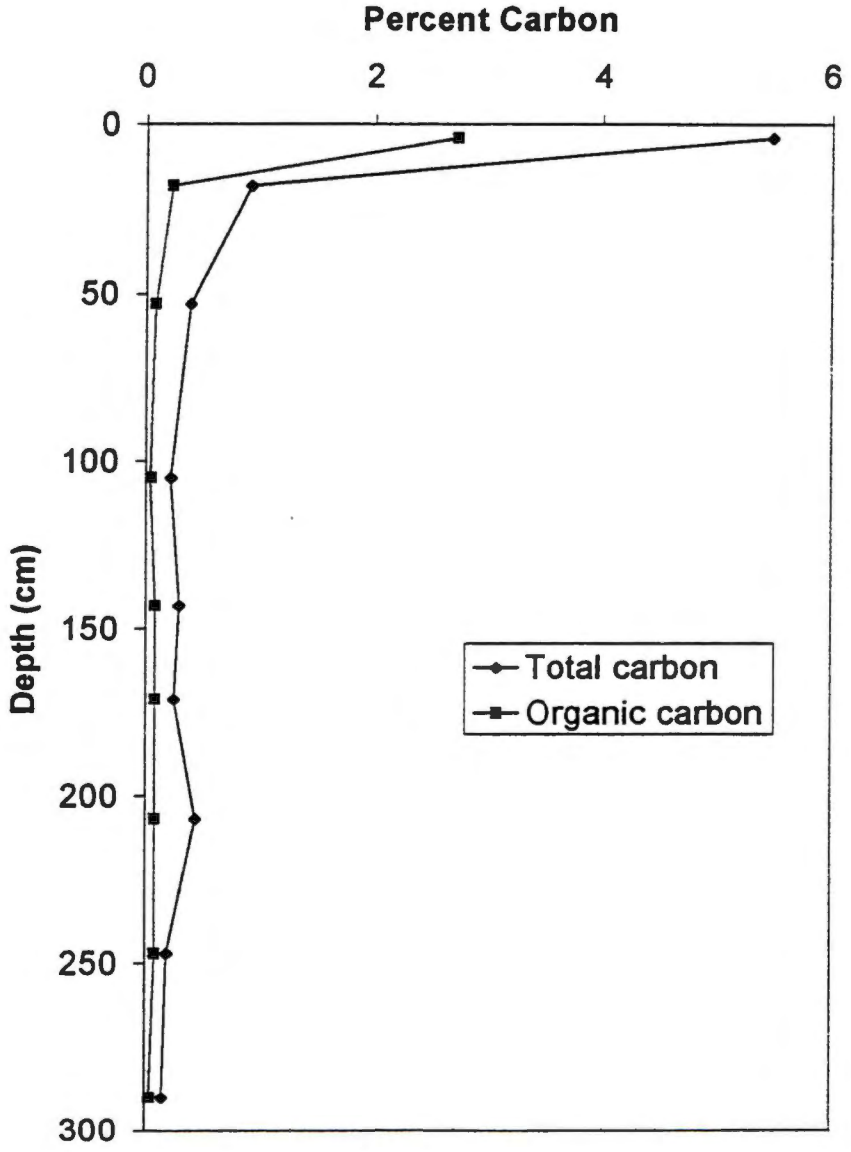


Figure 9. Plot of total and organic carbon for site 1.

discontinuity (Fig.10). Using the data obtained discrepancies within the loess were not discernable. The loess was most likely part of the Peoria deposition.

A layer of alluvium was identified from 105 cm to 247 cm. There was an irregular carbon distribution throughout this layer, which is a common characteristic of alluvial environments (Fig. 9). Total sand percentage increased with depth from 35% in the 2BC2 horizon (105 - 143 cm) to a maximum of 68.4% in the 2BC4 horizon (171 - 207 cm) before falling slightly to 65.8% in the 2BC5 horizon (207 - 247 cm) (Fig.6). The fining upward trend in the particle size data is indicative of a meandering stream depositional system. Free iron oxides and total iron concentration decreased steadily with depth until the 2BC5 horizon (171 - 207 cm), at which point there was a slight increase (Fig. 8). Bulk densities were high and increased with depth throughout this layer (Fig. 7). Abnormally high bulk densities in this zone were most likely due to compaction from the Giddings hydraulic probe, although the data in this layer were most likely influenced, they still serve to highlight differences in the soil fabric. At a depth of 247 cm below the surface there was a sharp decrease in both fine sand percentage and titanium to zirconium ratio as well as an increase in total and fine clay percentages confirming the presence of another lithologic discontinuity (Figs. 8,10).

The Tertiary aged sand began at 247 cm below the surface and extended throughout the pedon sampled. Both fine clay and total clay percentages increased sharply indicating that material has been illuviated, and thus an argillic horizon has formed at this depth (Fig. 8). This argillic horizon could have resulted from prior exposure to the surface and subsequent soil development. Bulk densities were much lower than in the

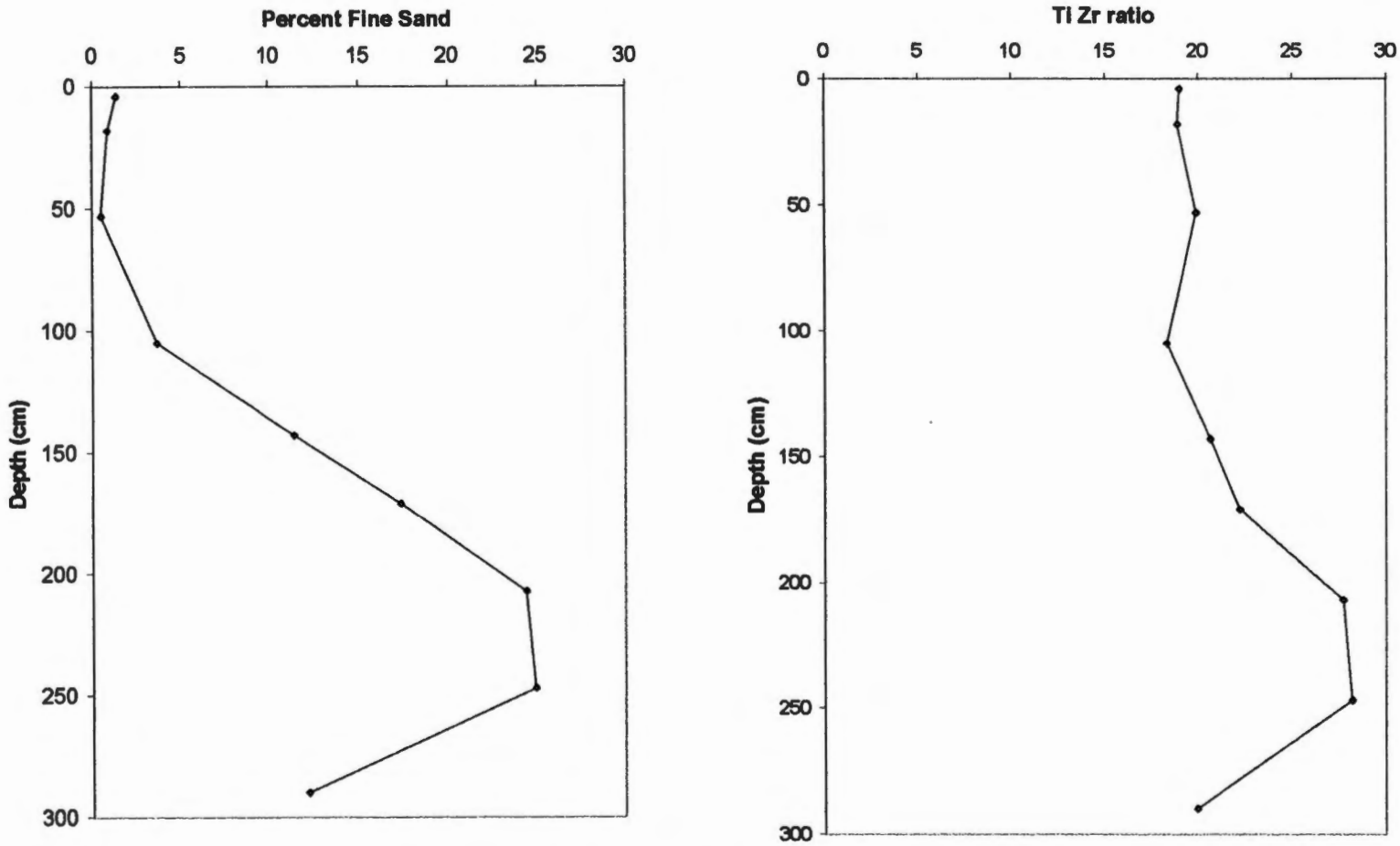


Figure 10. Plots of fine sand and titanium to zirconium for site 1.

overlying alluvium, which may be due to the higher clay content (Fig. 7). The high degree of weathering in this zone was best indicated by the soil color which was 2.5YR 4/8. This red color is influenced by the accumulation of iron oxides due to the formation of iron bearing accessory minerals.

Saturated hydraulic conductivity (K_{sat}) measurements were taken above the loess/alluvium interface, at a depth of 102 cm, and below this interface at a depth of 129 cm. K_{sat} above the interface was 0.0315 cm/ hr (fig. 11), putting it into the low K_{sat} class (Soil Survey Staff, 1993). Below the interface, the K_{sat} was 0.0558 cm hr^{-1} (Fig. 11), also in the low Ksat class (Soil Survey Staff, 1993). Although the K_{sat} values were both in the low class, it is clear that material below the interface is more conductive, and that water could be restricted above the interface. This vertical restriction of the water could possibly cause lateral water movement at this site.

The particle size control section had 9.4 percent sand and 29 percent clay, making it fine-silty (Fig. 6). Mineralogy class was mixed. The CEC/clay ratio in the control section (upper 50 cm of the argillic) was .63, putting it into the superactive cation exchange activity class. This soil had an ochric epipedon, an argillic horizon, and a base saturation by sum of cations of 35 percent at 125 cm below the top of the argillic horizon which barely makes it an alfisol. Since the base saturation by sum of cations was less than 60 percent, this site is in the Ultic subgroup of the alfisol order. This site was classified as a Fine-silty, mixed, superactive, thermic Ultic Hapludalf.

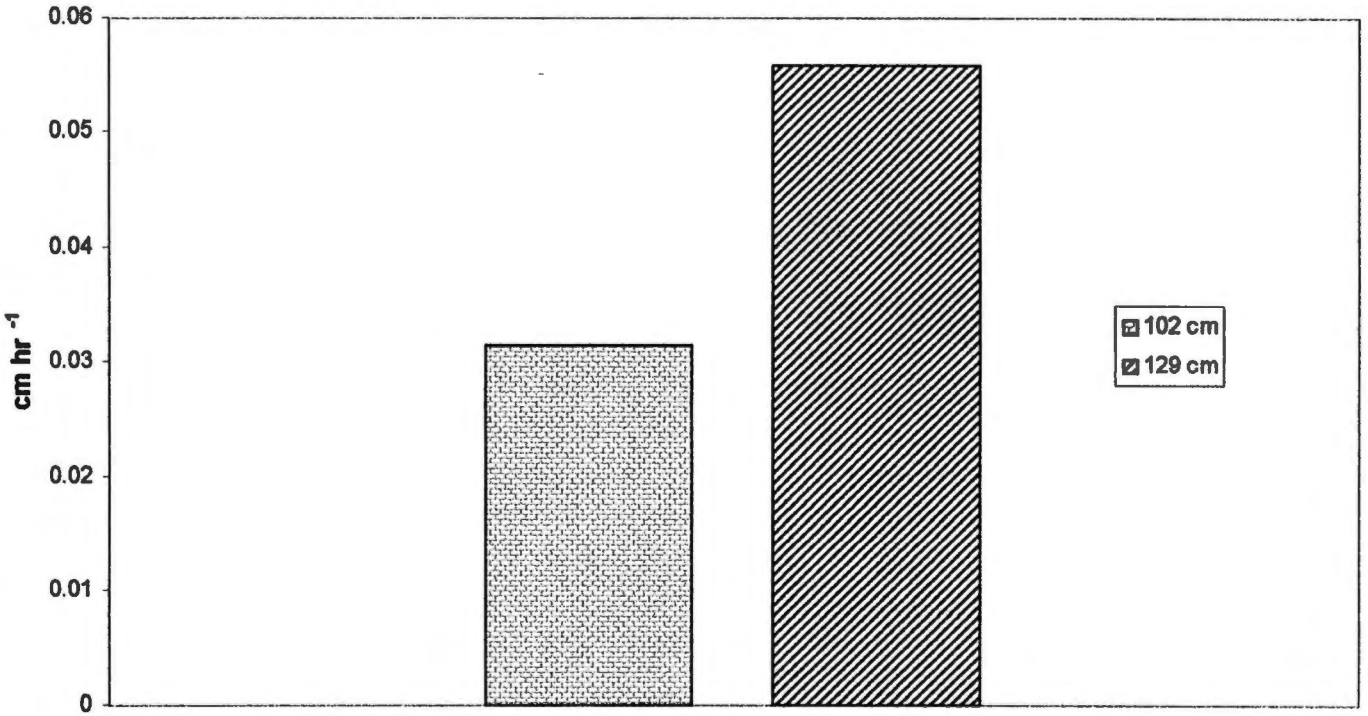


Figure 11. Graph of saturated hydraulic conductivity values at 102-cm and 129-cm depths for site 1.

Site Two

Site two was located at N 35° 8' 4.6", W 89°13' 23.8" on an upland position under a forage cropping system at an elevation of 164.75 meters above mean sea level. Soil morphology was sampled and described to a depth of 300 cm. The parent material sequence was loess over alluvium over Tertiary aged sand.

Loess was identified from the surface to a depth of 115 cm. Like site one, soil color throughout this layer was 7.5YR 4/4 except for the Ap horizon, which was influenced by organic matter accumulation and was 10YR 4/4. Silt percentages ranged from 74 % to 58.6 % (Fig.12). There was a slight bulge in both free iron oxide concentration and total iron in the Bt2 horizon (39 - 74 cm), indicating a typical weathering pattern as in site one (Fig.13). A bulge in both fine and total clay percentage was seen in the first Bt1 horizon (5 - 39 cm), before falling steadily throughout the remainder of the loess (Fig.13), indicating active illuviation of material. Both total and organic carbon decreased regularly below the Ap horizon with depth throughout the upper 115 cm (Fig.14). Bulk density values were similar to site one, with the highest value in the Bt1 horizon (5 - 39 cm) (Fig. 7). Again, it is likely that the upper horizons have been compacted by vehicles. A sharp increase in fine sand percentage and titanium to zirconium ratio in the BC1 horizon (74 - 115 cm) suggests a lithologic discontinuity (Fig.15). Like site one, using the methods employed only one loess deposition was identified. This was most likely part of the Peoria loess deposit.

An alluvial layer was present from 115 cm to 244 cm. As in site one, a slightly irregular carbon distribution was present in this zone, indicating a cyclic depositional

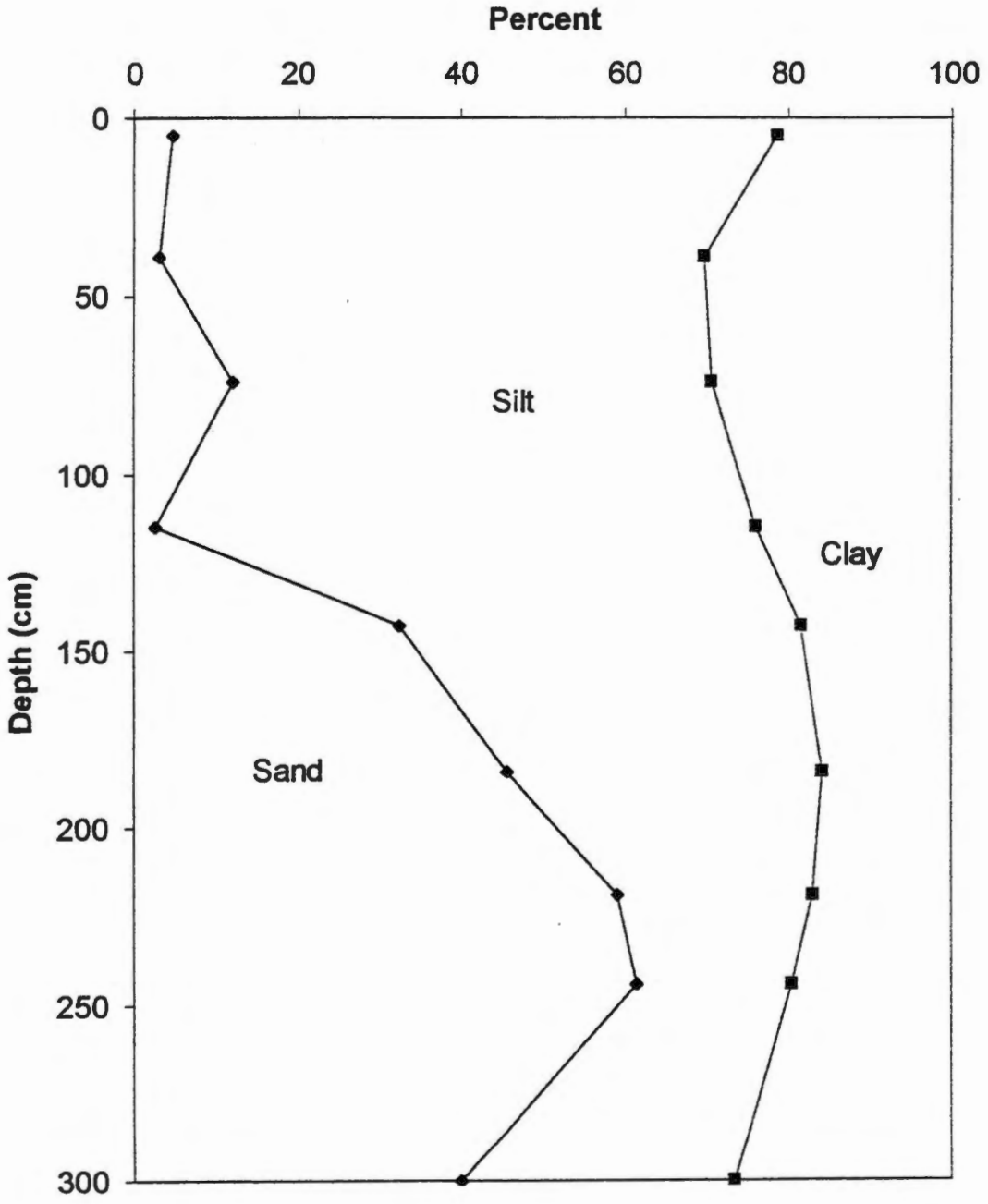


Figure 12. Cumulative particle size plot for site 2.

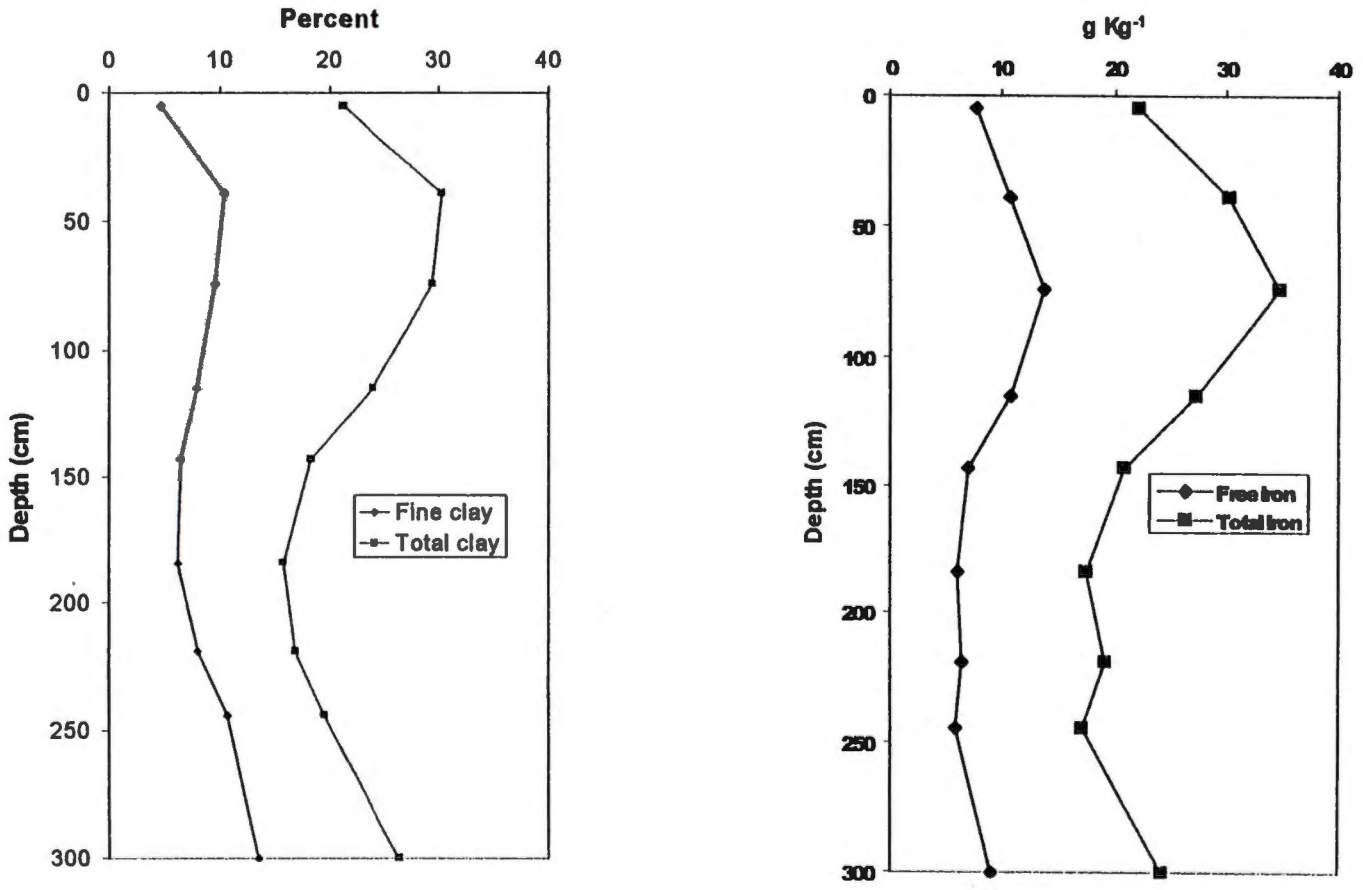


Figure 13. Plots of fine clay, total clay, free iron, and total iron for site 2.

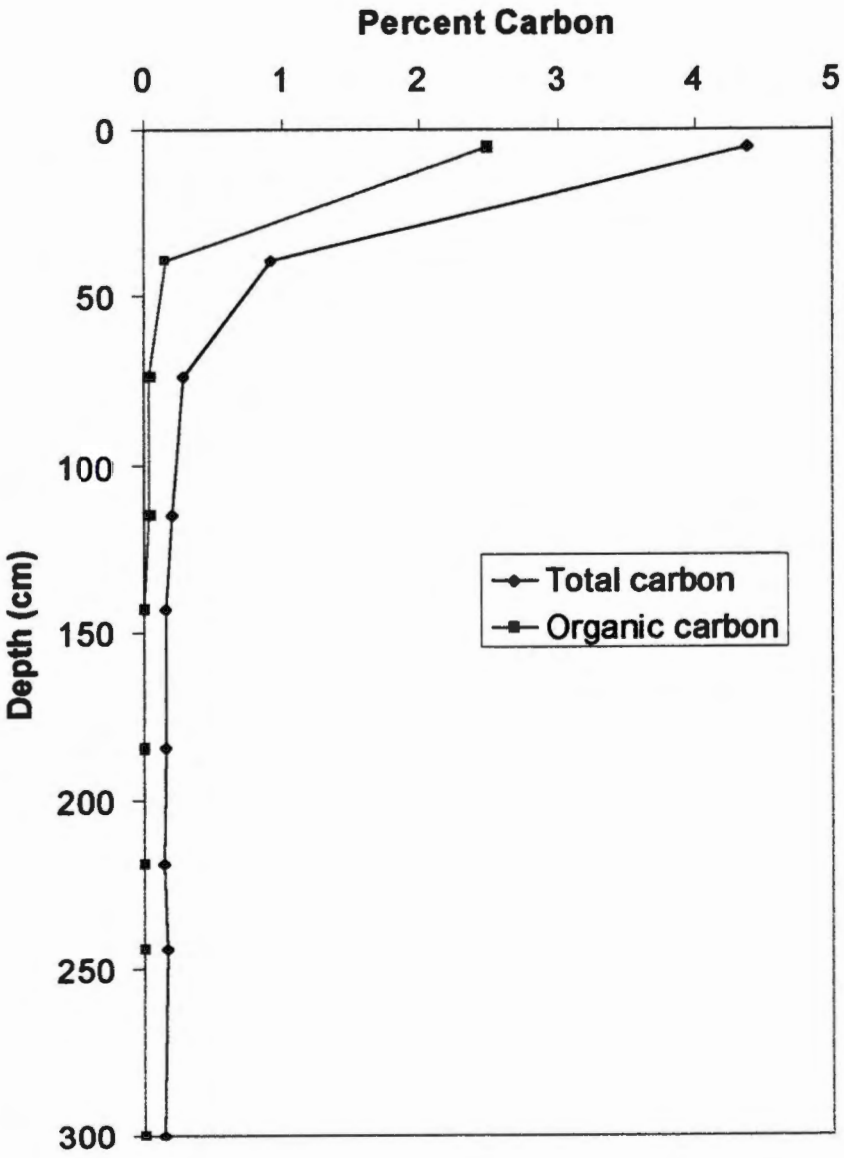


Figure 14. Plot of total and organic carbon for site 2.

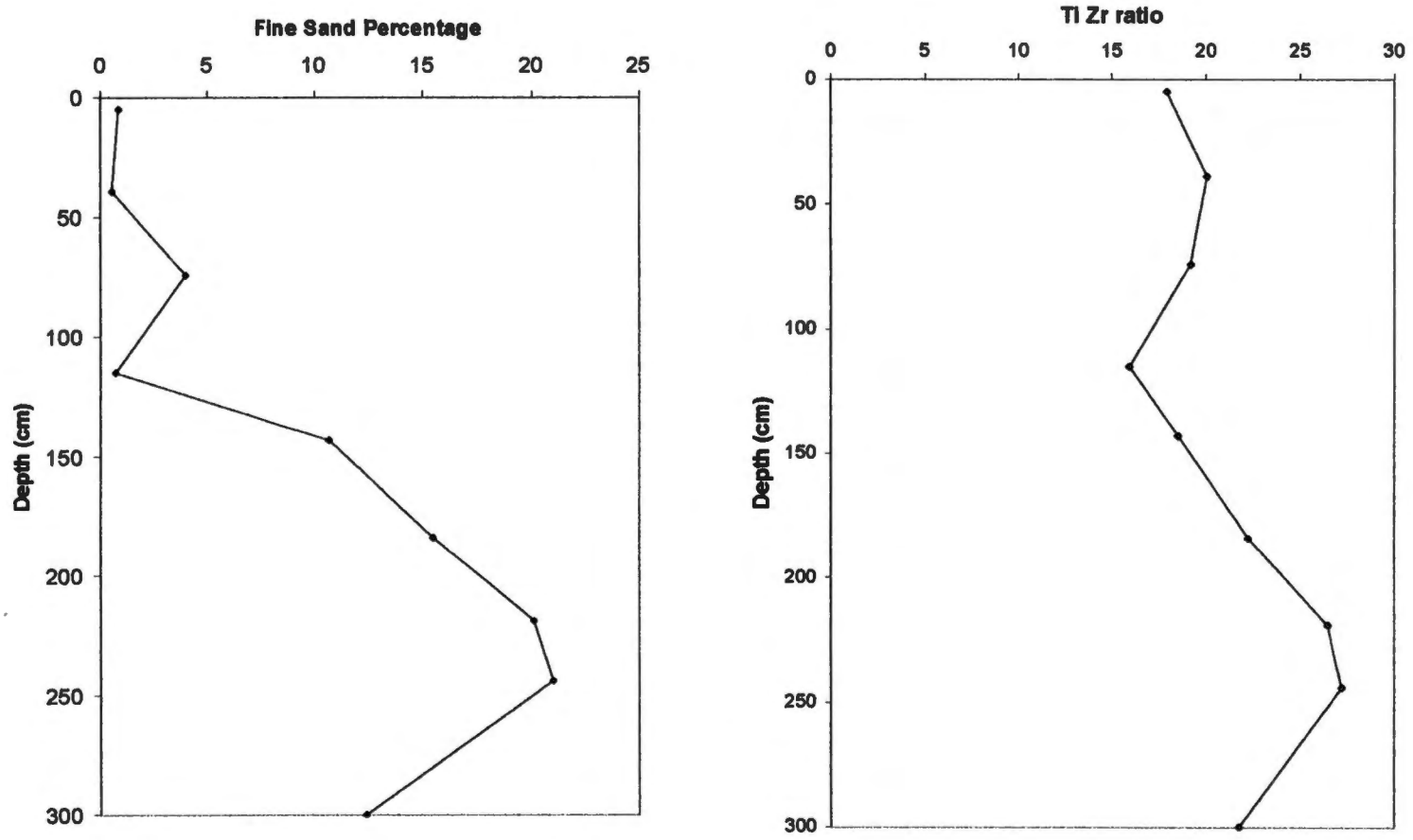


Figure 15. Plots of fine sand and titanium to zirconium for site 2.

environment (Fig.14). A fining upward sequence was present as in site one. Both fine sand and total sand percentages increased with depth to maximums of 21% and 61.5%, respectively (Figs.12,15). Both free iron oxide and total iron concentration throughout this layer was irregular, further indicating discontinuous weathering (Fig.13). Bulk densities were much higher than in the loess, most likely due to a combination of compaction from the Giddings probe and the sandier textures (Fig. 7). At a depth of 244 cm, there was a distinct reduction in fine sand percentage, titanium to zirconium ratio and a subsequent increase in total clay percentage, indicating a second lithologic discontinuity (Figs.13,15).

Tertiary sand was identified at 244 cm below the surface to the extent of the core sampled. Total sand percentage decreased significantly, while both fine and total clay percentages increased (Figs.12,13). As in site one, the clay increase was greater than 20%, making this argillic horizon. This argillic horizon could a result of this material being exposed to the surface prior to the alluvial processes taking place. Bulk density values were much lower than in the alluvium (Fig. 7). As seen in site one, the formation of iron bearing accessory minerals from weathering has influenced the soil color, making it a 2.5YR 4/8.

Saturated hydraulic conductivity measurements were made above and below the loess/alluvium interface at depths of 113 cm and 129 cm, respectively. In the zone above the interface (113 cm), the K_{sat} was 0.03280 cm/hr (Fig. 16), which is in the low Ksat class according to the USDA (Soil Survey Staff, 1993). Below the interface, the K_{sat} was 0.04435 cm hr^{-1} (Fig. 16), also in the low K_{sat} class (Soil Survey Staff, 1993). The soil

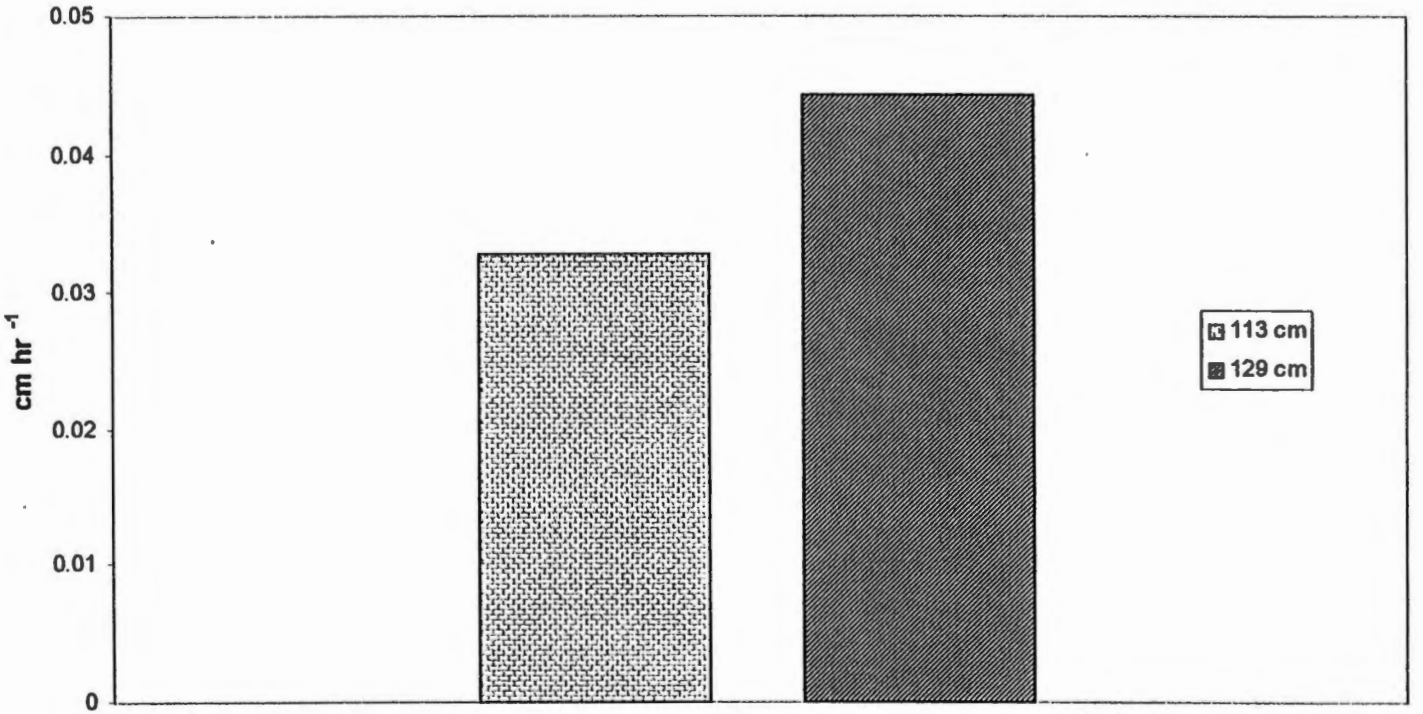


Figure 16. Graph of hydraulic conductivity values at 113-cm and 129-cm depths for site 2.

above the interface is slightly less conductive than the material below. Although this discrepancy is not as great as in site one, it could still result in lateral water movement

The particle size control section had 7.6 percent sand and 29.9 percent clay, making it fine-silty (Fig. 12). In the control section, mineralogy is mixed. The CEC/clay ratio was .43, putting it into the active cation exchange activity class. Site two had an ochric epipedon, an argillic subsurface horizon with a base saturation (sum of cations) at 125 cm below the top of the argillic of 35.3 percent, making this soil an alfisol. It is in the Ultic subgroup of the alfisol order because the base saturation by sum of cations was less than 60 percent. Site two was classified as a Fine-silty, mixed, active, thermic Ultic Hapludalf.

Site three

Site three was located at N 35° 8' 4.2", W 89° 13' 24.2" on an upland position under a forage cropping arrangement, at an elevation of 164.39 meters above mean sea level. Soil morphology was sampled and described to a depth of 300 cm. The parent material sequence was loess over alluvium over Tertiary aged sand.

Loess was present in the upper 109 cm of the core described. Soil color below the Ap horizon alternated between 7.5YR 4/6 and 7.5YR 4/4 throughout the layer. Silt percentage ranged from 72.3 % in the Ap horizon to 66.2 % in the underlying Bt1 horizon (Fig. 17). There was a slight bulge in free iron oxide concentration in the first Bt1 horizon (5-36 cm) before tapering off steadily throughout the remainder of the loess (Fig. 18), indicating typical weathering. This free iron oxide bulge coincided with a bulge in both total and fine clay percentages (Fig. 18). Total and organic carbon percentages decreased

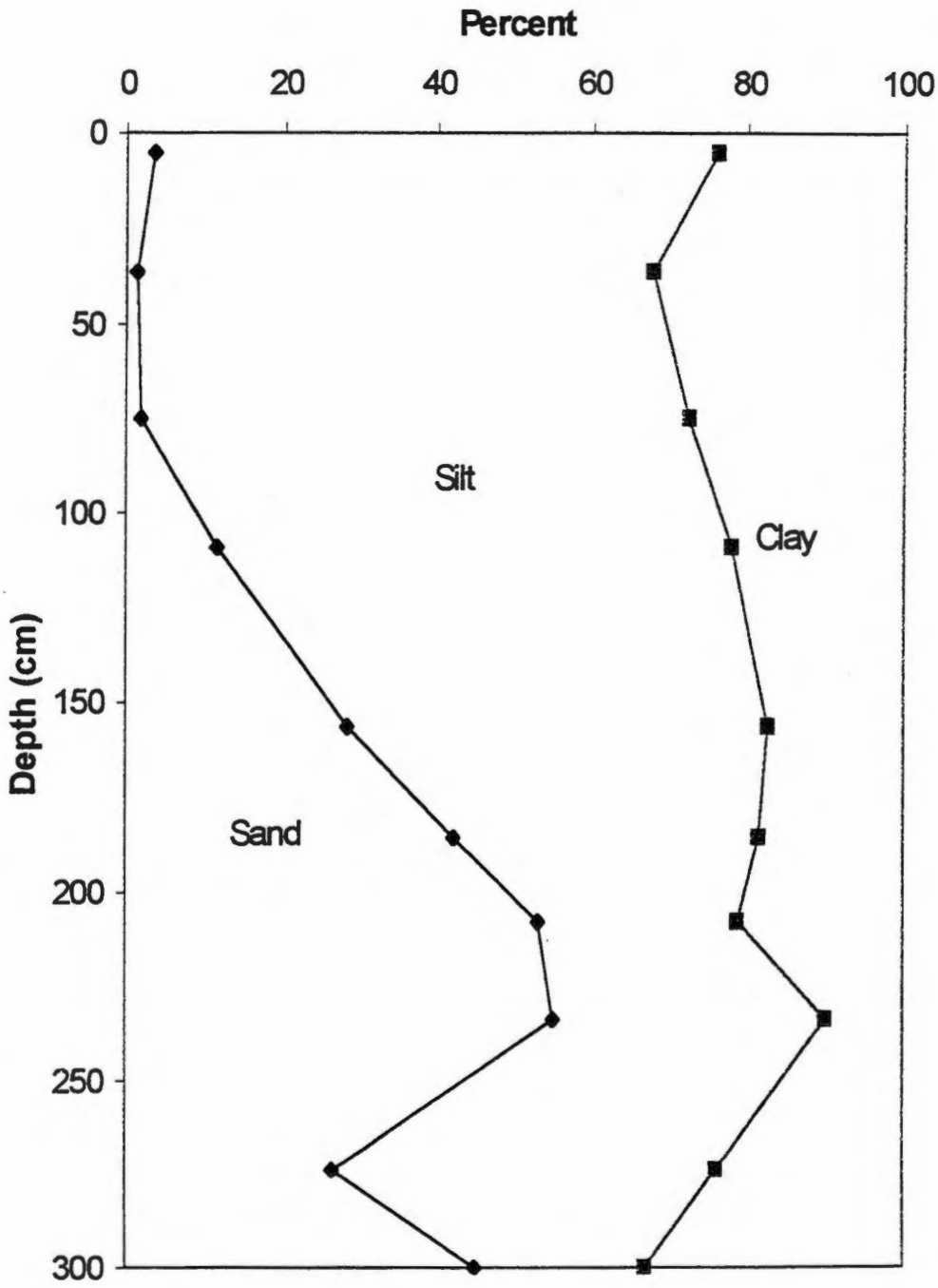


Figure 17. Cumulative particle size plot for site 3.

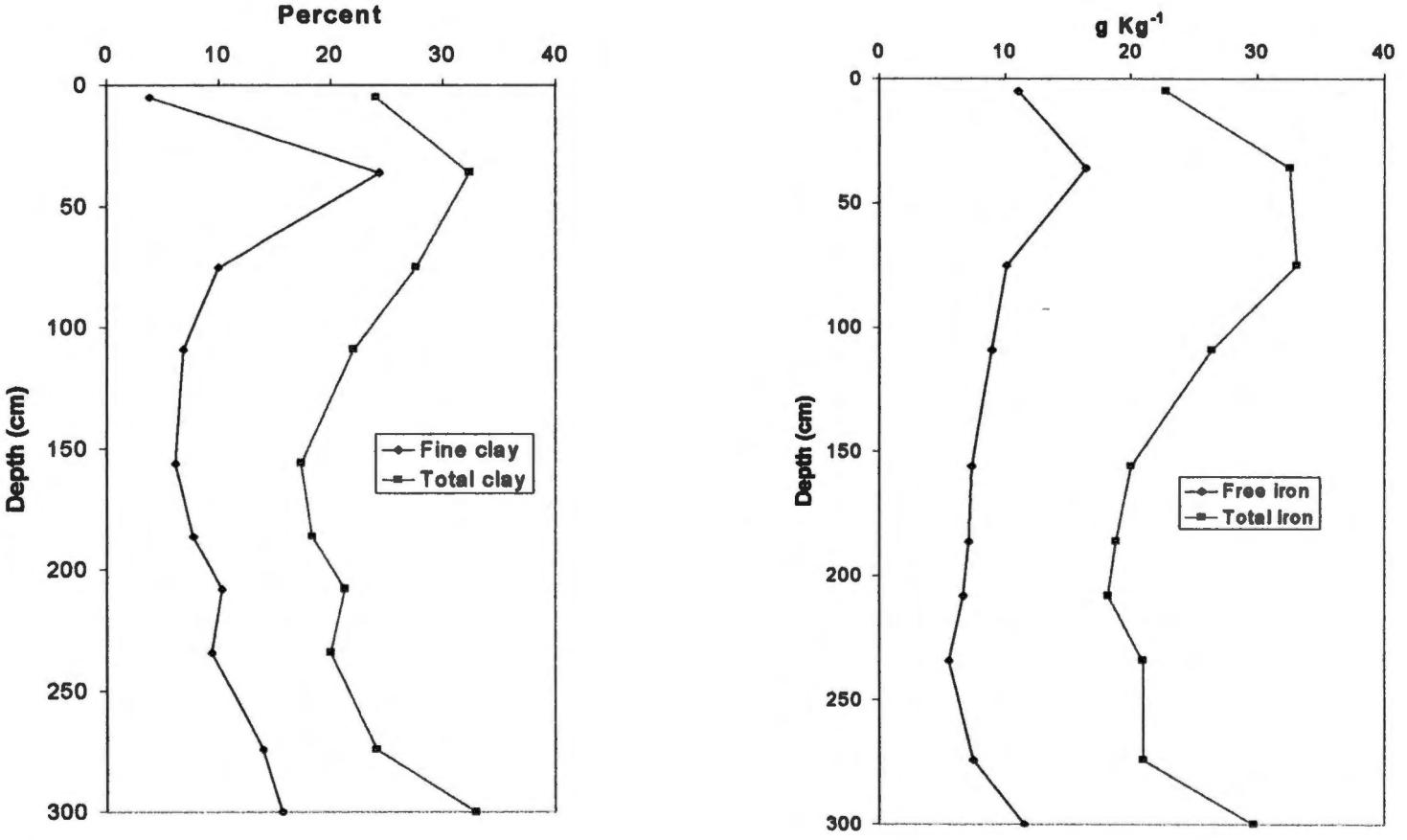


Figure 18. Plots of fine clay, total clay, free iron, and total iron for site 3.

rapidly with depth below the Ap horizon, as would be expected (Fig. 19). Bulk density was highest in the Bt1 horizon, as in sites one and two (Fig. 7). There was a marked increase in fine sand percentage between 109 cm and 156 cm indicating a change in parent material sequence (Fig. 20). No salient discrepancies were detected within the loess. Any loess deposited prior to the loess observed was likely truncated by erosion. The loess described was most likely part of the Peoria loess deposition.

Alluvium was present from 109 cm to 234 cm. Both total carbon and organic carbon had a slightly irregular distribution, as seen in the previous sites (Fig. 19). Again, an irregular carbon distribution could be due to a series of depositions, as one would observe in an alluvial depositional environment. Both total and fine sand percentages increased with depth (Figs. 17, 20). Sand percentage ranged from 28.3 % in the 2BC2 horizon (109 - 156 cm) to 55.2 % in the 2BC5 horizon (208 - 234 cm) (Fig. 17). As in sites one and two, this was a fining upward sequence, indicating a meandering stream system. Free iron oxides decreased steadily throughout the alluvium, as did the total iron concentration (Fig. 18). Bulk densities were much higher than seen in the overlying loess, possibly due to compaction from the hydraulic soil probe (Fig. 7). Fine sand percentage dropped over 50% between 234 cm and 274 cm, while the titanium to zirconium ratio dropped noticeably, marking the second lithologic discontinuity (Fig. 20).

Tertiary sands were found from 234 cm to the extent of the core sampled. Total clay and fine clay percentages increased significantly and an argillic horizon was present, likely from previous exposure to the surface (Fig. 18). Free iron oxides and total iron increased with depth (Fig. 18). Bulk densities were much lower than in the alluvium above, probably due to the increased porosity associated with more clayey materials (Fig.

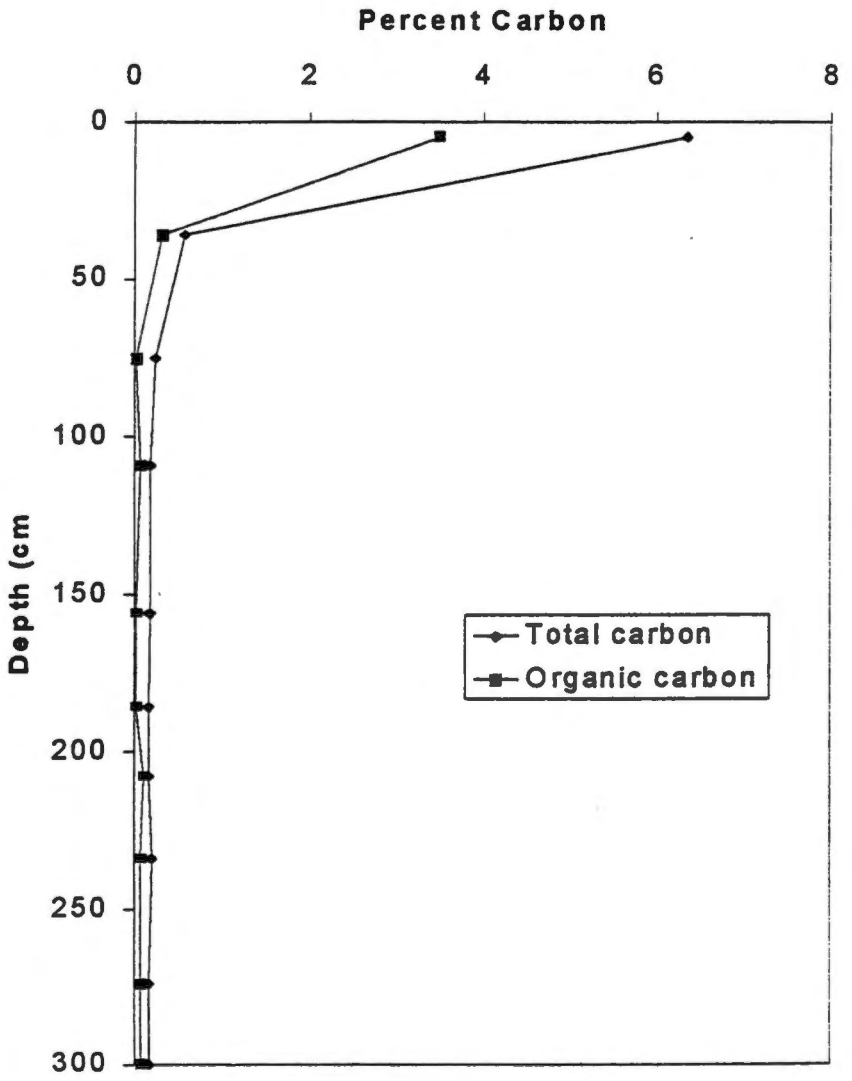


Figure 19. Plot of total and organic carbon for site 3.

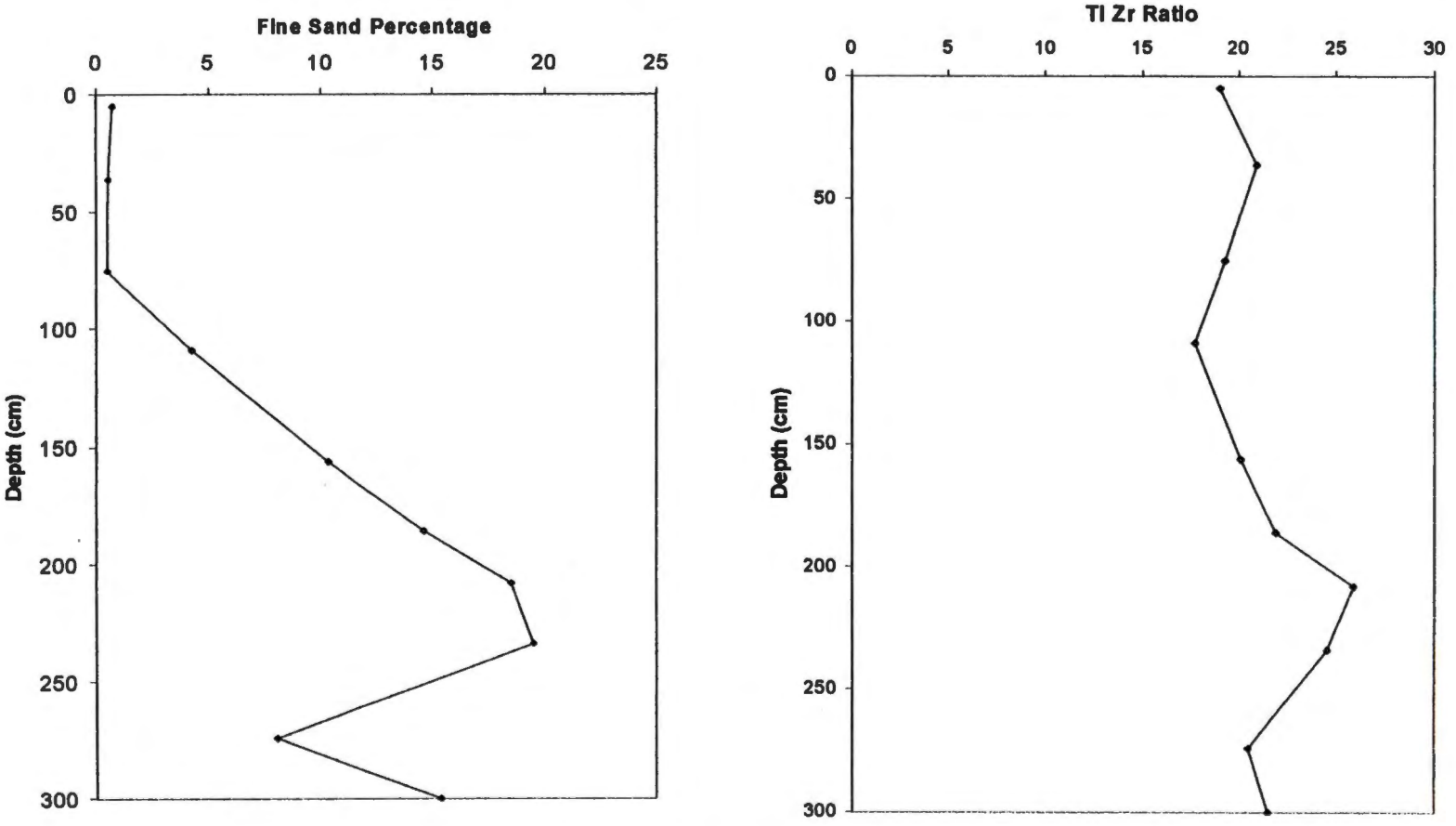


Figure 20. Plots of fine sand and titanium to zirconium for site 3.

7). Soil color was 2.5YR 4/8 throughout the portion sampled.

Saturated hydraulic conductivity measurements were made above the loess/alluvium interface at 102 cm, and below the interface at 135 cm. Above the interface the K_{sat} was 0.01474 cm/hr (Fig. 21), putting it into the low K_{sat} class (Soil Survey Staff, 1993). Below the interface, the K_{sat} was 0.06225 cm/hr (Fig. 21), again, low according to the USDA K_{sat} classes (Soil Survey Staff, 1993). The horizon above the loess/alluvium interface was much less conductive than the underlying horizon. This restriction probably results in some lateral water movement above the interface.

The particle size control section had 1.74 percent sand and 29.9 percent clay, making it be fine-silty (Fig. 17). Mineralogy was determined to be mixed. The CEC/clay ratio in the control section (upper 50 cm of the argillic) was .59, putting it into the active cation exchange capacity class. This soil had an ochric epipedon, an argillic sub-surface horizon, and a base saturation of 38 percent by sum of cations at 125 cm below the top of the argillic horizon, making this soil an alfisol. Since the base saturation was less than 60 percent in the control section, this soil is in the Ulitc subgroup. Site three was classified as a Fine-silty, mixed, active, thermic Ultic Hapludalf.

Site four

Site four was located at N 35° 8' 4.5", W 89° 13' 23", on an upland position under a forage cropping system, at 165.76 meters above mean sea level. Soil morphology was sampled and described to a depth of 247 cm. The parent material sequence was loess over alluvium over Tertiary sand.

A loess layer was identified from the surface to a depth of 114 cm. Below the Ap

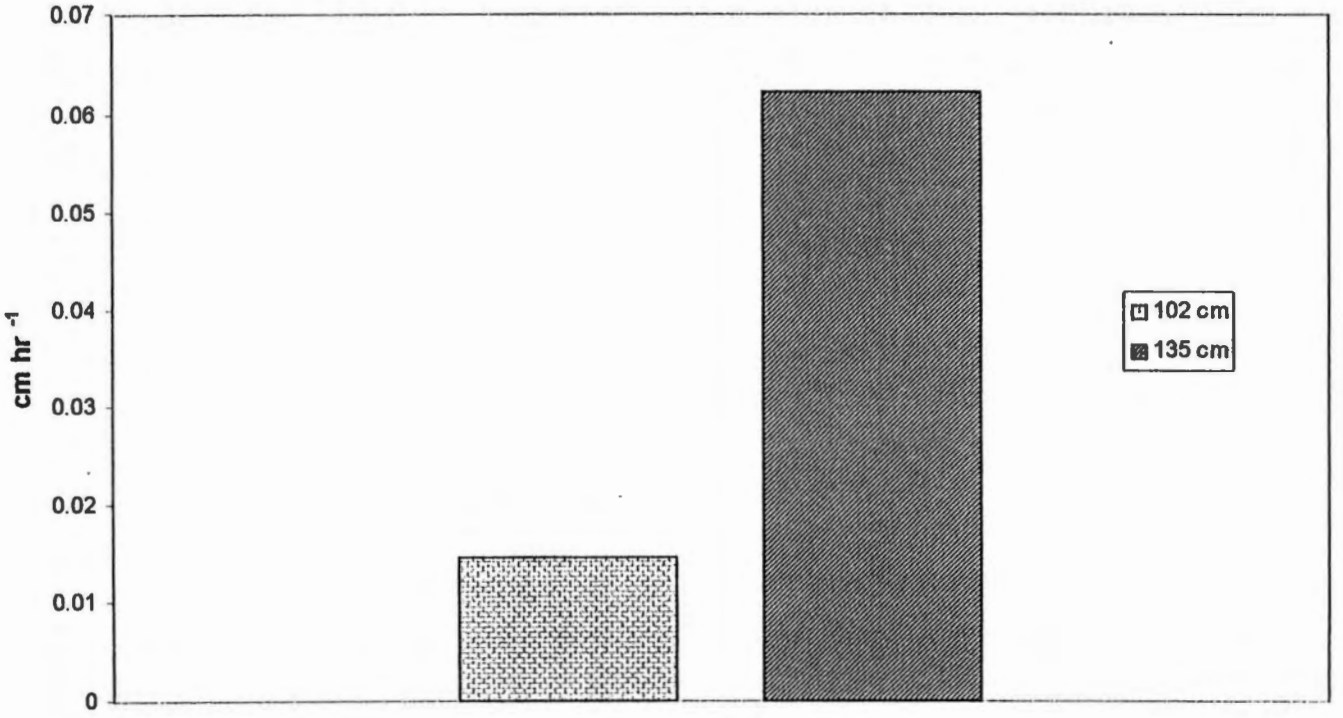


Figure 21. Graph of hydraulic conductivity values at 102-cm and 135-cm depths for site 3.

horizon, the soil color was 7.5YR 4/6 throughout most of the loessr. Total silt percentage ranged from 73.3 % in the Ap horizon to 57.7 % in the BC2 horizon (87 - 114 cm) (Fig. 22). As in the other sites, bulk density was highest in the Bt1 horizon, most likely a result of the overlying parking lot (Fig. 23). There was a bulge in both free iron oxide and total iron concentration in the Bt2 horizon (26 - 60 cm), before falling throughout rest of the layer (Fig. 24). The iron bulge coincided with a bulge in both total and fine clay, which indicates that this soil is pedogenically mature (Fig. 24). Total and organic carbon decreased steadily below the Ap horizon (Fig. 25). Fine sand percentage increased significantly while there was a slight increase in the titanium to zirconium ratio in the BC2 horizon (87 - 114 cm), indicating a change in parent material (Fig. 26). Discrepancies within the loess that could indicate more than one deposit were not identifiable using the data collected. The loess present is most likely the Peoria.

An alluvial layer was identified from 114 cm through the extent of the core sampled. There was a fining upward sequence throughout the alluvial layer, both total sand and fine sand percentages increased with depth, indicating a meandering stream system (Figs. 22,26). Free iron oxides and total iron decreased with depth throughout the alluvium (Fig. 24). Bulk density values were much higher than in the loess, most likely from both the compaction from the hydraulic probe and the material being more sandy and thus less porous (Fig. 23). Total and organic carbon percentages were somewhat capricious in the alluvial layer (Fig. 25). Like the previous sites, this was likely due to multiple depositions over time.

Saturated hydraulic conductivity was measured above and below the loess/alluvium interface at depths of 101 cm and 116 cm, respectively. Above the

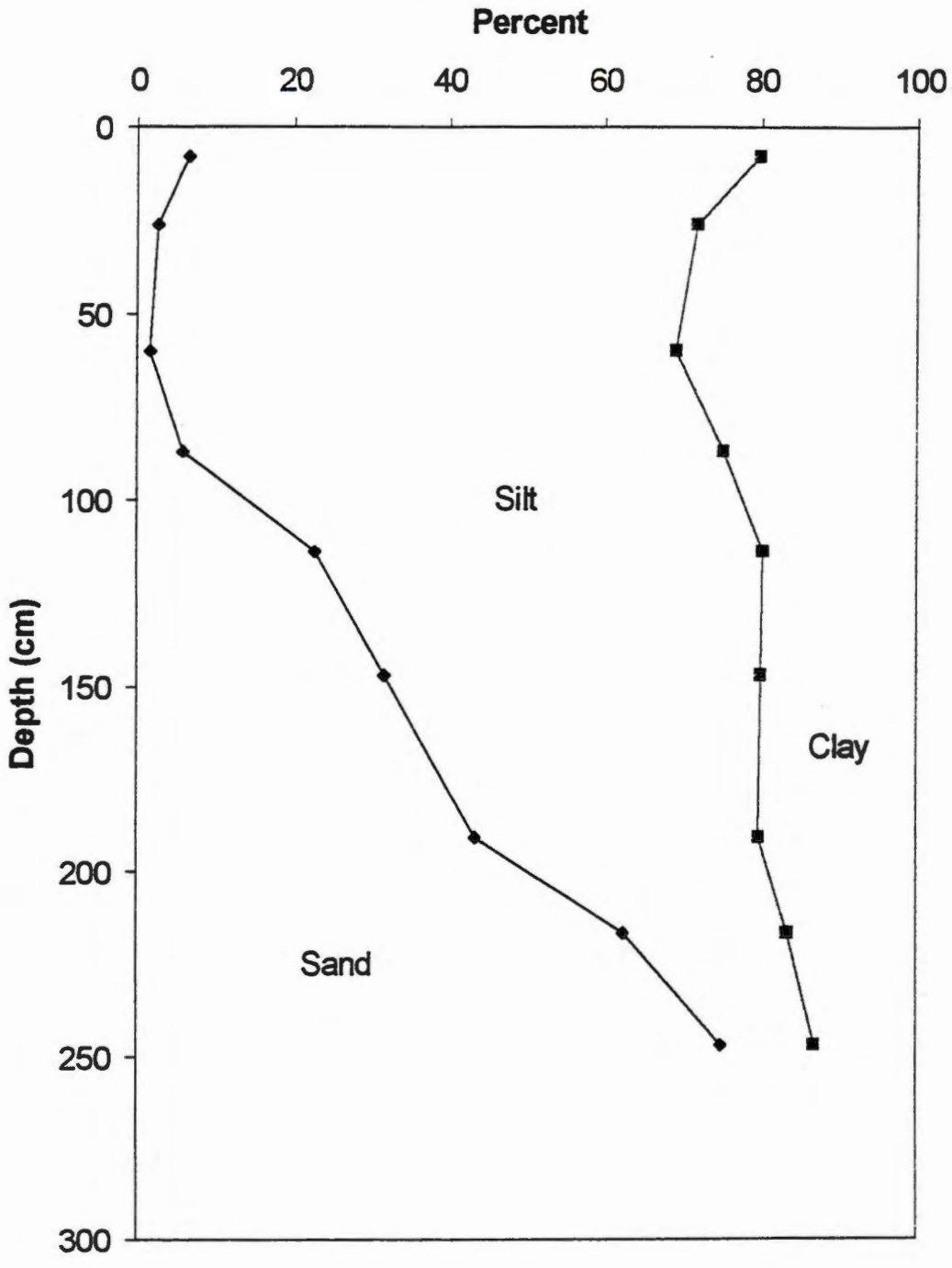
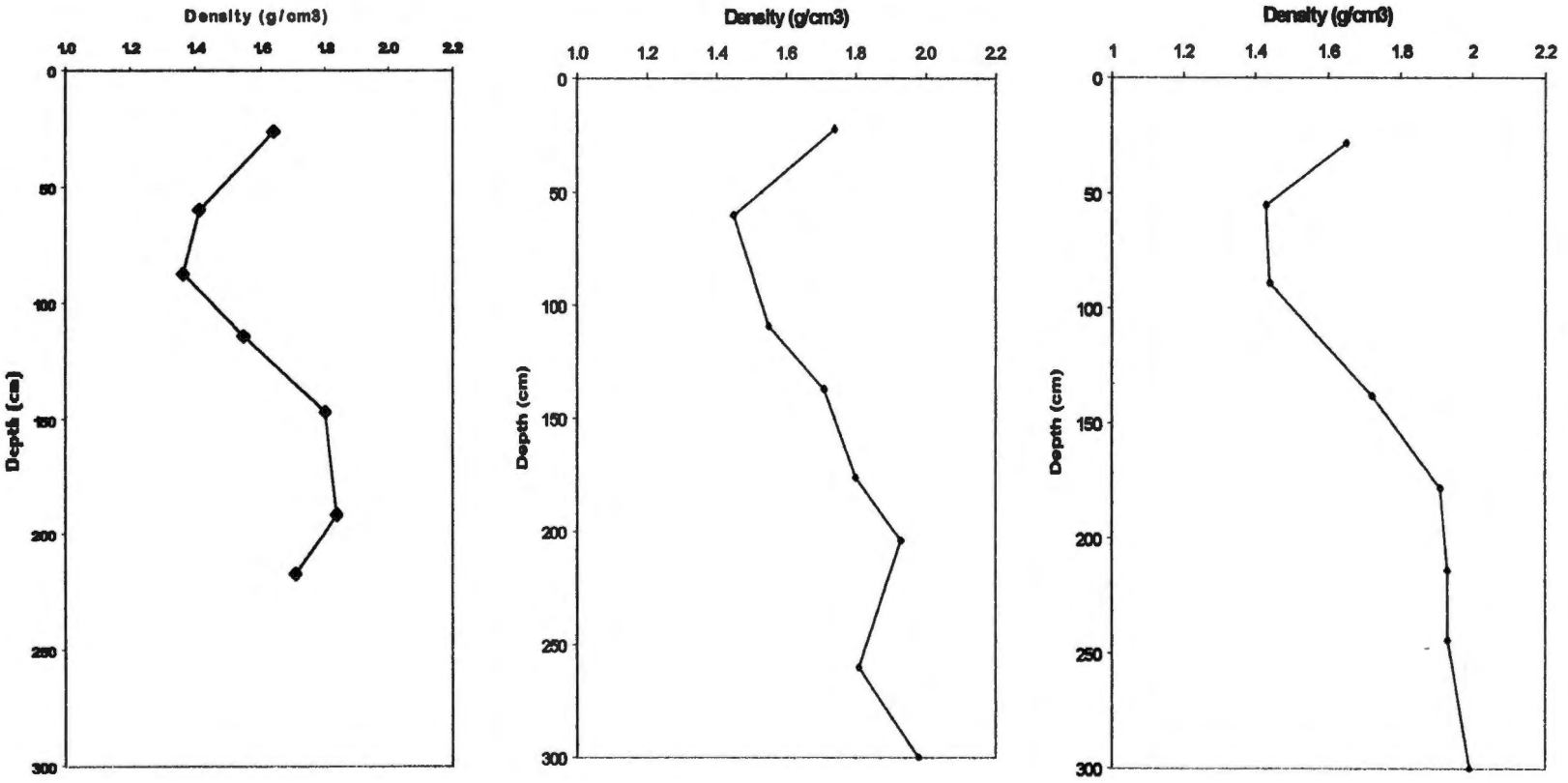


Figure 22. Cumulative particle size plot for site 4.



Site four. Site five. Site six.

Figure 23. Bulk densities for sites four, five, and six.

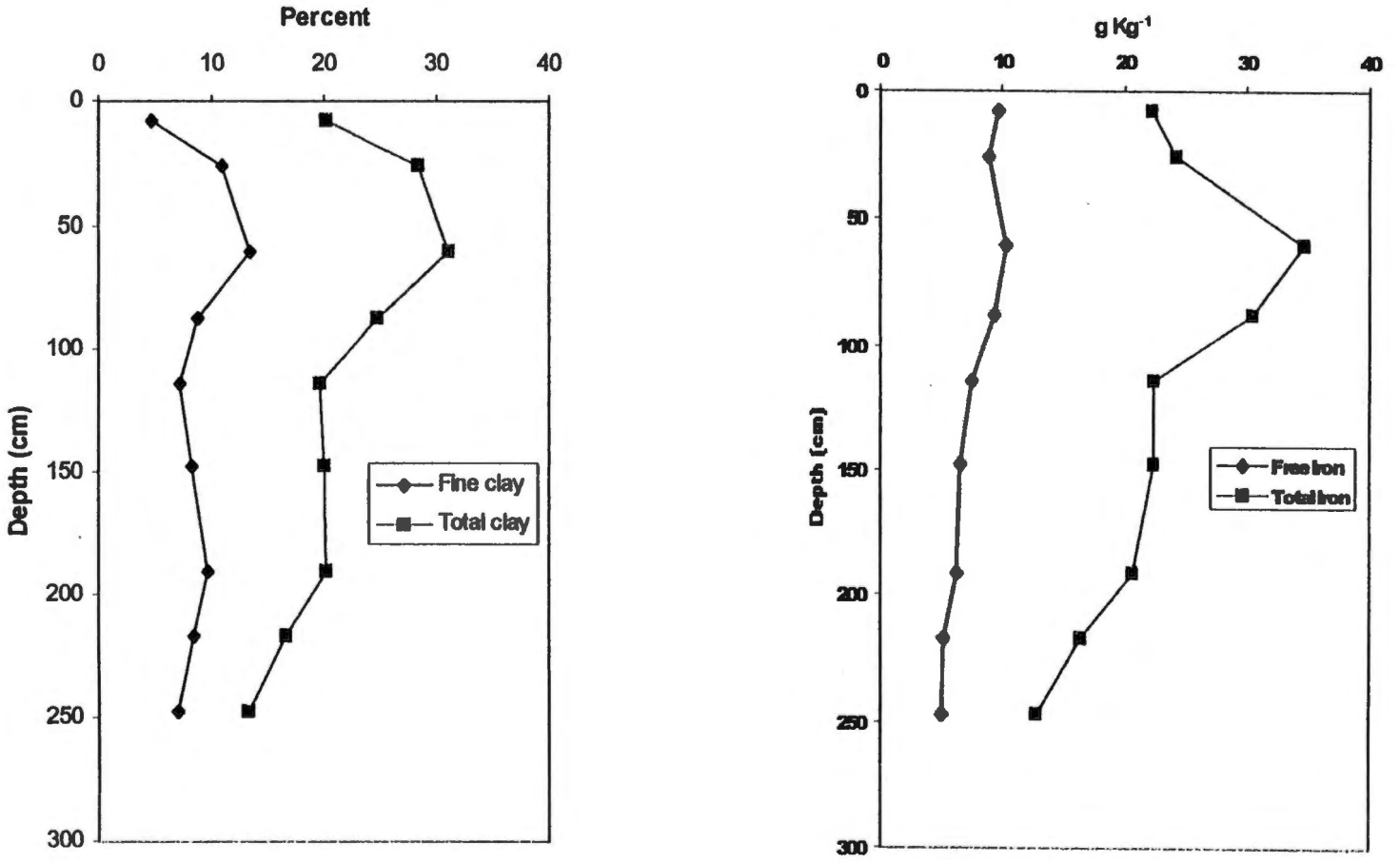


Figure 24. Plots of fine clay, total clay, free iron, and total iron for site 4.

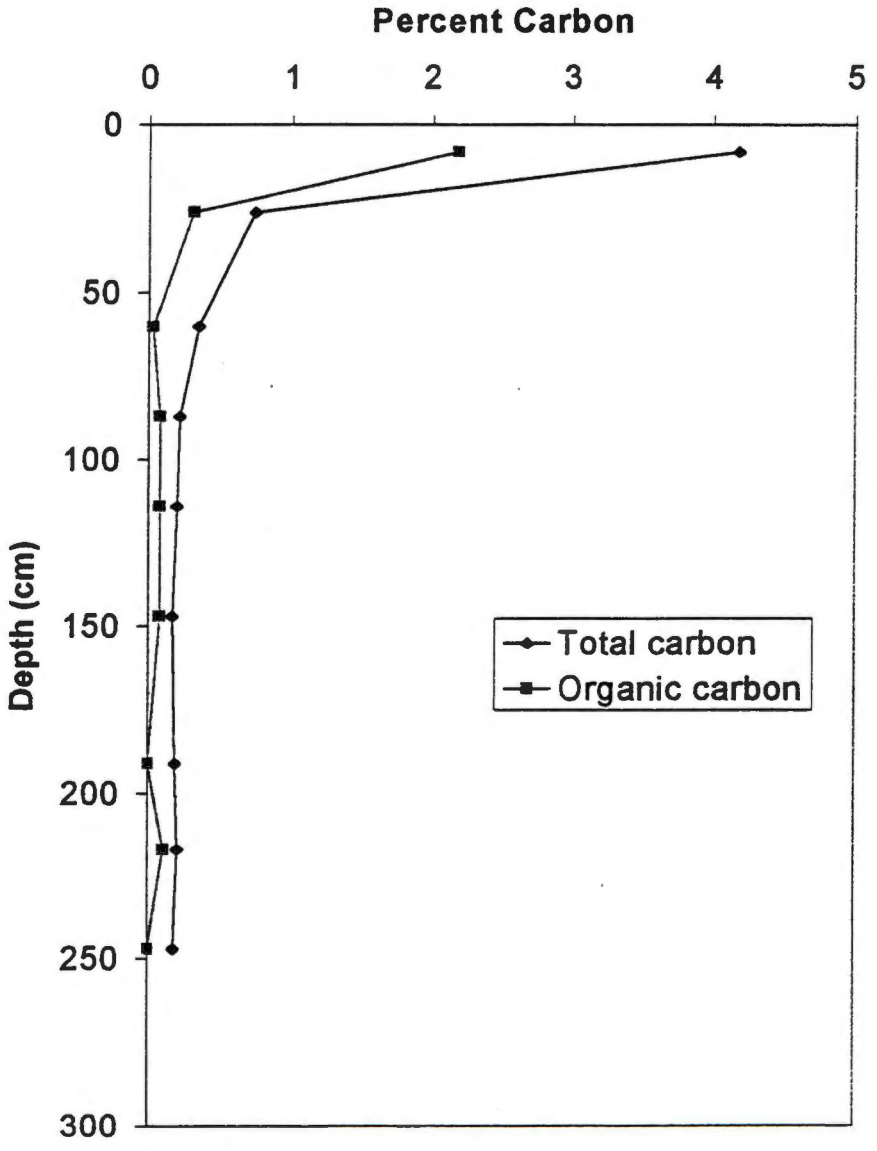


Figure 25. Plot of total and organic carbon for site 4.

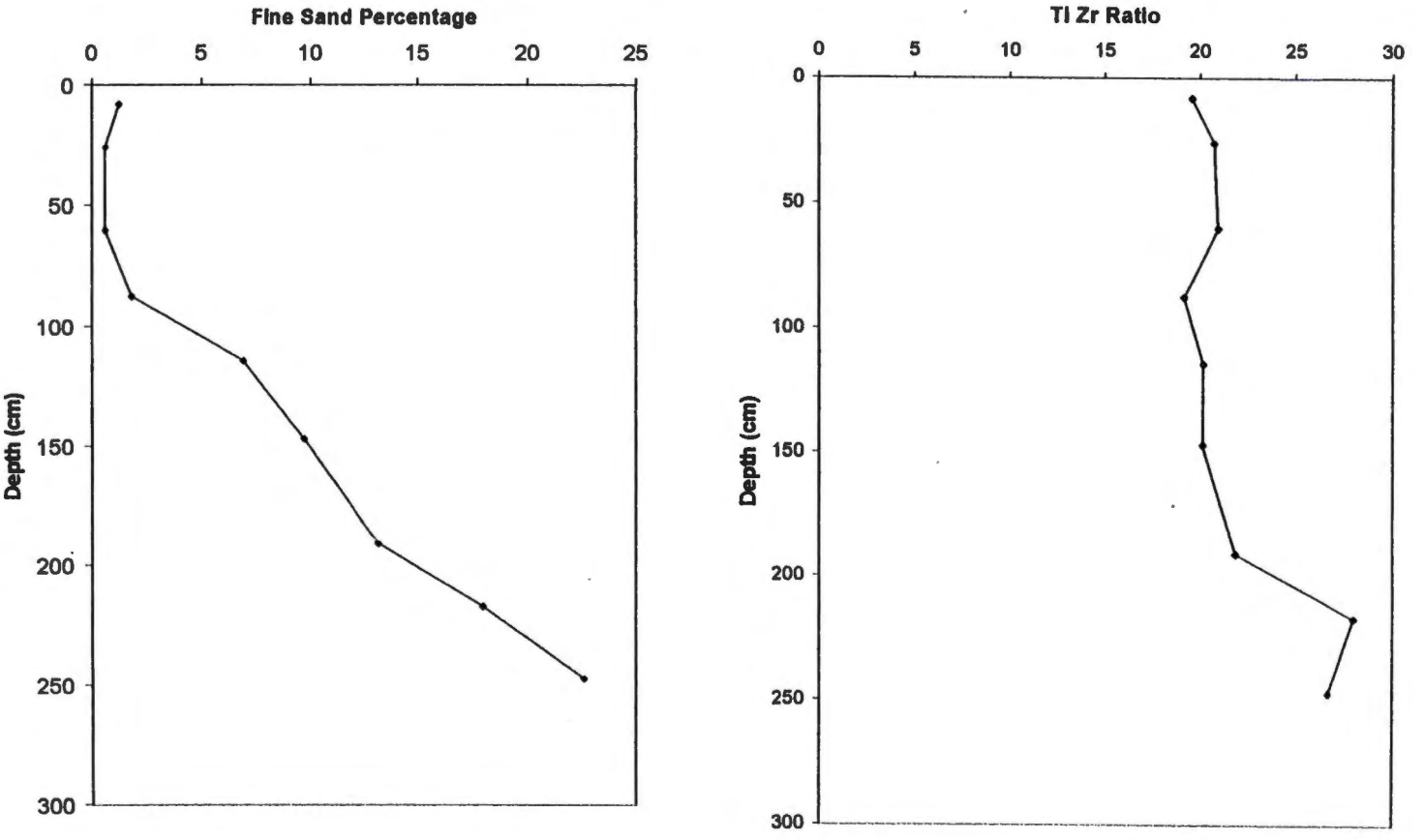


Figure 26. Plots of fine sand and titanium to zirconium for site 4.

interface the K_{sat} was in the low class, at 0.02046 cm/hr (Fig. 27). Below the interface, the K_{sat} was considerably higher, 0.09291 cm/hr (Fig. 27). However, it was still in the low K_{sat} class (Soil Survey Staff, 1993). As in the other sites, the low K_{sat} above the interface could induce lateral water movement.

The particle size control section had 2.3 percent sand and 29.7 percent clay, making it fine-silty (Fig. 22). Mineralogy class was mixed. The CEC/clay ratio in the control section (upper 50 cm of the argillic) was 0.57, putting it into the active cation exchange activity class. This soil had an ochric epipedon, an argillic horizon, and a base saturation by sum of cations of 35 percent at 125 cm below the top of the argillic horizon which made it an alfisol. It was in the Ultic subgroup of the alfisol order because the base saturation was less than 60 percent. This site was classified as a Fine-silty, mixed, active, thermic Ultic Hapludalf.

Site five

Site five was located at N 35° 8' 3.8", W 89° 13' 23.9", on an upland position, under a forage cropping arrangement, at an elevation of 164.98 meters above sea mean sea level. Soil morphology was sampled and described to a depth of 300 cm below the soil surface. Site five was formed in a loess over alluvium over Tertiary sand parent material sequence.

Loess was present from the surface to a depth of 109 cm. Soil color was 10YR 4/4 and 4/3 in the Ap and Bt1 horizon (6 - 22 cm), respectively. The remaining two horizons were 7.5YR 4/3 and 4/4. Total clay percentage remained somewhat steady, whereas the fine clay percentage had a bulge in the Bt2 horizon (22 - 60 cm) (Fig. 28).

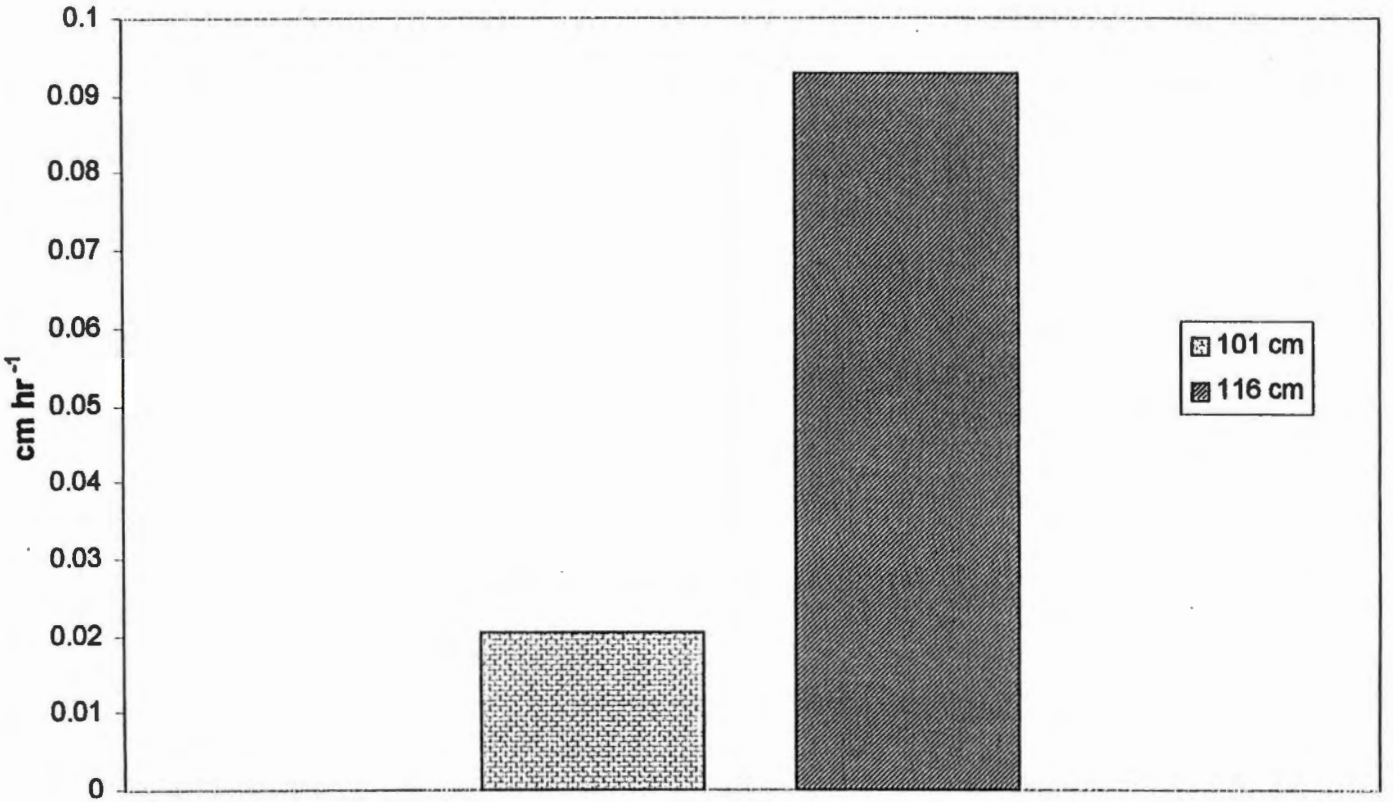


Figure 27. Graph of saturated hydraulic conductivity values at 101-cm and 116-cm depths for site 4.

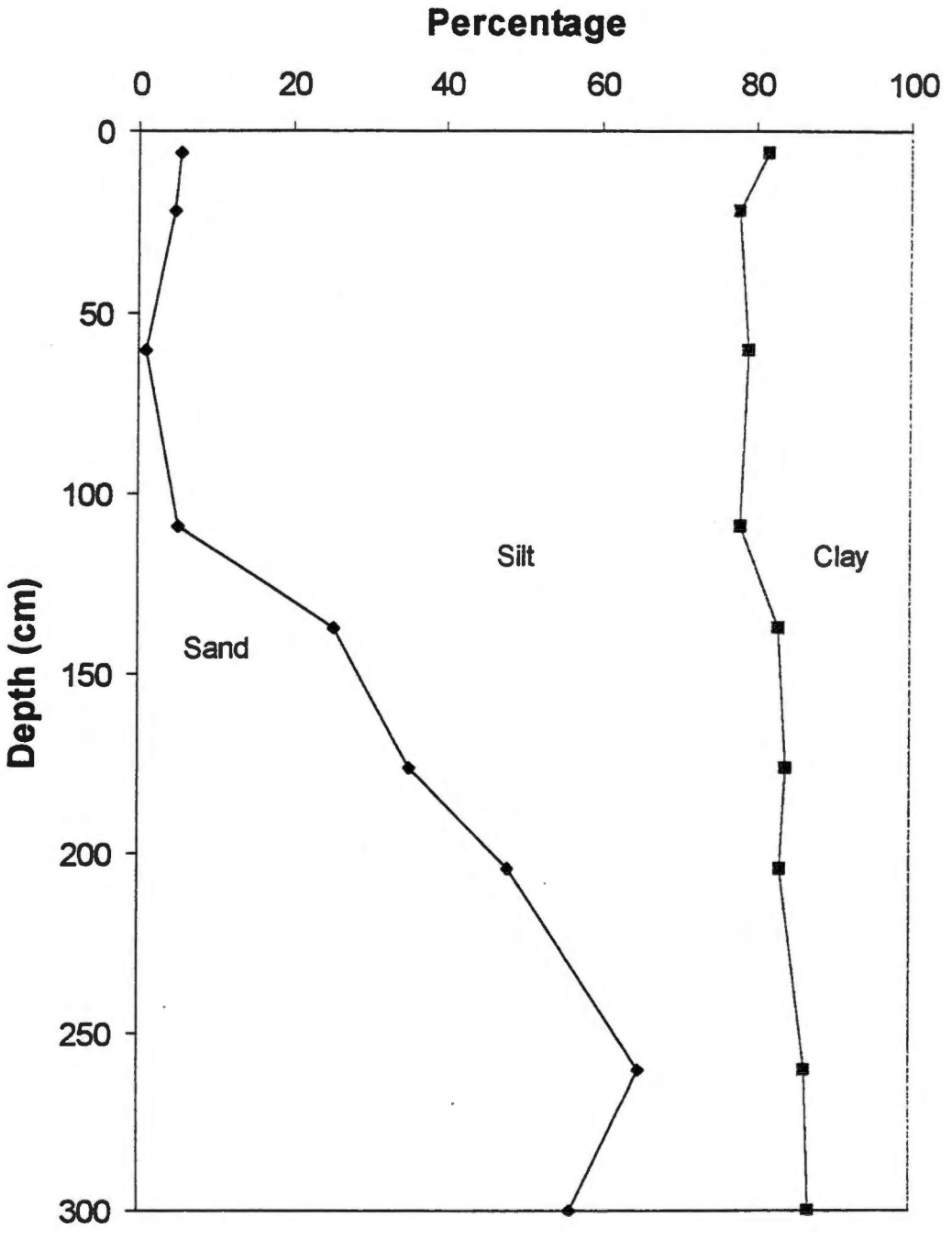


Figure 28. Cumulative particle size plot for site 5.

The bulge in fine clay percent is likely due to active illuviation of materials, and thus pedogenic maturity of the soil. Total silt percentage ranged from 76.0 % in the Ap horizon to a low of 73.1 % in the Bt3 horizon (60 - 109 cm) (Fig. 28). There was a bulge in total iron in the Bt2 horizon (22 - 60 cm), and a bulge in free iron in the Bt3 horizon (60 - 109 cm) (Fig. 29). Bulk density was highest in the Bt1 horizon (6 - 22 cm), like the previous sites, probably from vehicle compaction (Fig. 23). Both total and organic carbon decreased regularly below the surface horizon, as expected (Fig. 30). Fine sand percentage increased sharply at 109 cm, indicating a shift in the parent material sequence from loess to the alluvium (Fig. 31). There were no discrepancies found within the loess using the procedures outlined. The loess present at site five was likely part of the Peoria loess deposition.

Alluvium was present from 109 cm to 204 cm below the surface. Total carbon dropped slightly with depth (Fig. 30). However, the organic carbon distribution was slightly irregular, perhaps due to material being fluvially deposited. These processes will deposit material in a stratified manner, which will lead to differing degrees of weathering between depositions. Free iron oxide concentration was also variable, as would be expected in a fluvial material (Fig. 29). High bulk density values were observed throughout this layer, possibly due to a combination of the material being compacted while it was sampled and the material actually being significantly more dense than the overlying material as the sandier textures would suggest (Fig. 23). As in the other sites, this layer had a fining upward sequence, indicating material deposited by a meandering stream system (Figs. 28, 31). Both fine sand and titanium to zirconium ratio decreased sharply below 260 cm, indicating a discontinuity (Fig. 31).

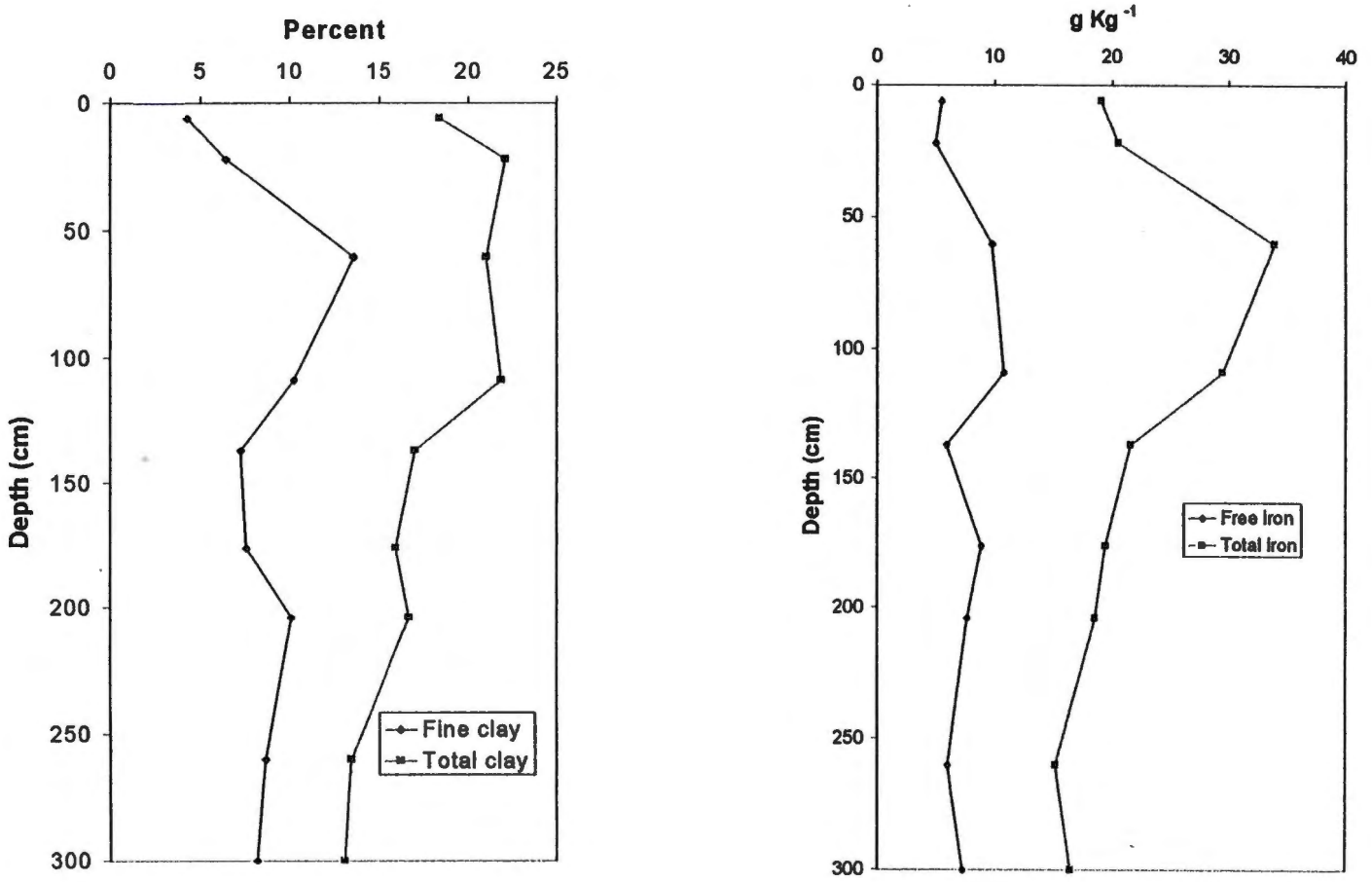


Figure 29. Plots of fine clay, total clay, free iron, and total iron for site 5.

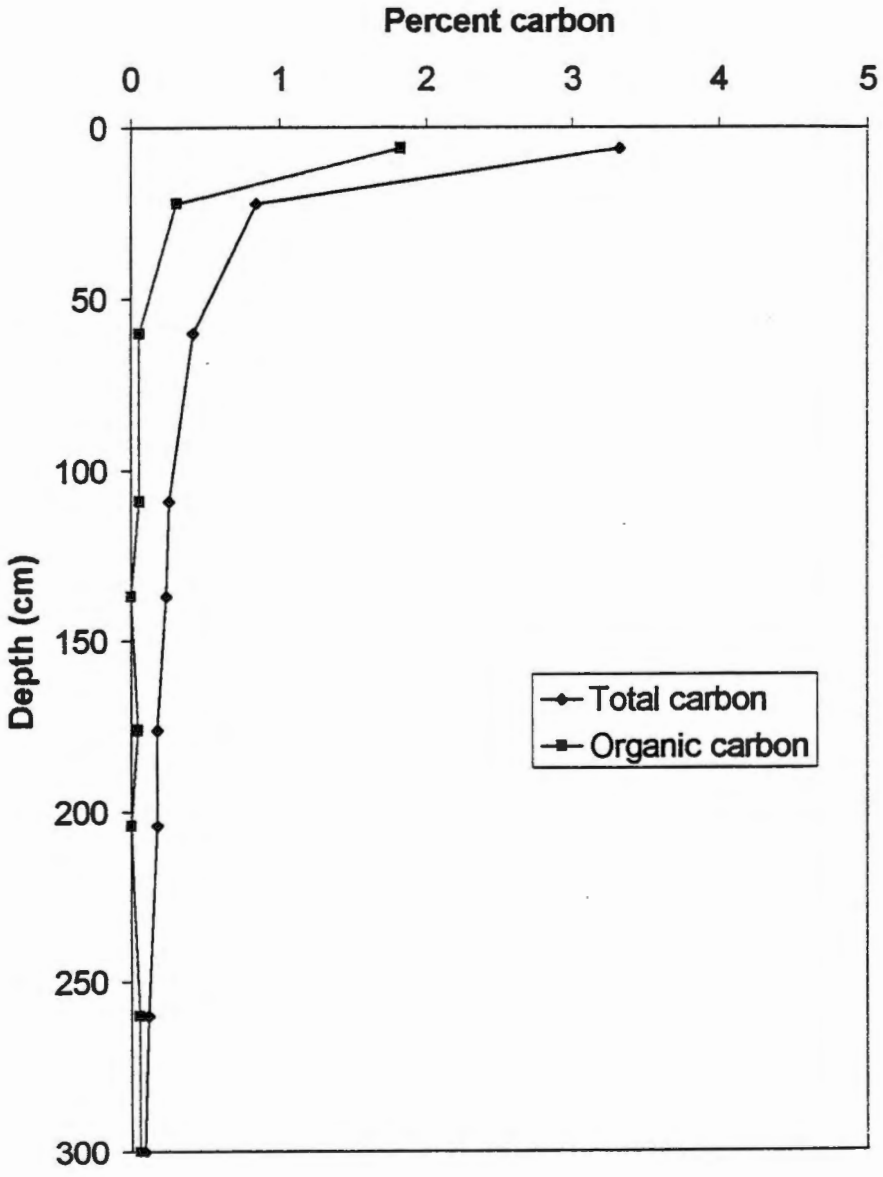


Figure 30. Plot of total and organic carbon for site 5.

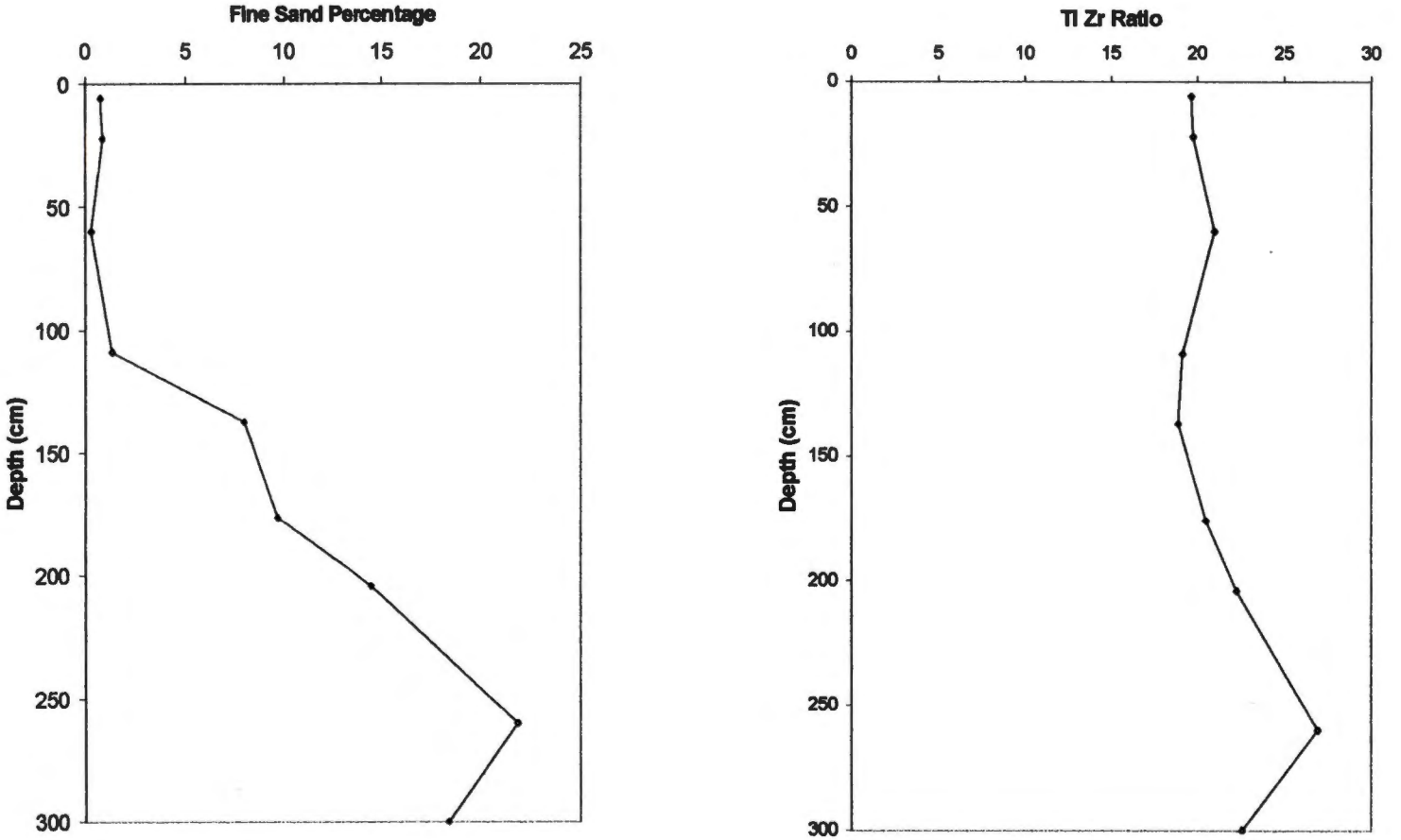


Figure 31. Plots of fine sand and titanium to zirconium for site 5.

Tertiary aged sand began at 260 cm and extended throughout the remainder of the core sampled. Unlike the previous sites, there was not an argillic horizon present (Fig. 28). Lack of an argillic horizon could be attributed to variation in the amounts of erosion and weathering prior to the influx of alluvium and/or the presence of a mixing zone between the alluvium and Tertiary sand. Unlike the Tertiary sand layers in the previous sites, the bulk density was very high, reflecting the increased sand content and associated low porosity (Fig. 23). Soil color in this horizon was 2.5YR 4/8.

Saturated hydraulic conductivity measurements were taken above the loess/alluvium interface at depths of 104 cm and 122 cm, respectively. Above the interface the K_{sat} was 0.03047 cm/hr, while below the interface the K_{sat} was 0.03096 cm/hr , both in the low class (Soil Survey Staff, 1993) (Fig. 32). K_{sat} values above and below the interface were very similar.

The particle size control section had 2.9 percent sand and 21.6 percent clay, making it fine-silty (Fig. 28). Mineralogy was determined to be mixed. The CEC/clay ratio in the control section (upper 50 cm of the argillic) was 0.60, putting it into the superactive cation exchange capacity class. This soil had an ochric epipedon, an argillic sub-surface horizon, and a base saturation of 36 percent by sum of cations at 125 cm below the top of the argillic horizon making this soil an alfisol. Since this site had a base saturation of less than 60 percent, it is in the Ultic suborder. Site five was classified as a Fine-silty, mixed, superactive, thermic Ultic Hapludalf.

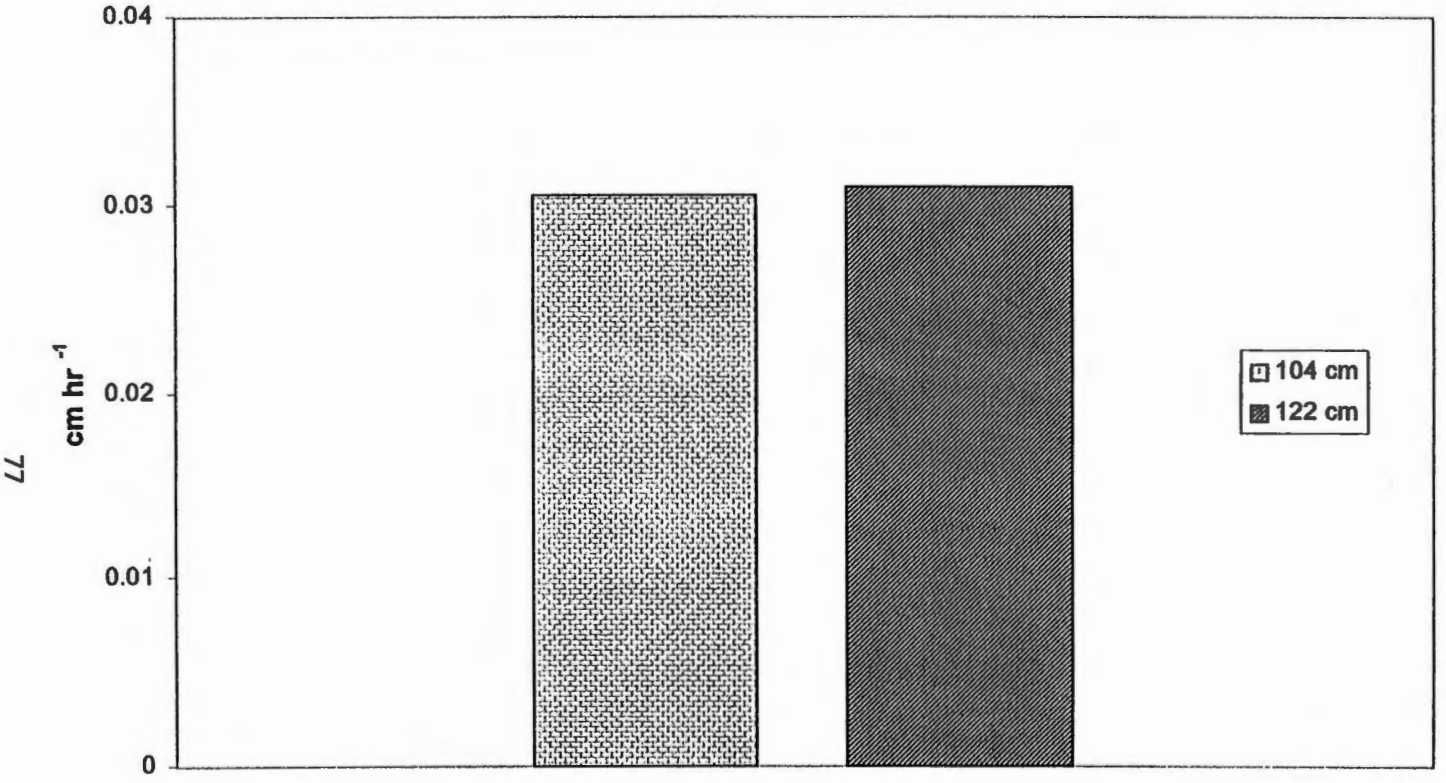


Figure 32. Graph of hydraulic conductivity values at 104-cm and 122-cm depths for site 5.

Site six

Site six was located at N 35° 8' 3.8", W 89°13' 23.9" on an upland position under a forage crop arrangement at 164.98 meters above sea level. Soil morphology was sampled and described to a depth of 300 cm. The parent material was loess over alluvium over Tertiary sands.

Loess was present from the surface to a depth of 138 cm. Soil color was 7.5YR 4/4 except for the Ap and Bt1 horizons (4 - 28 cm) which were both 10YR 4/4. Total silt percentage ranged from 77.3 % in the Ap horizon to 56.2 % in the BC2 horizon (89 - 138 cm) (Fig. 33). A bulge in free iron oxides, total iron concentration, fine clay, and total clay percentage occurred in the Bt2 horizon (28 - 55 cm) before falling off steadily (Fig. 34). Both total and organic carbon decreased rapidly below the Ap horizon (Fig. 35). As seen in the other sites, the Bt1 horizon (4 - 28 cm) had a high bulk density, probably from surface compaction (Fig. 23). Fine sand percentage increased significantly at 138 cm below the soil surface, indicating a lithologic discontinuity (Fig. 36). There were not any distinct differences in the loess that could be used to differentiate multiple depositions. The loess present was most likely part of the Peoria loess deposition.

Alluvium was present from 138 cm to 244 cm. Unlike the other sites, carbon distribution was stable (Fig. 35). However, free iron oxide and total iron concentration was somewhat irregular (Figs. 34). Total sand and fine sand percentages increased with depth as in the previous sites. (Figs. 33, 36). Bulk density was much higher than in the loess, as one would expect in sandier materials (Fig. 23). However, the bulk density values are unusually high, likely due to compaction from the soil probe. There was an increase in fine sand percent and titanium to zirconium ratio at 244 cm below the surface,

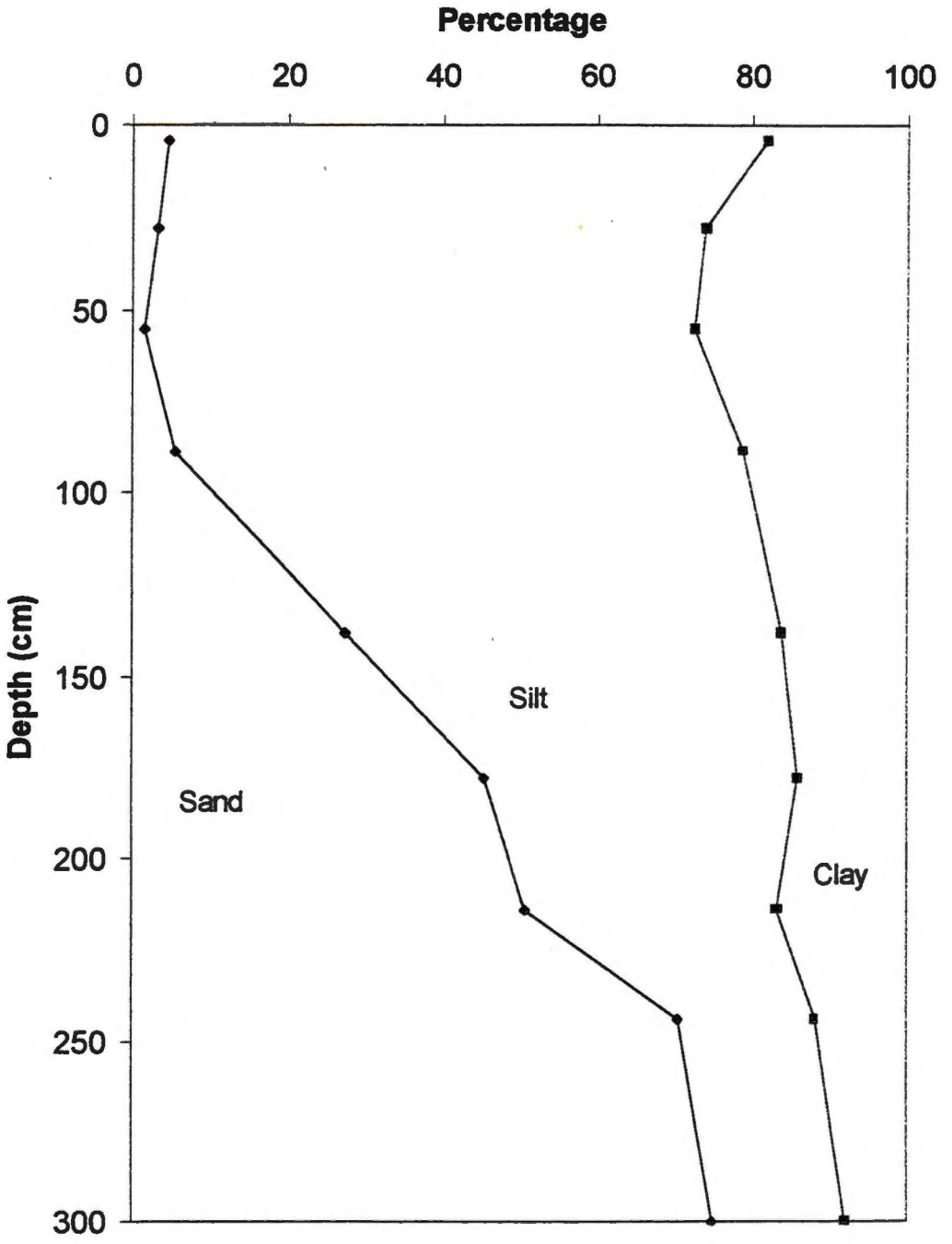


Figure 33. Cumulative particle size plot for site 6.

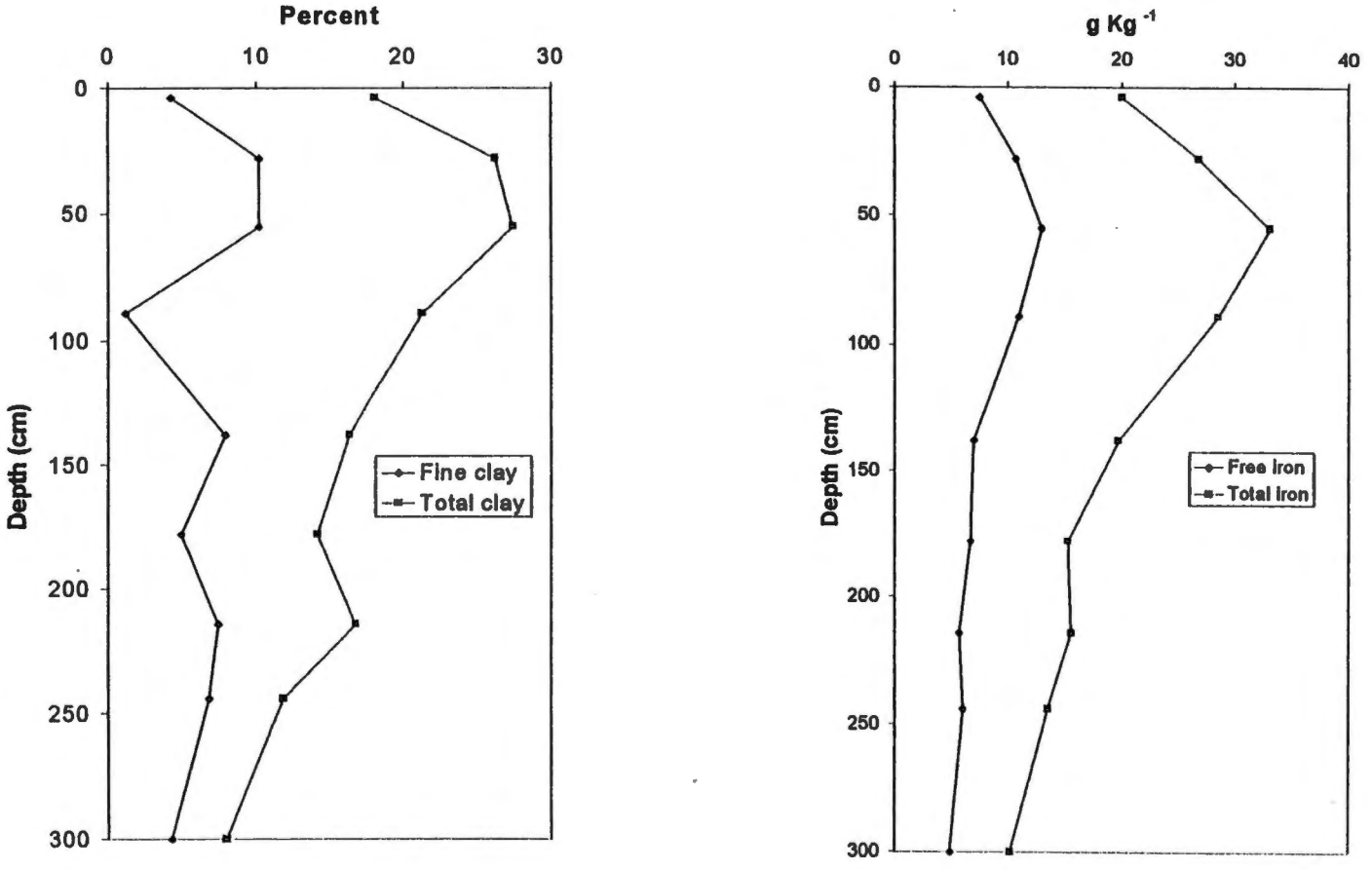


Figure 34. Plots of fine clay, total clay, free iron, and total iron for site 6.

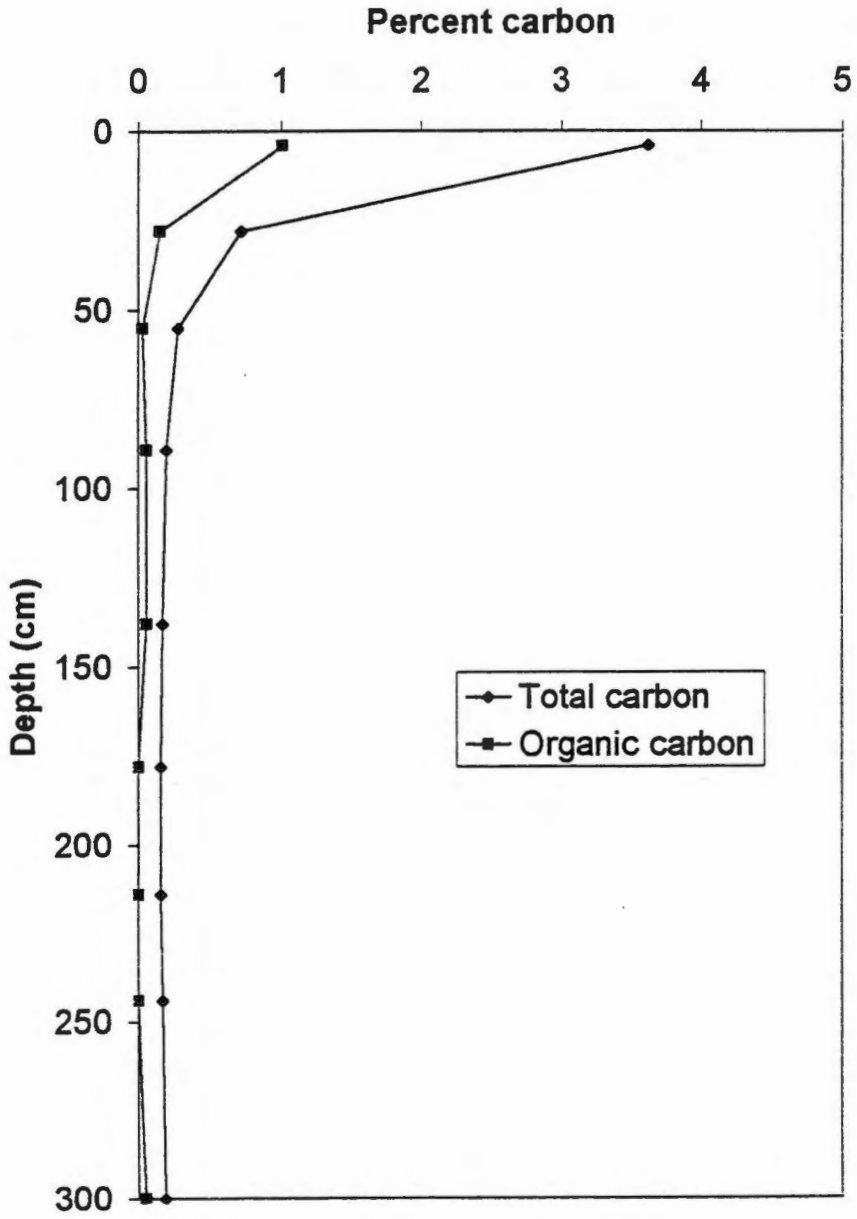


Figure 35. Plot of total and organic carbon for site 6.

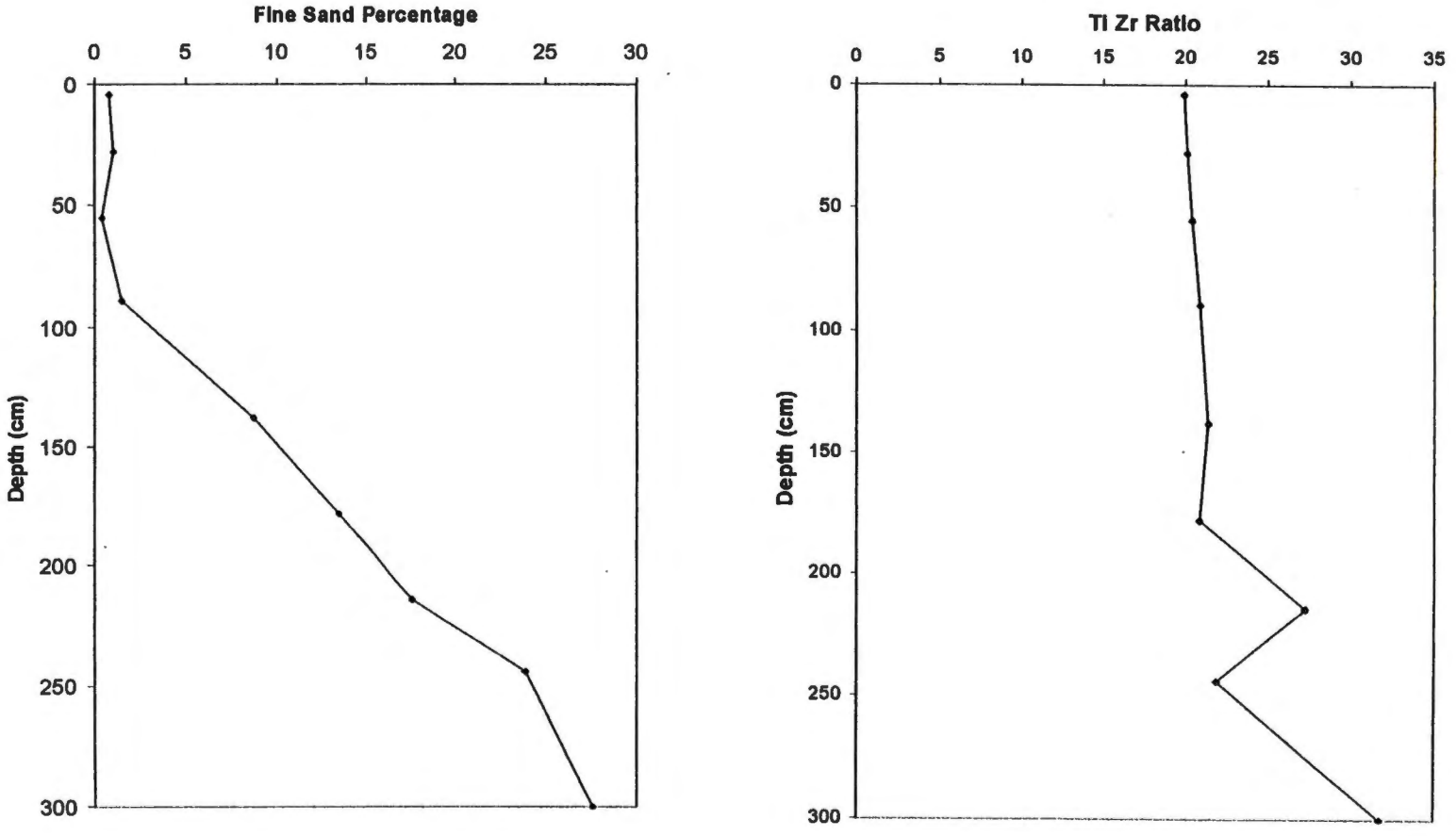


Figure 36. Plots of fine sand and titanium to zirconium for site 6.

indicating a lithologic discontinuity (Fig. 36).

Tertiary sands began at a depth of 244 cm and continued throughout the extent of the core sampled. Like site five, an argillic horizon was not present (Fig. 33). Lack of an argillic horizon could be due to attrition of the landscape prior burial. Also like site five, bulk density was much higher than in the overlying layer (Fig. 23). Soil color was 2.5YR 4/8, indicating that rubification has occurred. As in site five, differences between the Tertiary sand found in sites one through four and that found in this site are due primarily to variability in erosion and degree of weathering during Tertiary time before the area was inundated with alluvium.

Saturated hydraulic conductivity measurements were made above and below the loess/alluvium interface, at depths of 116 cm and 142 cm, respectively (Fig. 37). K_{sat} above the alluvium was 0.07349 cm/hr, and 0.09865 cm/hr below the interface, both are in the low K_{sat} class (Soil Survey Staff, 1993). The less conductive horizon above the interface could cause lateral water movement.

The particle size control section had 2.4 percent sand and 26.8 percent clay, making it fine-silty. Mineralogy was mixed. The CEC/clay ratio in the control section (upper 50 cm of the argillic) was 0.44, putting it into the active cation exchange capacity class. This soil had an ochric epipedon, an argillic sub-surface horizon, and a base saturation of 42 percent by sum of cations at 125 cm below the top of the argillic horizon making this soil an alfisol. Since it had a base saturation of less than 60 percent it will be in the Ultic subgroup of the alfisol order. Site six was classified as a Fine-silty, mixed, active, thermic Ultic Hapludalf.

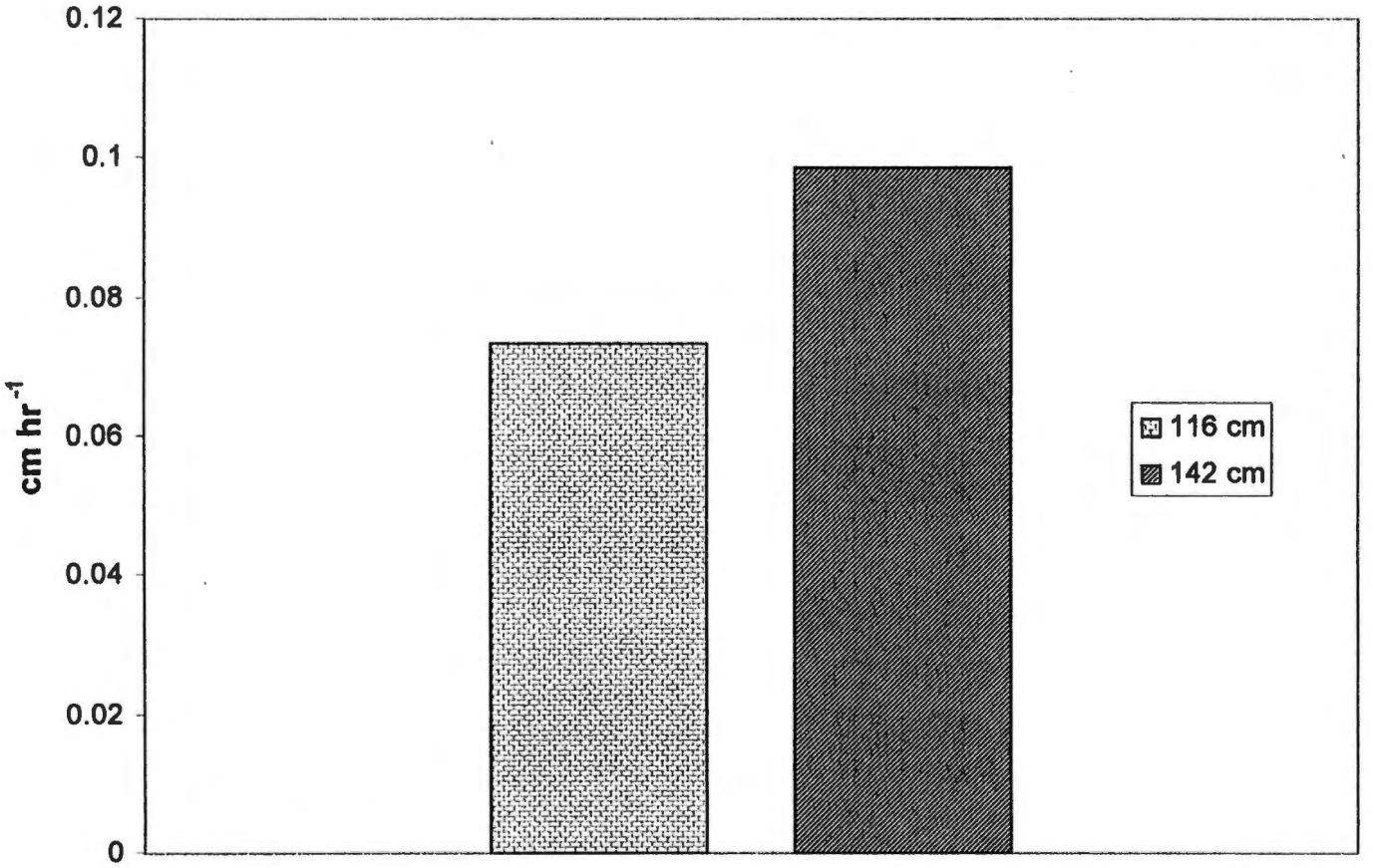


Figure 37. Saturated hydraulic conductivity values at 116-cm and 142-cm depths for site 6.

Site seven

Site seven was located at N 35° 8' 3.5", W 89° 13' 23", on an upland position under a forage cropping arrangement at an elevation of 165.06 meters above mean sea level. Soil morphology was sampled and described to a depth of 238 cm below the soil surface. Parent material was loess over alluvium over Tertiary aged sands.

Loess was present from the surface to a depth of 106 cm. Soil color in the upper two horizons was 10YR 4/3 and 4/4, while the remainder was 7.5YR 4/4. Total silt percentage ranged from 74.4 % in the Ap horizon to 68.1 % in the Bt2 horizon (31 - 60 cm) (Fig. 38). Bulk density values had the same trend as in the previous sites, with the upper horizon being affected by surface compaction (Fig. 39). Free iron oxides and total iron increased with depth until the Bt2 horizon (31 - 60 cm) before dropping off in the BC1 horizon (60 - 106 cm), illustrating a typical weathering profile (Fig. 40). There was a bulge in both fine and total clay in the Bt2 horizon (31 - 60 cm), indicating that material has been illuviated and an argillic horizon has formed (Fig. 40). Both total and organic carbon decreased rapidly with depth below the Ap horizon (Fig.41). There was a large increase in fine sand percentage and a slight increase in titanium to zirconium ratio at 106 cm, indicating a lithologic discontinuity (Fig. 42). Differences within the loess were not detected using the methods outlined. The loess was most likely part of the Peoria loess deposition.

Alluvium was present from 106 cm to the extent of the core sampled. Total carbon distribution was irregular as seen in the other sites, indicating an alluvial environment of deposition (Fig. 41). Both free iron oxides and total iron decreased with depth throughout the alluvium (Fig. 40). Bulk densities were quite high in this layer, as

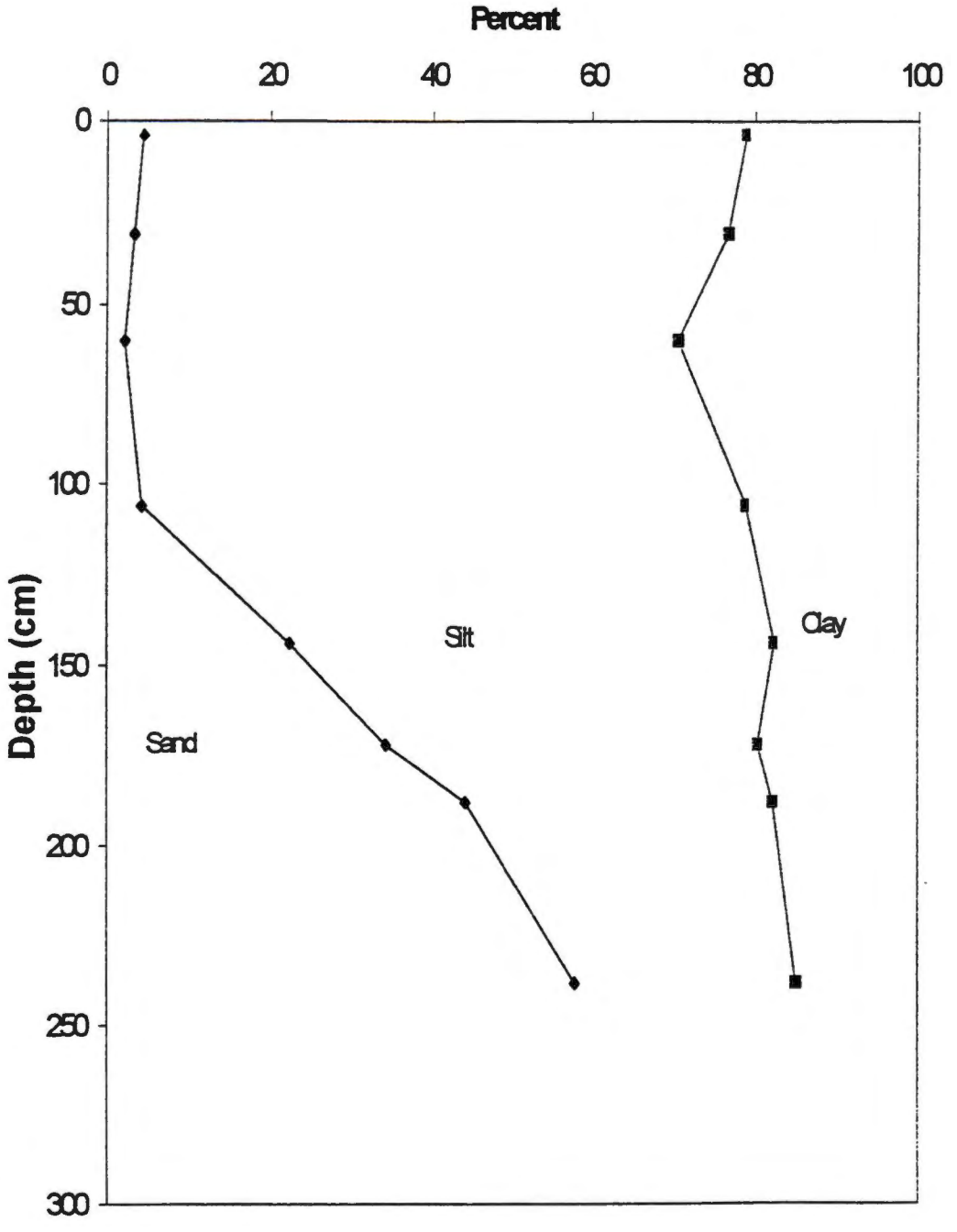


Figure 38. Cumulative particle size plot for site 7.

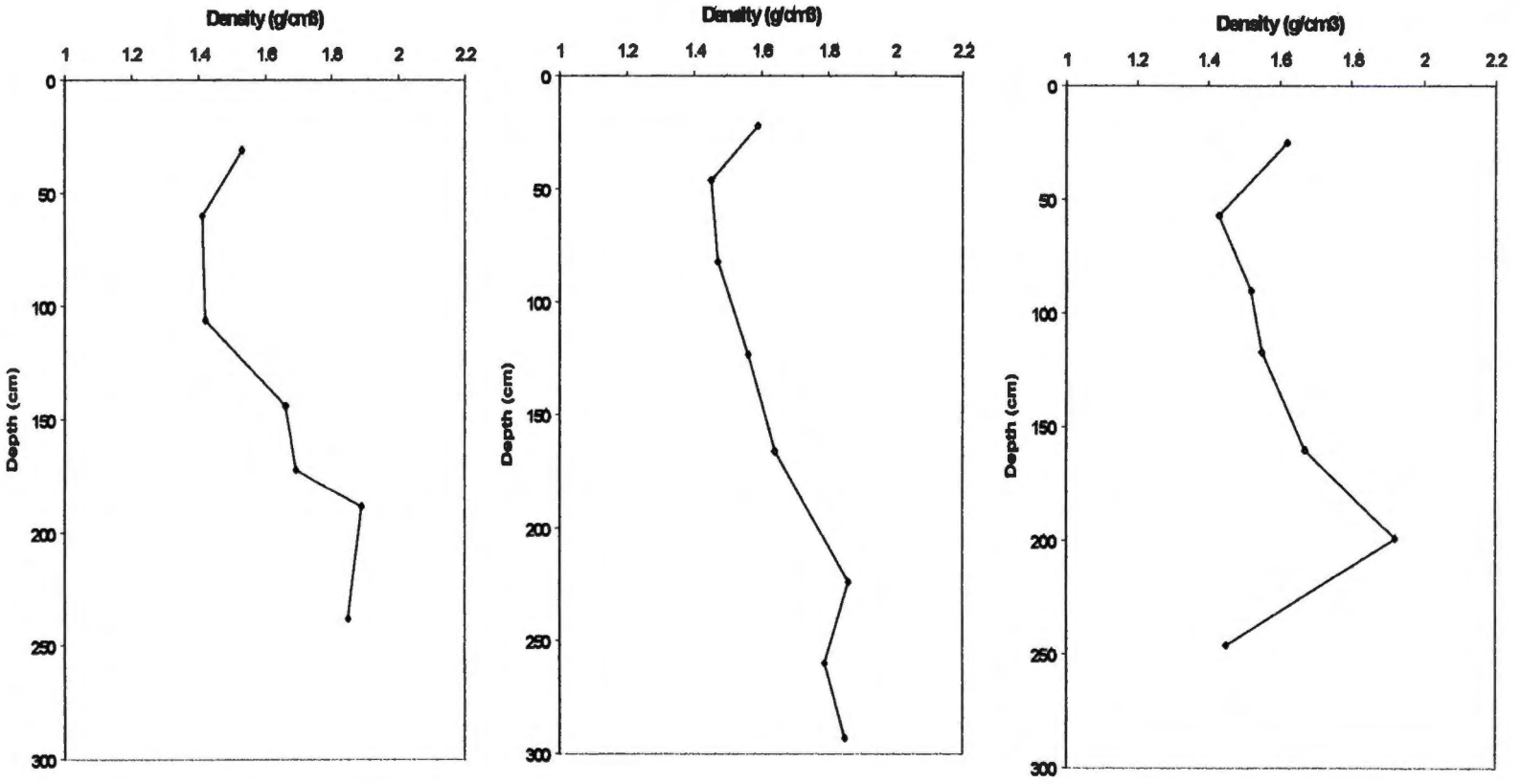


Figure 39. Bulk densities of sites seven, eight, and nine.

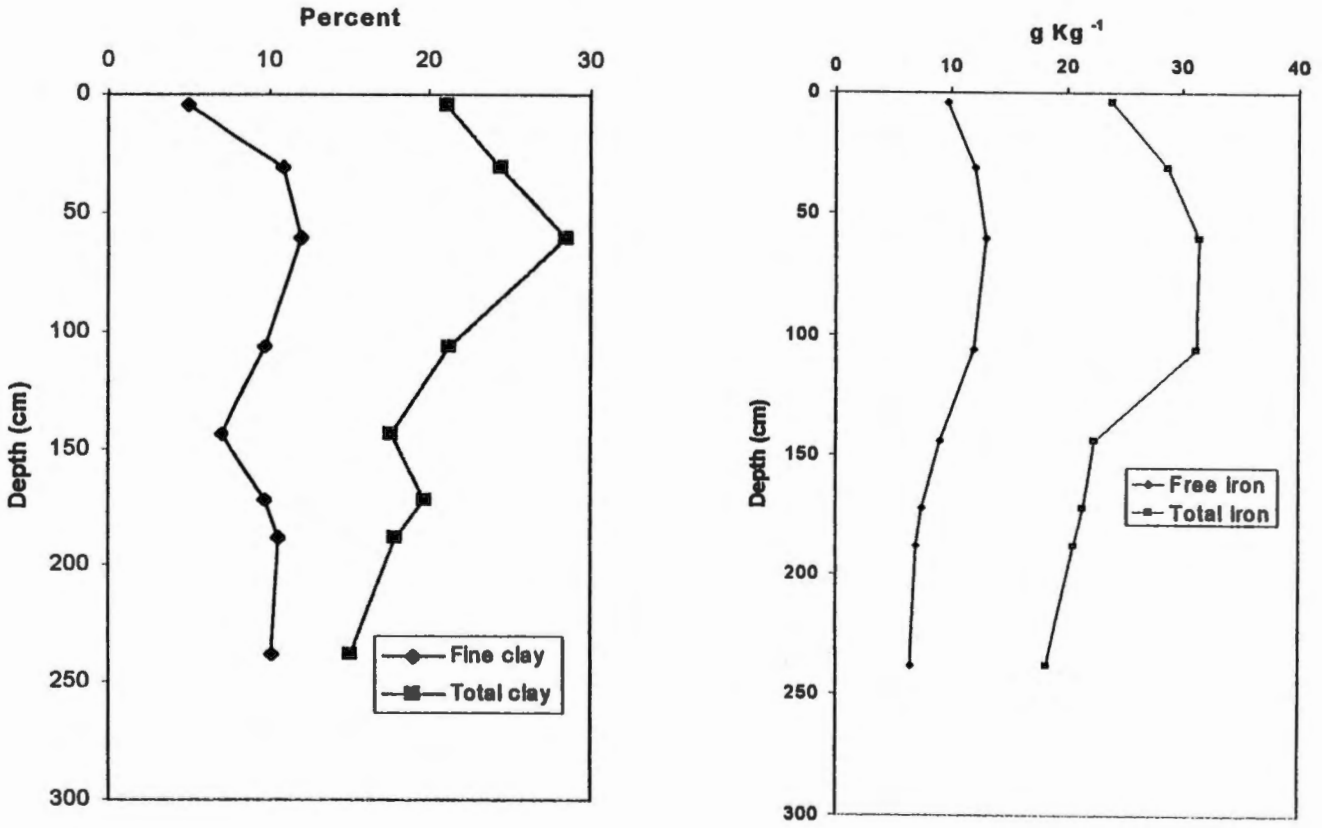


Figure 40. Plots of fine clay, total clay, free iron, and total iron for site 7.

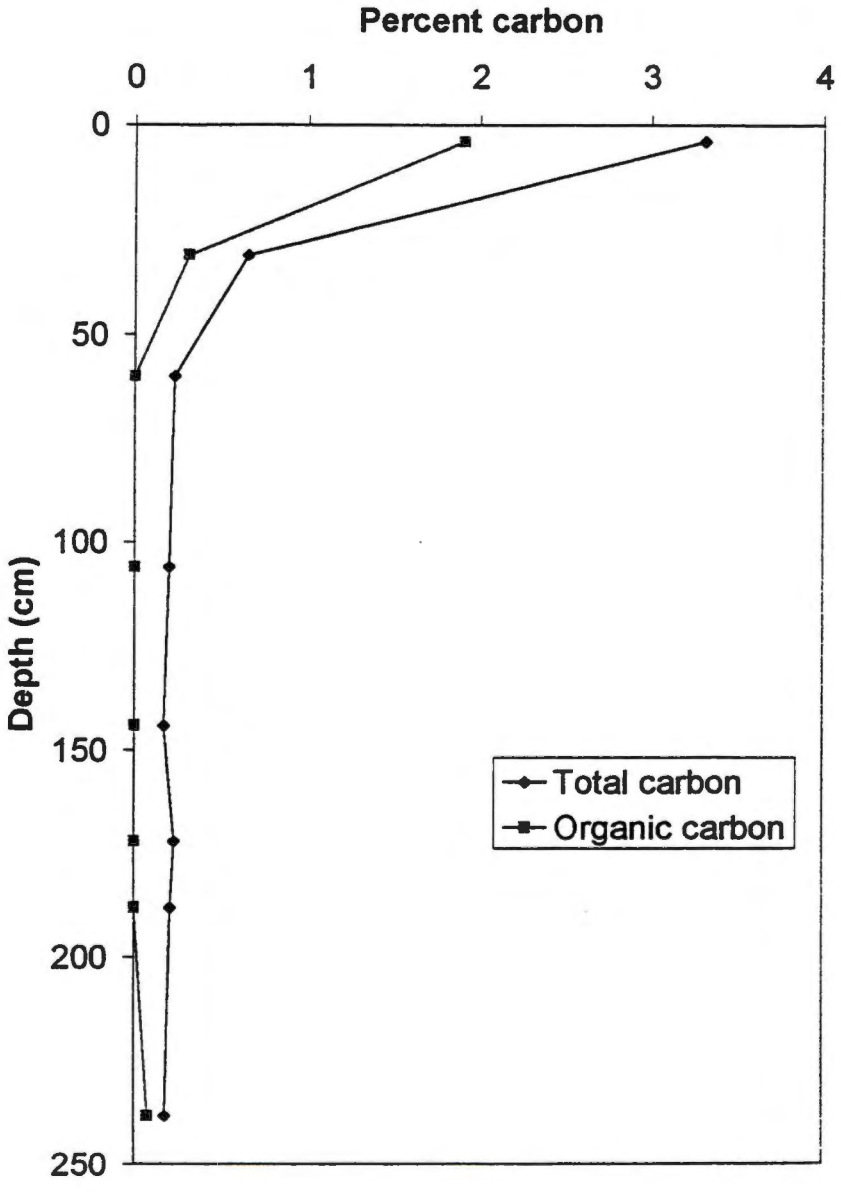


Figure 41. Plot of total and organic carbon for site 7.

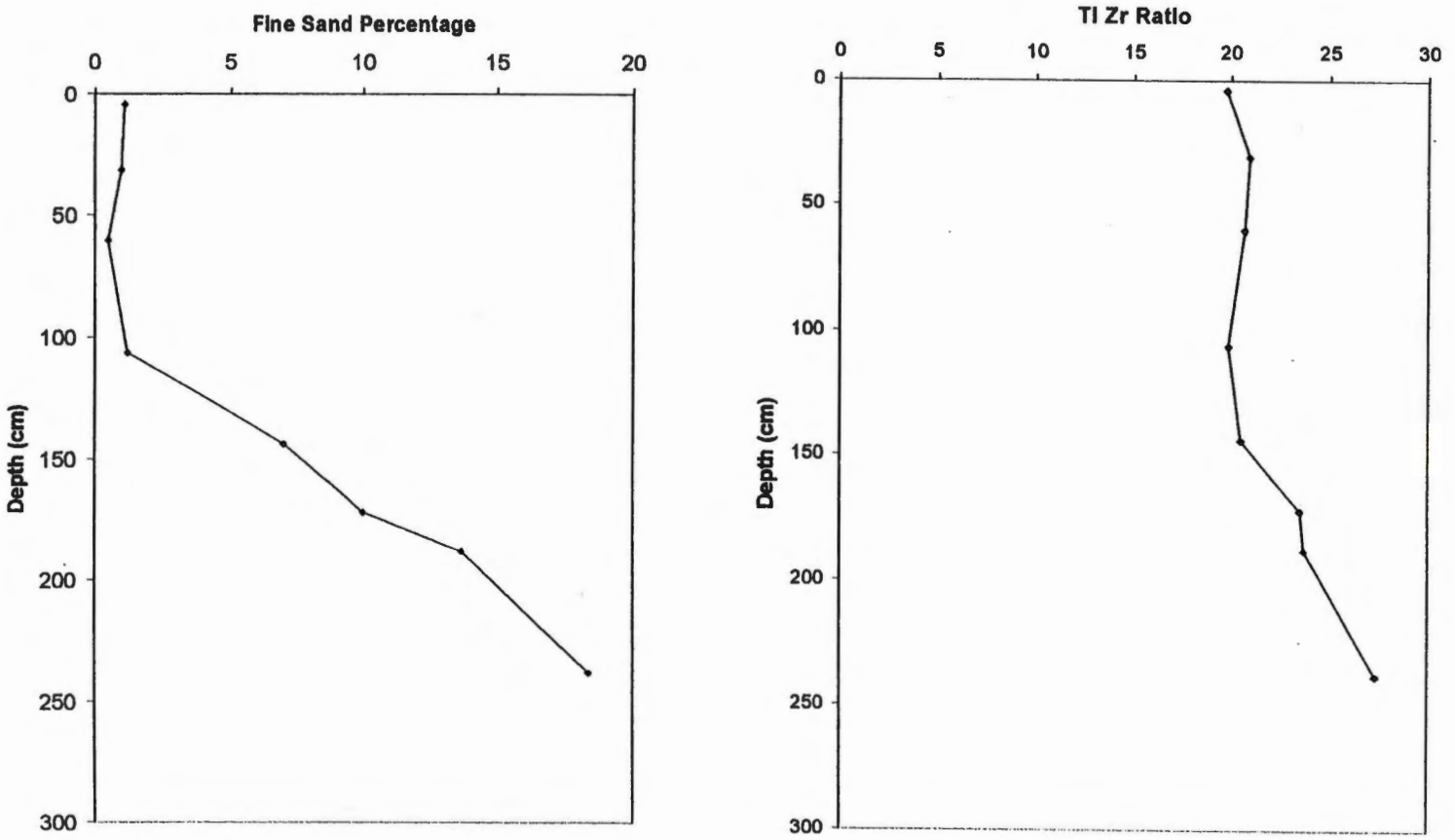


Figure 42. Plots of fine sand and titanium to zirconium for site 7.

seen in the other sites (Fig. 39). Total and fine sand percentage increased with depth throughout this layer (Figs. 38, 42). This fining upward sequence was likely caused from a meandering stream system.

Saturated hydraulic conductivity measurements were taken at depths of 101 cm and 127 cm, above and below the loess/alluvium interface (Fig. 43). As seen in the other sites, the horizon above the interface was less conductive than the underlying horizon. K_{sat} above the interface was 0.04174 cm/hr and below was 0.05897 cm/hr, both in the low K_{sat} class (Soil Survey Staff, 1993). This discrepancy in K_{sat} values could cause lateral movement of water at the interface.

The particle size control section had 2.8 percent sand and 26.9 percent clay, making it be fine-silty (Fig. 38). Mineralogy was mixed. The CEC/clay ratio in the control section (upper 50 cm of the argillic) was 0.55, putting it into the active cation exchange capacity class. This soil had an ochric epipedon, an argillic subsurface horizon, and a base saturation of 37 percent by sum of cations at 125 cm below the top of the argillic horizon making this soil an alfisol. Since this soil had a base saturation of less than 60 percent by sum of cations it was in the Ultic subgroup of the alfisol order. Site seven was classified as a Fine-silty, mixed, active, thermic Ultic Hapludalf.

Site eight

Site eight was located at N 35° 8' 3.8", W 89° 13' 22.8" on an upland position under a forage cropping system, at an elevation of 165.41 meters above mean sea level. Soil morphology was sampled and described to a depth of 293 cm. The parent material was loess over alluvium over Tertiary sands.

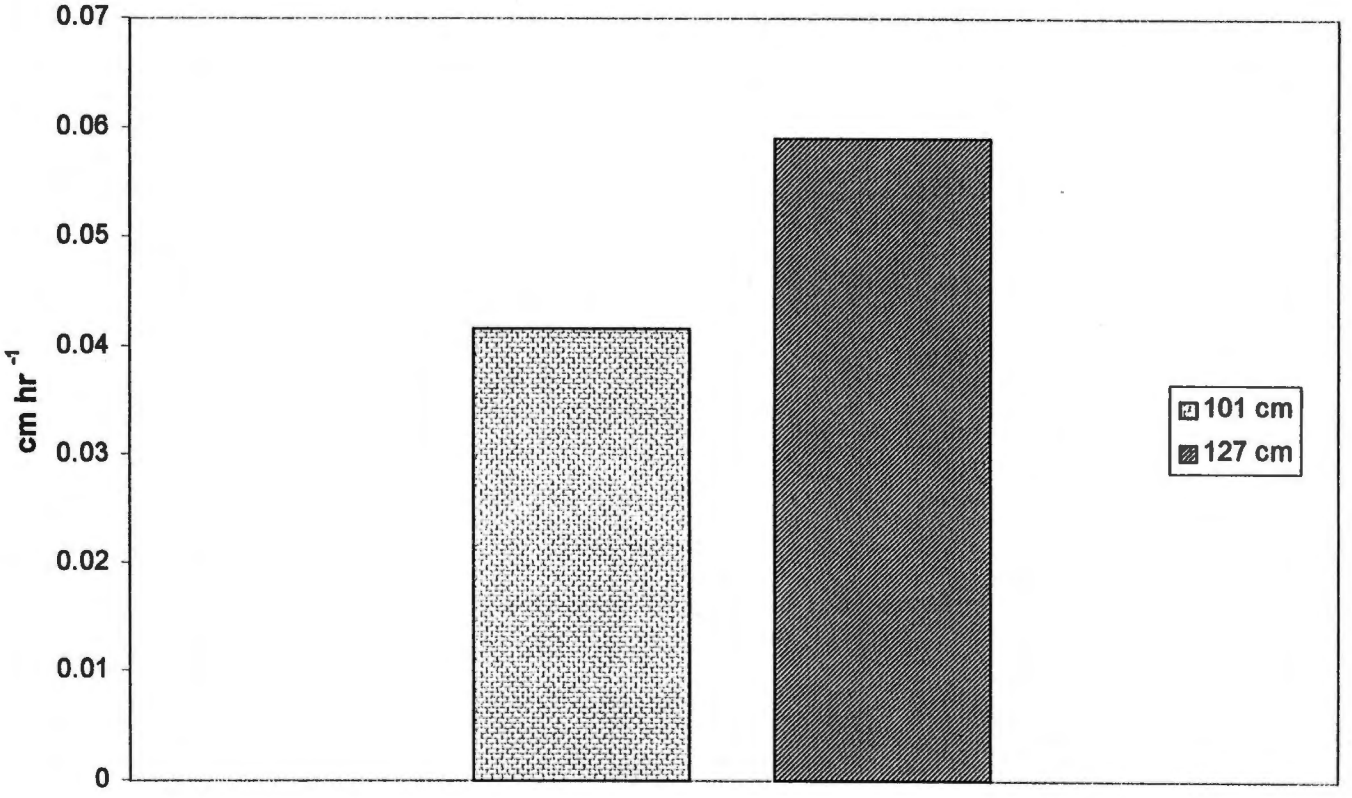


Figure 43. Graph of hydraulic conductivity values at 101-cm and 127-cm depths for site 7.

Loess extended from the surface to a depth of 123 cm. Soil color was 10YR 4/4 in the uppermost horizon and 7.5YR 4/4 throughout the remainder of the loess. Total silt percentage ranged from 78.73 % in the Ap horizon to 68.46 % in the Bt2 horizon (22 - 46 cm) (Fig. 44). There was a bulge in free iron oxides, total iron, total clay, and fine clay in the Bt2 horizon (22 - 46 cm) before dropping steadily throughout layer (Fig. 45). Total and organic carbon decreased in a regular pattern throughout the loess (Fig. 46). Bulk densities were similar to the other sites, with surface compaction affecting the Bt1 horizon (Fig. 39). There was a significant increase in fine sand percentage and a slight increase in titanium to zirconium ratio at 123 cm, suggesting a lithologic discontinuity between the loess and alluvium (Fig. 47).

Alluvium was present from 123 cm to 224 cm. Carbon distribution was irregular, suggesting a cyclic depositional pattern (Fig. 46). Free iron and total iron concentration decreased with depth through out this layer as did the fine and total clay percentage (Fig. 45). Both fine and total sand percentages increased with depth, illustrating a fining upward trend (Figs. 44, 47). Like the previous sites, bulk density values were higher than in the loess, possibly from compaction caused by the hydraulic probe and/or sandier material (Fig. 39). Soil color throughout the alluvium was 5YR 4/4. Fine sand and titanium to zirconium ratio had a sharp increase at 224 cm, indicating a second discontinuity (Fig. 47).

Tertiary sand began at 224 cm and continued throughout the sampling depth. Soil color was 2.5YR 4/4. Like sites five and six, an argillic horizon was not present (Fig. 44). Both fine sand and total sand percentages increased with depth throughout this layer (Figs. 44, 47). This was most likely a result of there being variation in the amount of erosion

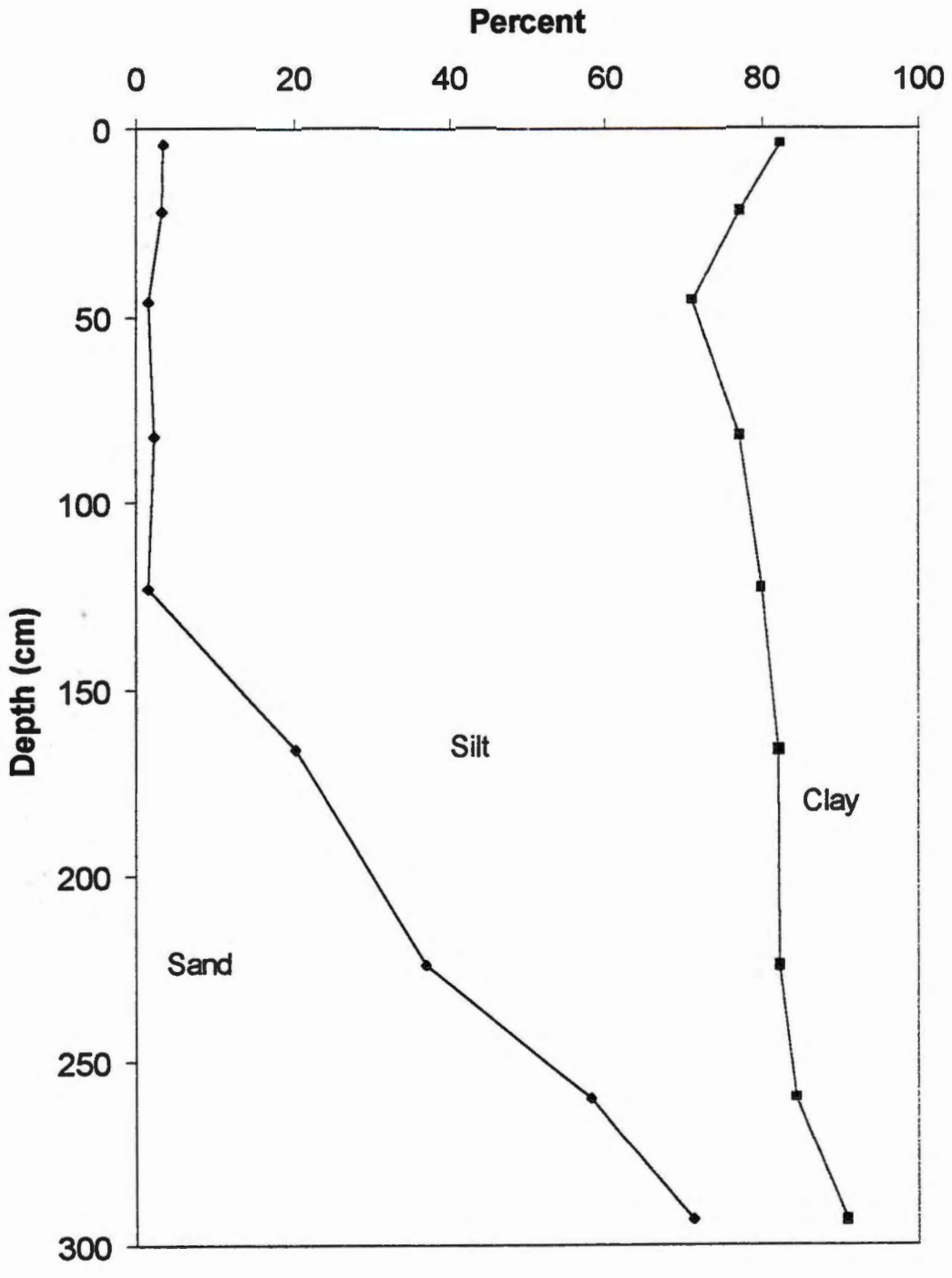


Figure 44. Cumulative particle size plot for site 8.

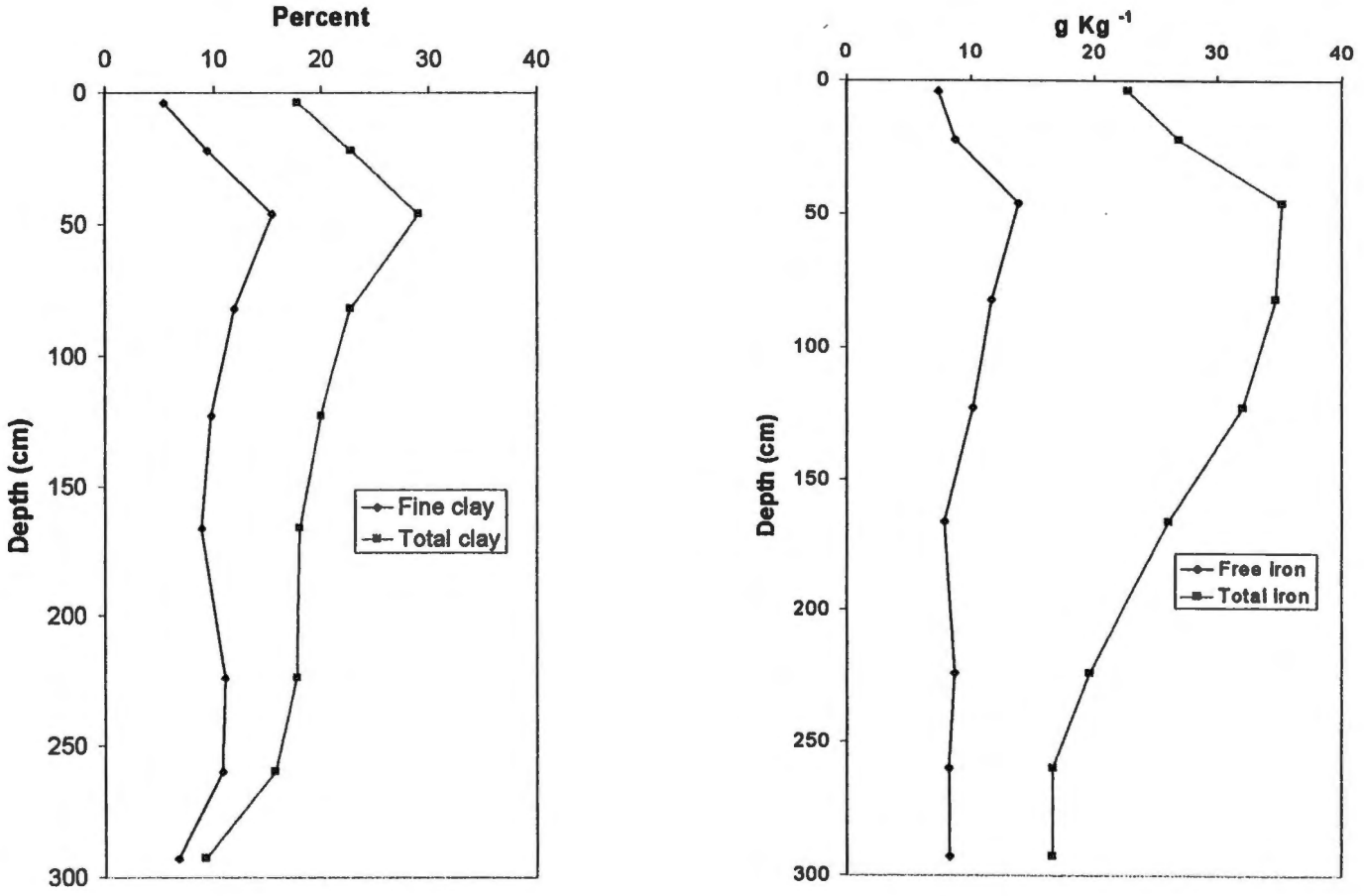


Figure 45. Plots of fine clay, total clay, free iron, and total iron for site 8.

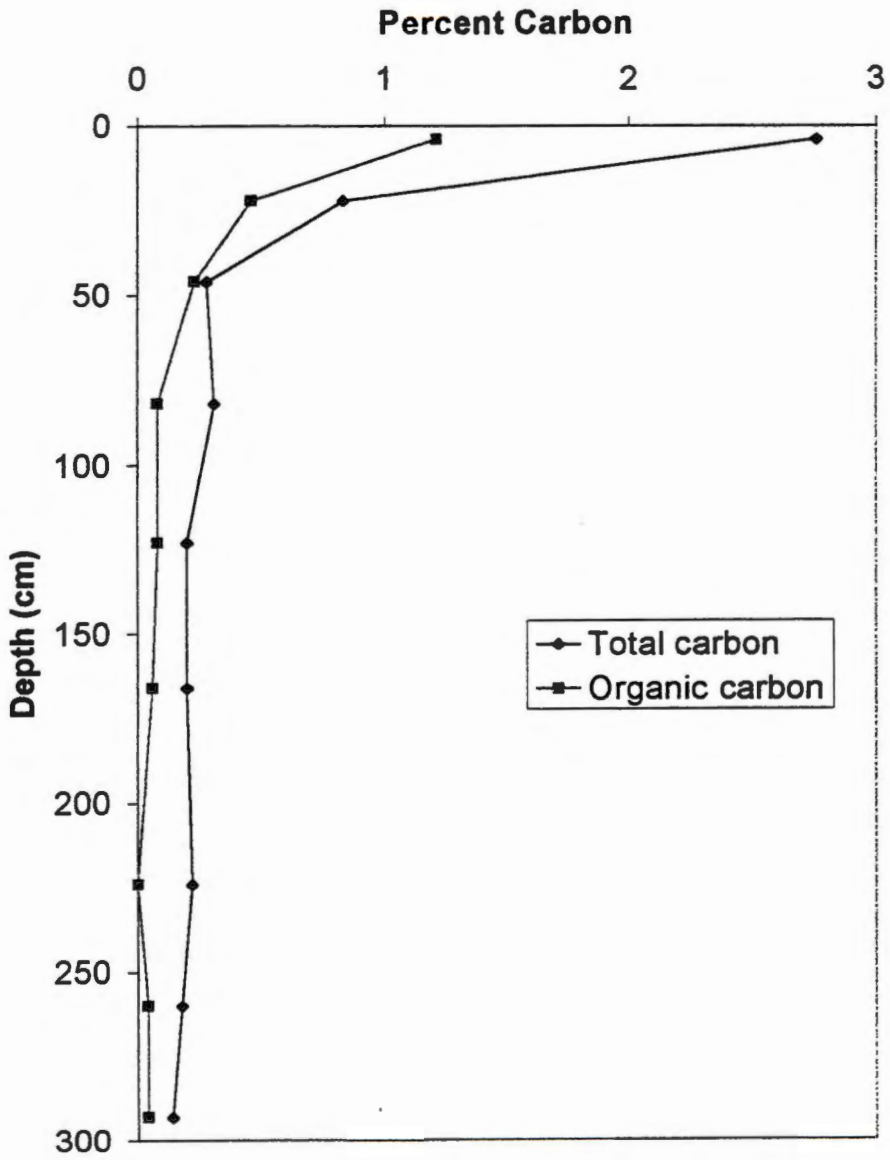


Figure 46. Plot of total and organic carbon for site 8.

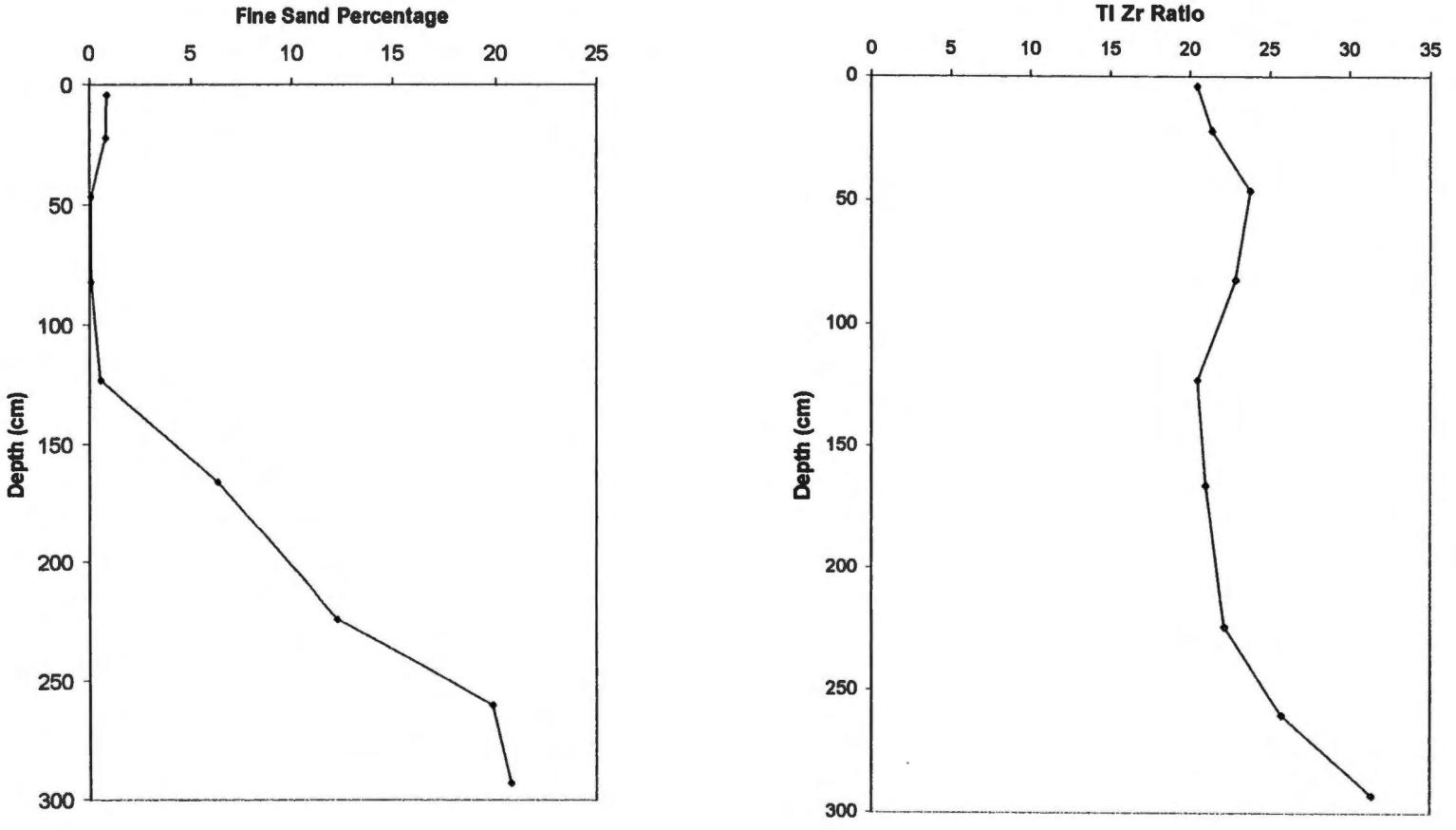


Figure 47. Plots of fine sand and titanium to zirconium for site 8.

prior to its burial and/or the presence of a mixing zone between the alluvium and the Tertiary sands. Bulk densities increased with depth, coinciding with the sand increase (Fig. 39). Free iron oxides changed very little in this layer (Fig. 45). Total carbon decreased steadily through out the remainder of the Tertiary sand, indicating that this material has undergone a relatively typical weathering pattern prior to burial (Fig. 46).

Saturated hydraulic conductivity was measured above and below the loess/alluvium interface at depths of 102 cm and 122 cm, respectively (Fig. 48). As in the previous sites, K_{sat} above the interface was lower than below the interface. Above the interface the K_{sat} was 0.04223 cm/hr, while below the interface the K_{sat} was 0.06225 cm/hr, both in the low K_{sat} class (Soil Survey Staff, 1993). Again, this difference could initiate lateral water movement.

The particle size control section had 2.4 percent sand and 25.9 percent clay, making it fine-silty (Fig. 44). Mineralogy was mixed. The CEC/clay ratio in the control section (upper 50 cm of the argillic) was .51, putting it into the active cation exchange capacity class. This soil had an ochric epipedon, an argillic sub-surface horizon, and a base saturation of 44 percent by sum of cations at 125 cm below the top of the argillic horizon making this soil an alfisol. Since base saturation was less than 60 percent this soil will be in the Ultic subgroup of the alfisol order. This site was classified as a Fine-silty, mixed, active, thermic Ultic Hapludalf.

Site nine

Site nine was located at N 35° 8' 4.2", W 89° 13' 22.8", on an upland position, under a forage cropping arrangement, at an elevation of 165.9 meters above sea level.

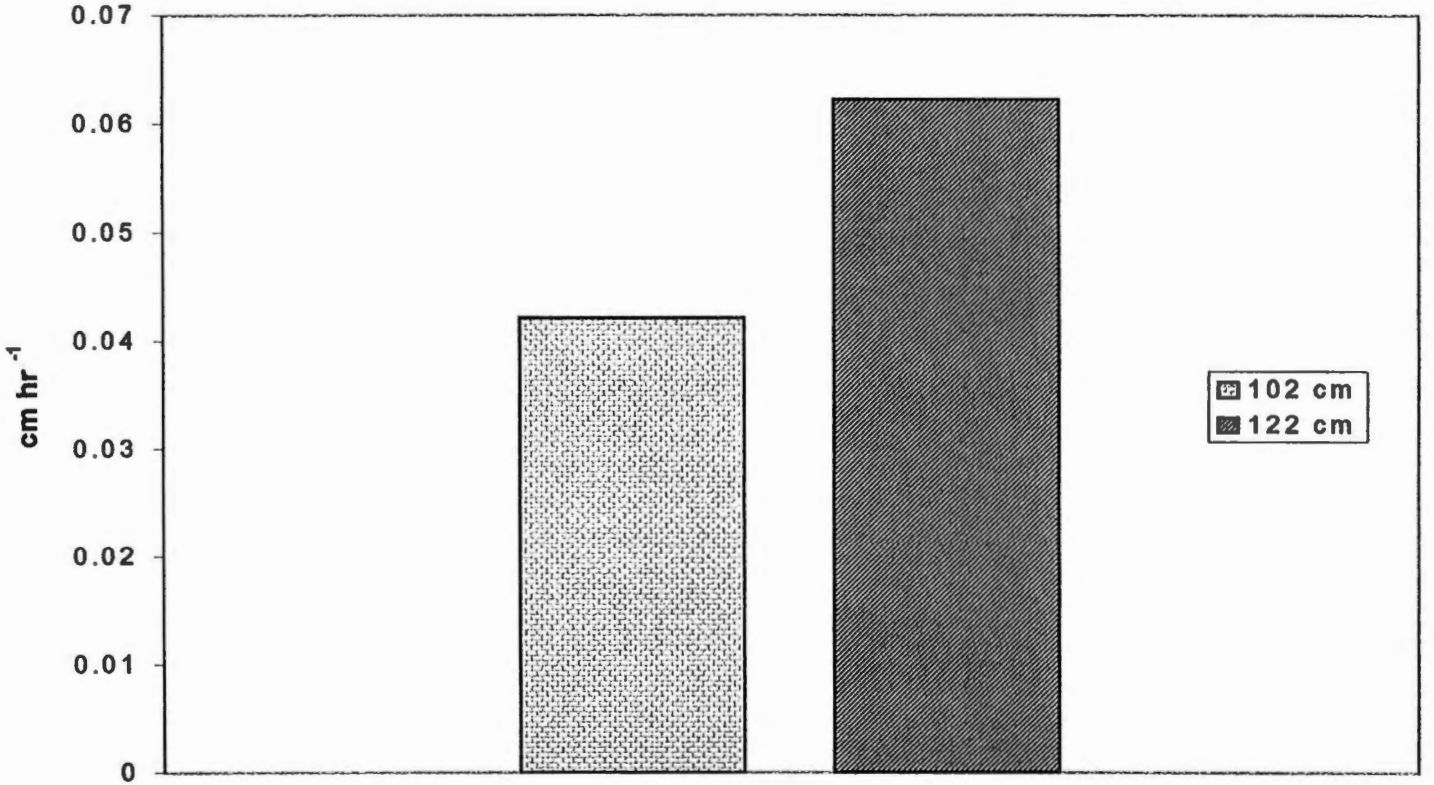


Figure 48. Graph of hydraulic conductivity values at 102-cm and 122-cm depths for site 8.

Soil morphology was sampled and described to a depth of 246 cm. Parent material was loess over alluvium over Tertiary aged sand.

Loess was present from the surface to a depth of 90 cm. Soil color was 10YR 4/4 and 10YR 4/3 in the Ap and Bt1 horizons, respectively. Soil color throughout the remainder of the loess was 7.5YR 4/4. Silt percentage ranged from 80.3 % in the surface to 70.4 % in the Bt2 horizon (25 - 57 cm) (Fig. 49). Free iron oxide and total iron concentration increased with depth until the Bt2 horizon (25 - 57 cm) before dropping off steadily (Fig. 50). Total and fine clay percentages also had their maximums in the Bt2 horizon, as expected (Fig. 50). Total and organic carbon had a regular decrease with depth indicating a typical weathering pattern (Fig. 51). Bulk density was highest in the Bt1 horizon, most likely from vehicle compaction (Fig. 39). Fine sand percentage increased sharply below the BC1 horizon (57 - 90 cm), indicating a lithologic discontinuity between the loess and alluvium (Fig. 52). Data in the loess was uniform, thus discrete depositions could not be detected within the loess. The loess present was most likely part of the Peoria loess deposit.

Alluvium was present from 90 cm to 199 cm below the surface. Carbon distribution throughout this layer was somewhat capricious (Fig. 51). Fine sand and total sand percentages increased with depth throughout this layer (Figs. 49, 52). Again, this deposit was likely the result of cyclic depositions from meandering streams. Free iron oxides decreased sharply at first then leveled out in the 2BC3 (117 - 160 cm) and 2BC4 (160 - 199 cm) horizons (Fig. 50). As seen in the other sites, the bulk density values were much higher than in the overlying loess (Fig. 39). Soil color in this layer was 5YR 4/4 in the 2BC2 and 2BC3 horizons and 2.5YR 4/4 in the 2BC4 horizon (160 - 199 cm). At 199

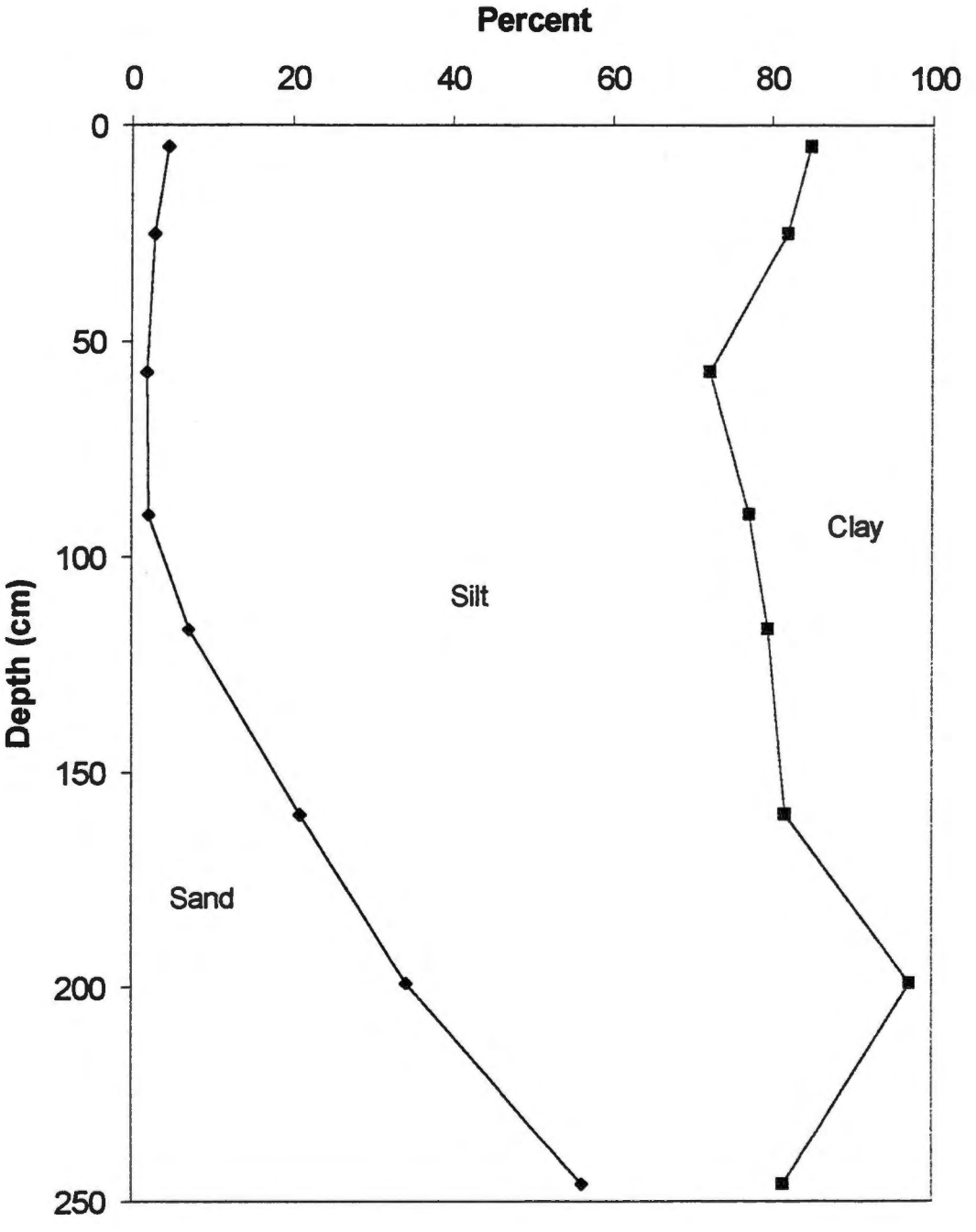


Figure 49. Cumulative particle size plot for site 9.

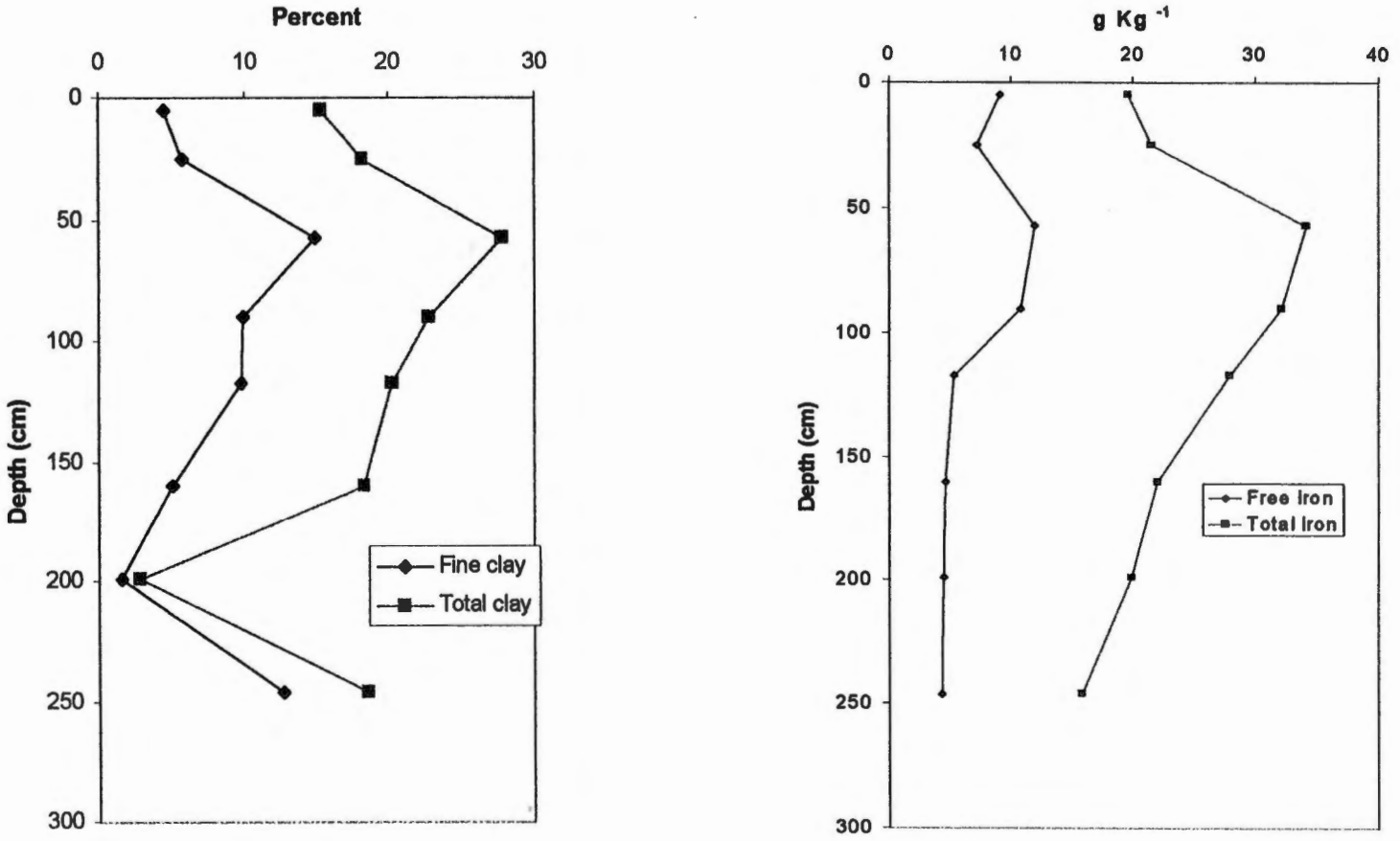


Figure 50. Plots of fine clay, total clay, free iron, and total iron for site 9.

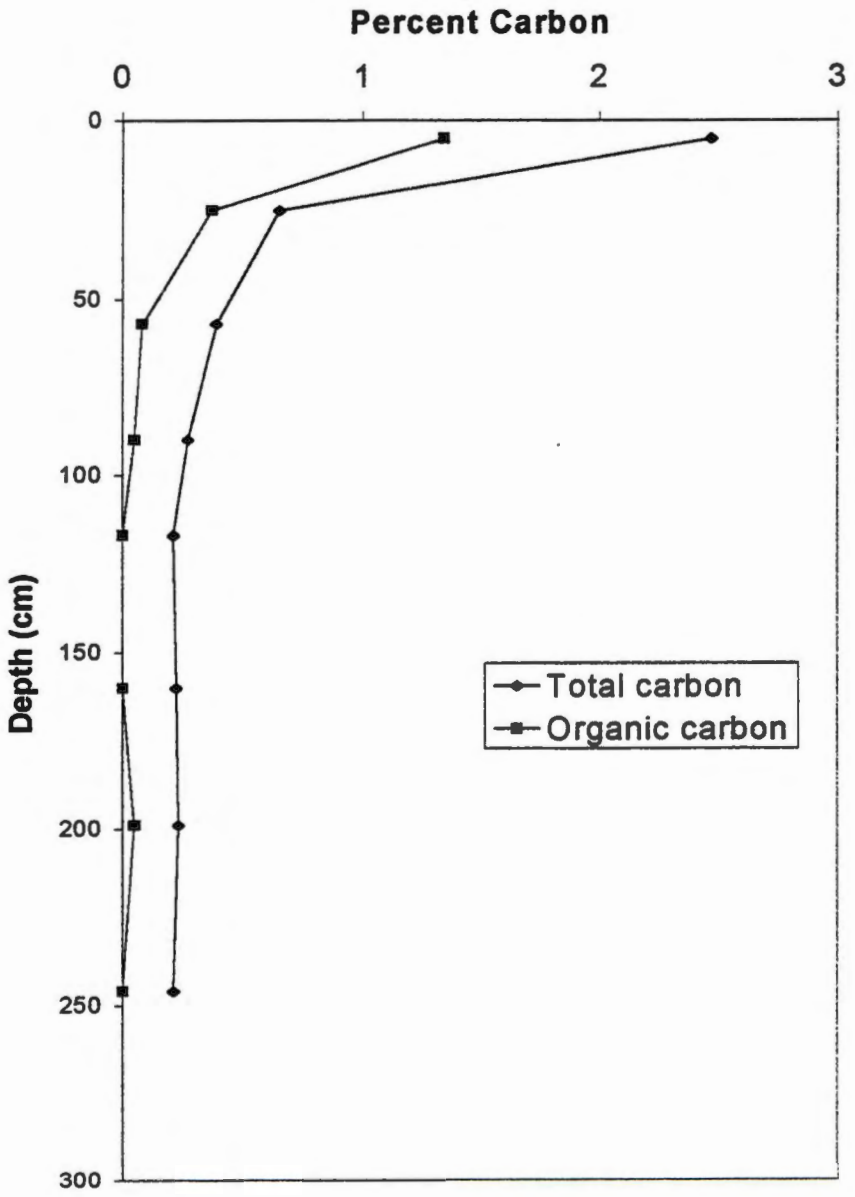


Figure 51. Plot of total and organic carbon for site 9.

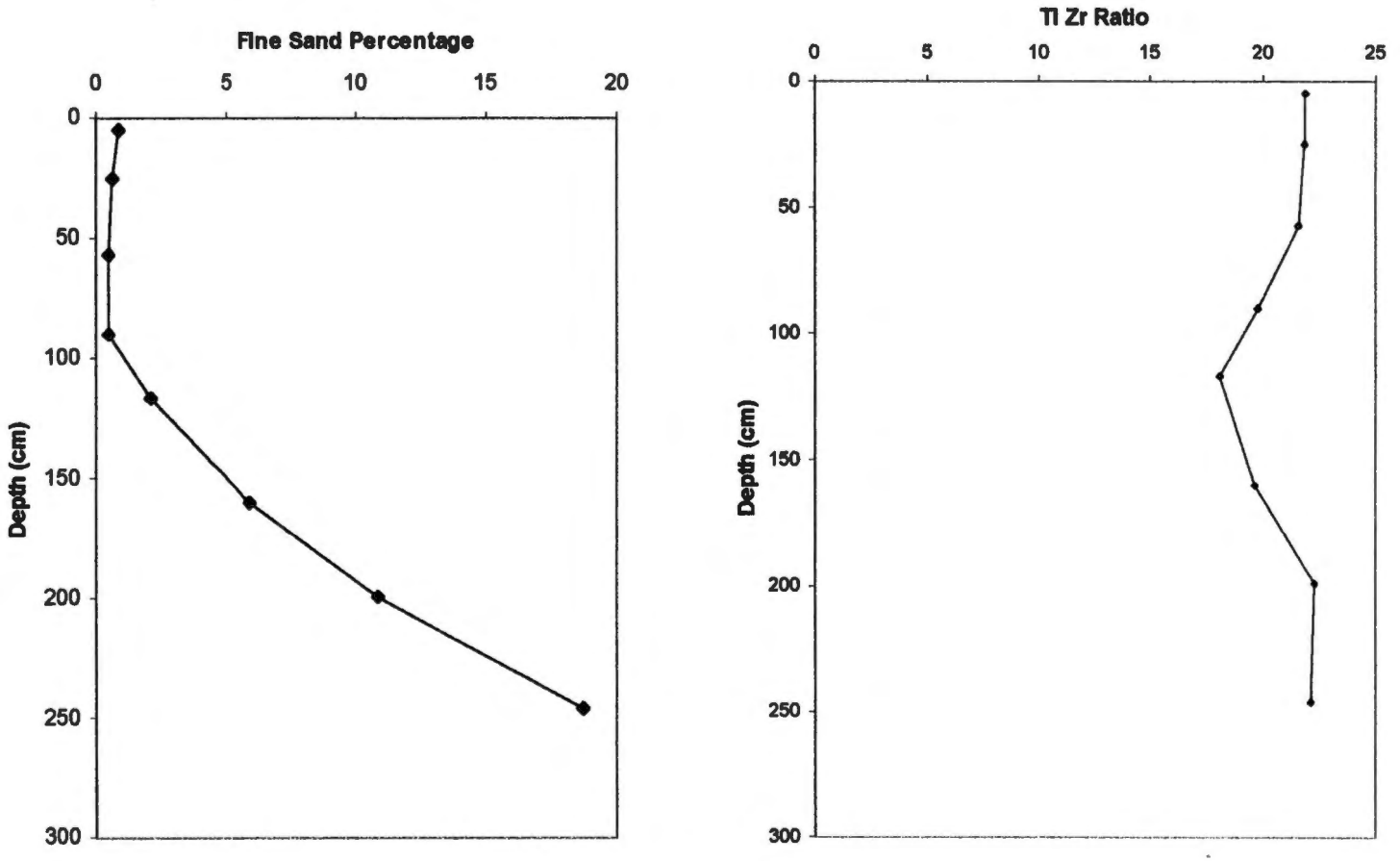


Figure 52. Plots of fine sand and titanium to zirconium for site 9.

cm there was a sharp increase in both fine sand and titanium to zirconium ratio, marking the second discontinuity (Fig. 52).

Tertiary sand was present from 199 cm through the extent of the core sampled. Like sites one, two, and three; material has been illuviated and enough clay has formed to create an argillic horizon (Fig. 49). Unlike sites five, six, and eight; this site was not eroded to the same degree prior to the influx of alluvium, and thus more of the former soil was preserved. The bulk density was significantly lower than in the overlying layer, most likely due to the increase in clay (Fig. 39). Soil color in this layer was 2.5YR 4/4.

Measurements of saturated hydraulic conductivity were made above and below the loess/alluvium interface at 111 cm and 125 cm, respectively (Fig. 53). As seen in the other sites, the horizon above the interface is less conductive, 0.03221 cm/hr, while below the interface the K_{sat} is 0.06225 cm/hr. Both horizons are in the low K_{sat} class (Soil Survey Staff, 1993). The less conductive horizon could possibly cause lateral water movement above the interface.

The particle size control section had 2.4 percent sand and 22.9 percent clay, making it fine-silty (Fig. 49). Mineralogy was mixed. The CEC/clay ratio in the control section (upper 50 cm of the argillic) was 0.51, putting it into the active cation exchange capacity class. This soil had an ochric epipedon, an argillic sub-surface horizon, and a base saturation of 49 percent sum of cations at 125 cm below the top of the argillic horizon making this soil an alfisol. Having a base saturation less than 60 percent put this soil into the Ultic subgroup of the alfisol order. This site was classified as a Fine-silty, mixed, active, thermic Ultic Hapludalf.

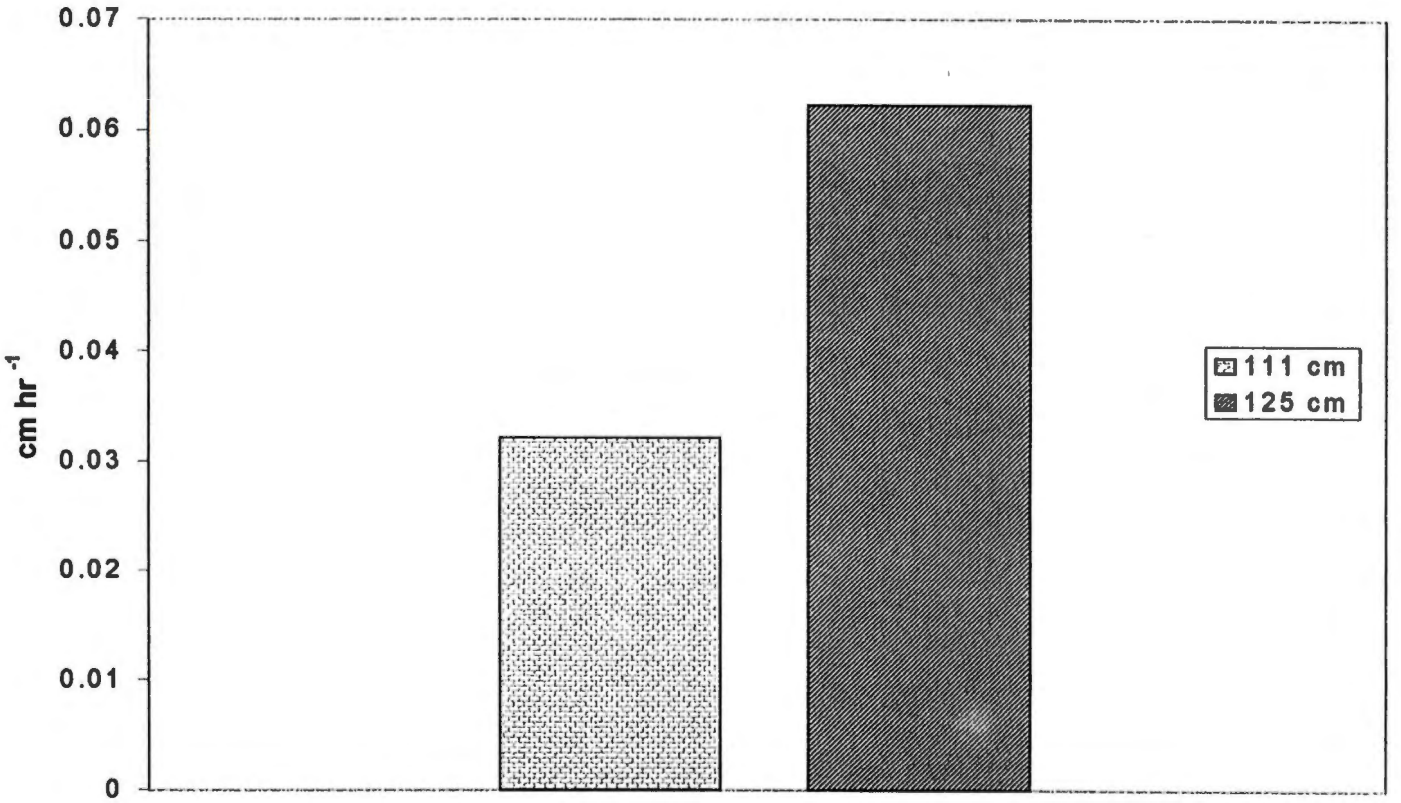


Figure 53. Graph of hydraulic conductivity values at 111-cm and 125-cm depths for site 9.

Conclusions

1. Sites one and five were classified as fine-silty, mixed, superactive, thermic, Ultic Hapludalfs. Sites two, three, four, six, seven, eight, and nine were classified as fine-silty, mixed, active, thermic, Ultic Hapludalfs. All sites were located on upland landscape positions. Parent material was loess over alluvium over Tertiary sand for all sites.

2. Data were insufficient to differentiate different loess depositions. The loess present at all sites was most likely the Peoria loess deposit.

3. Loess thickness ranged from 90 cm to 144 cm, mean thickness was 115 cm ± 10.3 cm. Thickness of the alluvium ranged from 82 cm to 151 cm, the mean thickness was 122 cm ± 20.5 cm. Neither pedons sampled at site four and seven were deep enough to reach the alluvium/Tertiary sand interface.

4. In all sites except site six, carbon distribution was somewhat irregular in the alluvial layer, indicating a cyclic depositional environment.

5. A fining upward trend was seen in the alluvium of all sites. Fining upward sequences are commonly associated with meandering stream systems.

6. The second horizon in all sites showed evidence of compaction, most likely due to the field being used as a parking lot. Further compaction was observed at depth, where bulk density values were abnormally high. This is likely due to a combination of: 1) compaction caused from the Giddings hydraulic probe and 2) actual differences due to porosity and texture.

7. There were no buried A horizons observed, indicating that erosional processes truncated the surfaces prior to burial. Argillic horizons were identified in the Tertiary sands in sites one, two, three, and nine; probably due to varying degrees of erosion prior to burial.

8. Saturated hydraulic conductivity was lower above the loess/alluvium interface in all sites studied, possibly causing lateral movement of fluids at this interface.

Chapter 3.

Non Intrusive Soil Investigation of a Landscape at the Ames Plantation

Introduction

Previous research at Ames has indicated water and thus agricultural chemicals move off-site via sub-surface preferential flow paths. Since the inception of the water quality project in 1990, researchers have been unable to identify preferential flow paths and predict water flow using traditional sampling techniques such as random sampling and grid sampling (Yoder, 1999). It is important to be able to identify and map the subsurface features that influence the lateral movement of water in the sub-surface. Use of non-intrusive soil investigation techniques such as EMI and GPR could prove to be an invaluable tool because sub-surface data can be obtained quickly and relatively inexpensively as well as nondestructively for an area. The objectives of this chapter were to 1) obtain EMI and GPR data collected from a second party, and 2) compare the soil morphological data obtained in chapter 2 to the EMI and GPR data to access the efficacy of both the EMI and GPR as a non-intrusive soil investigation tool.

Remote Sensing

Researchers began using electromagnetic signals to locate buried objects in the early twentieth century in Germany. In 1904, Hülsmeyer obtained the first patent on this new technology (Reynolds, 1997). Also in Germany, Leimbach and Löwy published the

first professional paper on locating buried objects using remote sensing in 1910 (Reynolds, 1997). Early researchers used what is called continuous wave (CW) transmission. In 1926, pulsed wave transmission was first used to locate buried objects in Germany by Hülsenbeck (Reynolds, 1997).

By 1960, remote sensing was being used to examine the polar ice sheets and conduct glaciological studies. With the onset of the Vietnam War, GPR was used heavily to locate unexploded ordinance, tunnels, and graves (Miller, 1996). After the war, GPR continued to be used by the military to find unexploded ordinance on bases in the U.S. During the late 1970s, GPR began being used in the private sector as an environmental tool. It is during this time that GPR was shown to be an effective tool to locate anthropogenic environmental problems such as contaminant plumes, landfill debris, voids beneath roads, and buried utility lines (Miller, 1996). Additionally, GPR was being used by geologists to locate depth to bedrock, mineral deposits, and in 1978 the first soil maps using GPR were produced.

Ground Penetrating Radar (GPR)

The design of a GPR unit is fairly simple, it consists of a portable GPR base unit (transmitter and receiver), a power source such as a 12- volt battery, an antenna in a box that can be pulled across the ground, and 30-60 meters of cable. Operation of such a unit can require up to four operators: 1) one person to operate the GPR itself, 2) one person who pulls the antenna, 3) two people who hold the lines to keep the unit straight within the grid (Miller, 1996).

When a GPR unit is pulled across a transect the transmitter antenna generates pulses of radio waves which propagate outward in a broad beam through the medium (Reynolds, 1997). These impulses travel through air at the speed of light (300,000 km/s). Once the impulse is reflected off an anomaly the receiver picks the signal up and records it as a function of two-way travel time. GPR output display is analogous to a seismograph in appearance, however, it uses electromagnetic energy while seismographs use an acoustic energy source (Smith and Jol, 1995).

GPR output is dependent upon the attenuation of electromagnetic waves and the speed of radiowave propagation in a material, both of which are functions of the electromagnetic properties of that material (table 1). The electromagnetic properties in a material are controlled by composition and water content of the material(s).

The speed of a radiowave through a material is dependent upon three factors: 1) the speed of light through free space, which is equal to c = 0.30 m/ns, 2) the dielectric constant of the material εr (table 2), and 3) the relative magnetic permeability of the material μ_r, which is equal to one for non-magnetic materials (Reynolds, 1997). The dielectric constant (ε_r) of a material is defined by the equation [$\varepsilon_r = Cd/Co$], which is the ratio of the capacitance of a condenser with the material in question being used as the dielectric (insulator) to the capacitance of the condenser with a vacuum being used as the dielectric (Buech,1972). For example, a material that has a low dielectric constant will be able to effectively reduce an electric field, whereas a material with a high dielectric constant will conduct electricity. Relative magnetic permeability is defined as the ratio of

Table 1. Relative success of GPR surveys in different media

Good Depth and High Resolution	**Attenuated Signal and Poor Resolution**
Sandy dunes	Clayey soil
Gravel	Shale
Upland volcanic deposits (tuff, loam, pumice)	Marsh
Upland coastal plain sediments	Caliche
Karst	Coastal marine
Urban areas i.e. pavement	Glacial till

Source: Reynolds (1997)

the magnetic permeability of the material in question to the magnetic permeability of free air (vacuum), which is denoted by μ_0, and has the value ($4\pi*10^{-7}$ Wb^{-1} A^{-1}), (Reynolds, 1997).

The speed of radiowaves through a material (Vm) is given by:

$$V_m = c/\{(\varepsilon_r\mu_r/2)[(1+P^2)+1]\}^{½}$$

Where c is the speed of light in free space, εr is the relative dielectric constant, μr is the magnetic permeability (=1 for non-magnetic materials), P is the loss factor, such that $P=\sigma/\omega\varepsilon$, σ is the conductivity, $\omega = 2\pi F$, where F is the frequency, ε is the permativity which equals $\varepsilon_r/\varepsilon_o$ where ε_o is the permittivity of free space ($= 8.854*10^{-12}$).

Table 2. Dielectric constants of ubiquitous materials.

MATERIAL	μ_r
AIR	1.006
ICE(-5 c)	2.9
MICA	6
WATER (pure)	81
COASTAL SAND (DRY)	10
SAND (WET)	25-30
CLAY (WET)	8-15
CLAY (DRY)	3
AGRICULTURAL LAND	15
GRANITE	5-8
LIMESTONE	7-9
DOLOSTONE	6.8-8
CONCRETE	6-30
ASPHALT	3-5

Source: Reynolds (1997)

The potential for successful GPR survey is high in areas that have coarse to moderately coarse textured soils with low amounts of expandable clays and low amounts of dissolved salts (Doolittle and Collins, 1995). Addition of water to the soil will cause minor signal attenuation while the presence of salts, clays, and saline conditions will cause severe attenuation (Smith and Jol, 1995). Doolittle and Collins (1995), found it

imperative to have soil morphology information prior to conducting a GPR investigation due to the discrepancies in output caused by soil variability.

Antenna Frequency

It is very important when conducting a GPR survey to choose an antenna frequency appropriate for the objectives of the survey. Most GPR units operate in the VHF-UHF region of the electromagnetic spectrum. The frequency used in a survey is a compromise between desired depth and acceptable resolution. As antenna frequency increases, depth of penetration decreases while quality of resolution increases. For most soil surveys, frequencies of 300 to 500 MHz are commonly used. However, for deep geologic investigations, frequencies as low as 20 MHz are used. For shallow high resolution surveys, frequencies as high as 900 MHz. Smith and Jol (1995) found a linear relationship between antenna frequency, travel time, and depth of maximum depth of penetration in Quaternary sand and gravel deposits in Lake Bonneville, Utah, USA.

GPR Applications

As technology improves, the application of GPR continues to expand. Today, it is used extensively in such varied fields as forensics, pedology, geology, and engineering. It has been used to successfully estimate depth to soil horizons (Collins and Doolittle, 1987), organic material extent and thickness (Doolittle et al., 1990; Collins et al., 1986; Doolittle, 1983), and depth to bedrock (Collins et al., 1989). Rebertus and Doolittle (1989) used GPR to determine loess thicknesses and to map the paleosol surface at two sites in Northern Delaware. In Southwestern Tennessee, Freeland et al. (1997)

determined loess thickness, paleo-surface topography, and ephemeral drainage areas within a paleosol. Miller (1996) located and determined the precise metric grid coordinates, size, shape, and depth of an object.

EMI

Conrad Schlumberger first mapped electrical conductivity and resistivity in the early twentieth century (McNeill, 1980). He employed a technique that involved injecting an electrical current into the ground and mapping the potential distribution. Today, the method has a wide variety of uses including: locating depth to bedrock, lithology of rock strata, location and mapping of clay deposits, mapping ground water distribution, detecting contaminant plumes, mapping permafrost and ice, and archeological mapping (McNeill, 1980).

The EMI (EM-31), produced by Geonics Limited, is designed to conduct a resistivity survey with one operator while walking. According to McNeill (1980), the EMI operates by sending out a sinusoidally varying magnetic field that induces currents in the ground, of which the amplitude is linearly proportional to the terrain conductivity. One can determine the magnitude of these currents by measuring the magnetic field generated (McNeill, 1980).

Electrical conductivity can be defined as the ease with which an electrical current will pass through the material in question. Resistivity is the reciprocal of conductivity and can be explained by Ohm's Law: $\rho = RA/L$ ohms · meter, where $R=V/I$ and is expressed as volts per amperes, or ohms (Tipler, 1991).

Physical and chemical properties of a material will affect the conductivity and resistivity. Conductivity through a material (soils and rocks) takes place through the moisture-filled pores (McNeill, 1980). Therefore, it is affected by porosity, moisture content, concentration of dissolved electrolytes, temperature of the interstitial liquid, and concentration of colloids (McNeill, 1980).

EMI Uses

The EMI is used to provide an above ground view of the bulk electrical conductivity of a soil. Often the EMI is used as a preliminary investigation tool to find anomalies in bulk electrical conductivity. The EMI can provide information up to 6 meters below the soil surface.

Ammons et al. (1989), used an EM-38 to separate saline from non-saline soils in Gibson County, TN. Jordon and Costanini (1995) found the EM-31 to be a very effective tool for obtaining information on buried drums, storage tanks, and utilities. The EM-31 was successfully used by Thamke (1999) to delineate the lateral extent of saline-water contamination plumes in Quaternary alluvial deposits in Northeastern Montana. Rogers et al. (1996) mapped shallow lithologic variations at a discontinuity that controlled off-site movement of hydrocarbons near Glenrock, Wyoming using both an EM-31 and an EM-34.

Materials and Methods

Field Methods

A grid was laid out with survey flags spaced 15.25-m apart. The perimeter was mapped as well as points taken at each flag (43 flags) using a Trimble Ag.GPS™ 132. A Geonics EM-31™ was used to take bulk conductivity readings to both the 3-m and 6-m depths. The data were merged with GPS data to produce electrical conductivity maps using Arc View ™. Ground-penetrating radar data was collected using an SIR System-10A, manufactured by GSSI, Inc., North Salem, NH, USA. Data from the GPR was interfaced with GPS to produce 3-D images of the subsurface.

Statistical Analysis

Soil morphological and physical data were analyzed using Ward's Minimum Variance Cluster Analysis (SAS Institute, 1998). Variables included: percent sand, silt, clay, texture, bulk density, particle density, and total porosity. Clusters of sites by horizon were made within the upper 130-cm of the pedons. Using clusters based upon the Ap, Bt1, Bt2, C1 horzons, a frequency table was created. From the frequency table, groups were separated based upon a clustering frequency of three or more, with a maximum frequency of four.

GPR and EM-31 data were analyzed and grouped visually based upon output similarities. Groups produced from the two methods were analyzed for degree of agreement using SAS (SAS Institute, 1998).

Results and Discussion

Ward's minimum variance clustering analysis of sites within the Ap horizons yielded the following clusters: i) sites 1, 2, 3, 4, 7; ii) sites 5, 6, 8; and iii) site 9 (table 3). Within the Bt1 horizons, the following clusters were formed: i) sites 5, 6, and 8; ii) sites 1, 2, 3, 4, and 7; and iii) site 9 (table 4). From the Bt2 horizons, clustering by site produced the following clusters: i) sites 1, 3, 4, 6, 7, 8, and 9; ii) site 5; and iii) site 2 (table 5). Clusters from the BC1 horizons were: i) sites 2, 5, 6, 7, 8, 9; ii) sites 1, and 3; and iii) site 4 (table 6). Clustering from the BC2 horizons were: i) site 8; ii) site 9; and iii) site 4 (table 7). BC2 clusters were not taken into account when determining the final grouping. From table 8, groups were formed based upon a clustering frequency of three or more. These groups were as follows: I) sites 1, 3, 4, and 7; II) sites 5, 6, and 8; III) sites 2 and 7 (table 9). From table 9, site seven is grouped into two groups, while site nine is not grouped at all.

Table 3. Table of cluster by site for horizon = Ap

Cluster	Site 1	Site 2	Site 3	Site 4	Site 5	Site 6	Site 7	Site 8	Site 9
1	1	1	1	1	0	0	1	0	0
2	0	0	0	0	1	1	0	1	0
3	0	0	0	0	0	0	0	0	1

Table 4. Table of cluster by site for horizon = Bt1

Cluster	Site 1	Site 2	Site 3	Site 4	Site 5	Site 6	Site 7	Site 8	Site 9
1	0	0	0	0	1	1	0	1	0
2	1	1	1	1	0	0	1	0	0
3	0	0	0	0	0	0	0	0	1

Table 5. Table of cluster by site for horizon = Bt2

Cluster	Site 1	Site 2	Site 3	Site 4	Site 5	Site 6	Site 7	Site 8	Site 9
1	1	0	1	1	0	1	1	1	1
2	0	0	0	0	1	0	0	0	0
3	0	1	0	0	0	0	0	0	0

Table 6. Table of cluster by site for horizon = BC1

Cluster	Site 1	Site 2	Site 3	Site 4	Site 5	Site 6	Site 7	Site 8	Site 9
1	0	1	0	0	1	1	1	1	1
2	1	0	1	0	0	0	0	0	0
3	0	0	0	1	0	0	0	0	0

Table 7. Table of cluster by site for horizon = BC2

Cluster	Site 1	Site 2	Site 3	Site 4	Site 5	Site 6	Site 7	Site 8	Site 9
1	NA*	NA*	NA*	0	NA*	NA*	NA*	1	0
2	NA*	NA*	NA*	0	NA*	NA*	NA*	0	1
3	NA*	NA*	NA*	1	NA*	NA*	NA*	0	0

*NA = BC2 horizon not present at that site.

Table 8. Frequency of clustering from horizon = Ap, Bt1, Bt2, and BC1.

	Site 1	Site 2	Site 3	Site 4	Site 5	Site 6	Site 7	Site 8	Site 9
Site 1	x	2	4	3	0	1	3	1	1
Site 2	2	x	2	2	1	1	3	1	1
Site 3	4	2	x	3	0	1	3	1	1
Site 4	3	2	3	x	0	1	3	1	1
Site 5	0	1	0	0	x	3	1	3	1
Site 6	1	1	1	1	3	x	2	4	2
Site 7	3	3	3	3	1	2	x	2	2
Site 8	1	1	1	1	3	4	2	x	2
Site 9	1	1	1	1	1	2	2	2	x

Groupings of sites based upon visual interpretation of GPR and EM-31 data were as follows: i) sites 1, 3, 4, and 7; ii) sites 6, 8, and 9; and iii) sites 2 and 5 (table 10). Groupings based upon GPR and EM-31 data matched well with groupings based upon clustering analysis of the soil data (table 11). Analysis of agreement between groupings at the 95 % level of confidence yielded a Kappa value of .8 +/- .34 (table 12). This was a

Table 9. Groups based upon frequency of 3 or more.

Group	Site 1	Site 2	Site 3	Site 4	Site 5	Site 6	Site 7*	Site 8	Site 9
1	x		x	x			x		‡
2		x					x		‡
3					x	x		x	‡

‡ = Did not appear with any site more than twice.
* = Appeared in more than one group.

Table 10. GPR/EM-31 Groups.

Group	Site 1	Site 2	Site 3	Site 4	Site 5	Site 6	Site 7	Site 8	Site 9
1	x		x	x			x		
2		x			x				
3						x		x	x

Table 11. Groups (by site) of soil data compared to GPR/EM-31 data.

Group	Soil Data	GPR/EM-31 Data
1	1, 3, 4, 7	1, 3, 4, 7
2	5, 6, 8	6, 8, 9
3	2, 7 *	2, 5

* Site 7 appeared in more than one group.

Table 12. Frequency statistics of final groupings.

Statistic	Value	95% Confidence Bounds
Simple Kappa	0.800	0.461 - 1.139
Weighted Kappa	0.846	0.583 - 1.109

strong agreement. The Weighted Kappa value was not taken into account because the unequal number of sites between techniques (site nine not being grouped) was significant. Based upon the data, the GPR and EM-31 were very effective tools for separating soils of differing physical properties formed on a loess/alluvium/Tertiary sand parent material. Further, with the aid of artificial intelligence such as Neural Networks, clustering of sites based upon remote sensing data will become more expeditious and reliable.

Conclusions

1. Final groupings of sites based upon soil morphological and physical properties were as follows: group 1) sites 1, 3, 4, 7; group 2) sites 5, 6, and 8; group 3) sites 2 and 7. Site 9 was not grouped with any of the other sites, while site 7 was grouped twice.

2. Groupings of sites based upon GPR and EM-31 were: group 1) sites 1, 3, 4, and 7; group 2) 6, 8, and 9; group 3) sites 2 and 5.

3. The groupings based upon the GPR and EM-31 data agreed very well with the groupings based upon clustering analysis of soil morphological and physical data, K = .8 +/- .34.

4. The GPR and EM-31 are promising non-intrusive soil investigation tools. As software is developed to assist with analysis of patterns the effectiveness of these tools will improve.

References

References

Ammons, J.T., M.E. Timpson, and D.L. Newton. 1989. Application of Aboveground Electromagnetic Conductivity Meter to Separate Natraqalfs and Ochraqualfs in Gibson County, Tennessee. Soil Survey Horizons, 30: 66-70.

Amoozegar, A. 1989a. A compact constant-head permeameter for measuring saturated hydraulic conductivty of the vadose zone. Soil Sci. Soc. Am. J. 53:1356-1361.

Amoozagar, A. 1989b. Comparison of the Glover solution with the simultaneous equations approach for measuring hydraulic conductivity. Soil Sci. Soc. Am. J. 53: 1362-1367.

Autin, W.J. 1996. Pleistocene Stratigraphy of the Lower Mississippi Valley. Engineering Geology: 45; 87-112.

Berg, L.S. 1964. Loess as a Product of Weathering and Soil Formation. Isreal Program for Scientific Translations. Jerusalem, Isreal

Blake, G.R. 1965. Particle Density. *In*: C.A. Black (ed.) Methods of Soil Analysis. Agronomy 9: 371-373. Am. Soc. of Agron., Madison, WI.

Boul, S.W., F.D. Hole, R.J. McCracken, and R.J. Southard. 1997. Soil Genesis and Classification (4th ed.). Iowa State University Press. Ames, Iowa

Buech, F. 1972. Principles of Physics. (2nd Ed). Mcgraw-Hill. New York.

Call, R.E. 1891. Annual Report of the Geological Survey of Arkansas for 1889. Vol. 2, The Geology of Crowley's Ridge. Woodruff Printing Co., Little Rock, AR, 283pp.

Campbell, Saundra. 1996. The Crown Jewel: Spanning Counties, Ames Plantation Also Has a Rich Tradition in Research. U.T. Agriculture, winter 1996.

Chapman, H.D. 1965. Cation Exchange Capacity. *In*: C.A. Black, et al (eds.) Methods of Soil Analysis. Part 1. 1st ed. Agronomy Monogr. 9. ASA and SSSA.

Collins, M.E and J.A. Doolittle. 1987. Using Ground Penetrating Radar to Study Soil Microvariability. Soil Sci.Soc Am. J. 51: 491-493.

Collins, M.E., G.W. Schellentrager, J.A. Doolittle, and S.F. Shih. 1986. Using Ground Penetrating Radar to Study Changes in Soil Map Unit Composition in Selected Histosols. Soil Sci.Soc Am. J. 50: 408-412.

Collins, M.E., J.A. Doolitte, and R.V. Rourke. 1989. Mapping Depth to Bedrock on a Glaciated Landscape using Ground Penetrating Radar. Soil Sci.Soc Am. J. 53: 1806-1812.

Doolittle, J.A. 1983. Investigating Histosols with Ground Penetrating Radar. Soil Survey Horizons. 23(3): 23-28.

Doolittle, J.A., P. Fletcher, and J. Turenne. 1990. Estimating the thickness and volume of organic materials in cranberry bogs. Soil Survey Horizons, 29(2): 46-54.

Doolittle, J.A. and M.E. Collins. 1995. Use of Soil Information to Determine Application of Ground Penetrating Radar. Journal of Applied Geophysics. 33:101-108.

Emerson, F.V. 1918. Loess depositing winds in the Louisiana region. J. Geol., 26: 532 - 541.

Follmer, L.R. 1996. Loess Studies in the Central United States: Evolution of Concepts. Engineering Geology: 45; 287-304.

Foth, H.D. 1984. Fundamentals of Soil Science. 7th ed. John Wiley & Sons. New York, New York.

Freeland, R.S., R.E. Yoder, and J.T. Ammons. 1997. Observing Preferential Flow Paths with Ground Penetrating Radar. Tennessee Agri. Science. Issue 181, Winter 1997.

Freeze, R.A. and J.A. Cherry. 1979. Groundwater. Prentice Hall. Englewood Cliffs, NJ.

Gallagher, A.O. 1993. A modified method of total elemental analysis for determining background metals in Tennessee. M.S. thesis. University of Tennessee.

Gambrell, R.P. and W.H. Patrick. 1982. Manganese. p. 313-322. *In* A.L. Page, et al. (ed.). Methods of soil analysis. Part 2. 2nd ed. Agron. Monogr. 9, ASA, Madison, WI.

Gee, G.W. and J.W. Bauder. 1986. Particle Size Analysis. *In:* A. Klute (ed.). Methods of Soil Analysis, Part 1. 2nd ed. Agronomy 9: 383-412.

Geyl, W.F. 1968. Tidal stream action and sea level change as of valley meanders and underfit streams. Aus. Geogr. Studies, 6:24-42.

Geyl, W.F. 1996. A geomorphical testament: tidal paleomorphs. NL Books, University of New Castle, NSW.

Hilgard, E.W. 1860. Report on the Geology and Agriculture of the State of Mississippi. E.Barksdale, State Printer. Jackson, Mississippi.

Hilgard, E.W. 1906. Soils, thier formation, properties, composition, and relations to climate and plant growth. The Macmillan Company. New York.

Hillel, D. 1982. Introduction to Soil Physics. Academic Press inc. San Diego, CA.

Jackson, M.L. 1958. Soil Chemistry: A First Course. 6th printing. Madison, WI.

Jenny, H. 1941. Factors of Soil Formation. McGraw-Hill. New York, New York.

Joeff, J.S. 1949. Pedology 2nd ed. Pedology Publications. New Brunswick, New Jersy.

Jordon, T.E. and D.J. Costantini. 1995. The Use of Non-Invasive Electromagnetic (EM) Techniques for focusing Environmental Investigations. The Professional Geologist, June 1995: 4-9.

Kellogg, C.E. 1941. The soils that support us. The Macmillan Co., New York.

Kilmer, V.J. and L.T. Alexander. 1949. Methods for Making Mechanical Analysis of Soils. Soil Sci. 68: 15-24.

Krinitzsky, E.L., and W.J. Turnbull. 1967. Loess deposits of the Mississippi. Geol. Soc. Am., Spec. Papers No. 94, New York, 64pp.

Leighton, M.M. and H.B. Willman. 1950. Loess formations of the Mississippi valley. Jour. Geology 58:599-623.

Leverette, F. 1899. Illinois glacial lobe. US Geol. Surv., Washington, DC, Monograph 38.

Livingston, R.L. 1993. Soil and Geomorphic Relationships on Two Water Quality Landscapes on the Ames Plantation. M.S. Thesis, Univ. of Tennessee.

Luxmoore, R.J. 1981. Micro-, meso-, and macroporosity of soil. Soil. Sci. Soc. Am. J. 45:671.

Lyell, C. 1834. Observations on the Loamy Deposit Called "Loess" of the Basin of the Rhine. Reprinted from *Edinburgh New Phil. Jour.*, 17(33), 110-113, 118-120. *In :* Smalley, I.J. (Ed.) Loess, its Lithology and Genesis. 1975. Dowden, Hutchinson, and Ross Inc. Stroudsburg, Pennesylvania.

Lyell, C. 1847. On the Delta and Alluvial Deposits of the Mississippi, and Other Points in the Geology of North America, Observed in the Years 1845-1846. Reprinted from *Amer. Jour. Sci.*,3 Ser.2, 34-35, 36-37. *In:* Smalley, I.J. (Ed.) Loess, its Lithology and Genesis. 1975. Dowden, Hutchinson, and Ross Inc. Stroudsburg, Pennesylvania.

Mabry, T.O. 1898. The brown or yellow loam of north Mississippi and it's relation to northern drift. J. Geol. 6: 273 - 302.

Markewich, H.W. (Ed.) 1994. Second progress report on chronostratigraphic and paleoclimatic studies, middle Mississippi River Valley, eastern Arkansas, western Tennessee, and northeastern Mississippi. US Geol. Surv. Open File Rept. 94 - 208.

McLean, E.O. 1982. Soil pH and Lime Requirement. *In:* A.L. Page et al. (eds.). Methods of Soil Analysis, Part 2. 2nd ed. Agronomy 9: 199-224.

McNeill, J.D. 1980. Electromagnetic Terrain Conductivity Measurmen at Low Induction Numbers. Geonics Limited. Technical Note TN-6. Mississauga, Ontario, Canada.

Miller, B.J. 1989. In: Autin, W.J., S.F. Burns, B.J. Miller, R.T. Saucier, and J.I. Snead. Quaternary Geology of the Lower Mississippi Valley. In: R.B. Morrison (ed.). Quaternary non-glacial geology: conterminous U.S. Geol. Soc. Am., Boulder, CO. Pp 564-573.

Miller, R.A. 1974. The Geologic History of Tennessee. Tennessee Dept. of Conservation, Div. of Geology. Bulletin 74. Nashville, Tn.

Miller, R.W. 1990. Soils, An Introduction to Soils and Plant Growth. 6th Ed. Prentice Hall. Englewood Cliffs, New Jersy.

Miller, P.S. 1996. Disturbances in the Soil: Finding Buried Bodies and Other Evidence Using Ground Penetrating Radar. Journal of Forensic Sciences. July 1996; 41(4): pp. 648-652

Moore, H.L. 1994. A Geologic Trip across Tennessee by Interstate 40. Knoxville, Tn.: The Univ. of Tennessee Press.

Nadkarni, R.A. 1984. Application of microwave oven sample dissolution in analysis. Anal. Chem. 56:2233-2237.

Olsen, R.V. and Ellis, R. (1982). Free Iron Oxides. *In:* A.L. Page et al. (eds.). Methods of Soil Analysis, Part 2. 2nd ed. Agronomy 9: 311-312.

Pecsi, M. 1990. Loess is not just the accumulation of dust. Quat. Intern. 7/8:1-22.

Rebertus, R.A. and J.A. Doolittle. 1989. Landform and stratigraphic Influences on Variability of Loess Thickness in Northern Deleware. Soil Sci.Soc Am. J. 53: 843-847.

Reynolds, J.M. 1997. An introduction to Applied and Environmental Geophysics. John Wiley and Sons. Chirchester, England.

Rogers, N.T., S.K. Sandberg, and G. Powell. 1996. The Effective Use of Electromagnetic Methods to Delineate A Fluvial Paleochannel System Controlling Oil Migration Near Glenrock, Wyoming. Proceedings of the SAGEEP, 1996, Keystone, Co. pp. 917-925. *From*: Geonics Limited, Ground Conductivty Meters for Environmental Site Evaluation. February 1999. Geonics Limited, Mississauga, Ontario, Canada.

Russell, R.J. 1944. Lower Mississippi Valley Loess. Reprited from *Bull. Geol. Soc. Amer.*, 55, 1-8, 23-30, 33-40. *In:* Smalley, I.J. (Ed.) Loess, its Lithology and Genesis. 1975. Dowden, Hutchinson, and Ross Inc. Stroudsburg, Pennesylvania.

Russell, E.E. and W.S. Parks. 1975. Stratigraphy of the Upper Cretaceous, Paleocene, and Lower Eocene in West Tennessee. TN. Division of Geology, Bulletin 79.

Shimek, B. 1902. The loess of Natchez, Mississippi. Am. Geologist, 30: 279 - 299.

Simonson, R.W. 1962. Soil Classification in the United States. Reprinted from *Science*, 137:1027-1034. *In*: Drew, J.V. (Ed.) Selected Papers in Soil Genesis and Classification. 1967. Soil Science Society of America, Inc. Madison, WI.

Smalley, I.J. (Ed). 1975. Loess, its Lithology and Genesis. Dowden, Hutchinson, and Ross Inc. Stroudsburg, Pennesylvania.

Smith, D.E. 1998. A Geomorphical Investigation of Soils Forming on the Humbolt Terrace in Western Tennessee. M.S. Thesis, Univ. of Tennessee.

Smith, G.D. 1942. Illinois loess - variation in its properties and distribution: a pedologic interpretation. Univ. IL Agric. Expt. Sta. Bull. 490, Urbana, IL. 184pp.

Smith, D.G. and H.M. Jol. 1995. Ground Penetration Radar Antenna Frequencies and Maximum Probable Depths of Penetration in Quaterary Seiments. Journal of Applied Geophysics. 33: 93-100.

Smith, R.M. 1957. Soil structural evaluation with a nonpolar liquid. Soil Sci. 84:311-322.

Snowden, J.O., Jr. and R.R. Priddy. 1968. Loess investigation in Mississippi. MS Geol., Econ. and Topo. Surv., Bull. 3. Jackson, MS.

Soil Survey Staff. 1993. Soil Survey Manual. USDA Handbook No. 18. U.S. Government Printing Office, Washington, D.C.

Soil Survey Staff. 1996. Soil Survey Laboratory Methods Manual. Soil Survey Investigation Report No.42 version 3.0. National Soil Suvey Center. Lincoln, NE.

Soil Survey Staff. 1999. Keys to Soil Taxonomy. U.S. Government Printing Office, Washington, D.C.

Stearns, R.G. 1957. Cretaceous, Paleocene, and lower Eocene geologic history of the northern Mississippi embayment. Bull. Geol. Soc. Am. 68:1077-1100.

Thamke, J.N. 1999. Use of Terrain Electromagnetic Geophysical Methods to Map Saline-Water Contamination, East Poplar Oil Field, Northeastern Montana. U.S. Geological Survey. *From*: Geonics Limited, Ground Conductivty Meters for Environmental Site Evaluation. February 1999. Geonics Limited, Mississauga, Ontario, Canada.

Thomas, G.W. 1982. Exchangable Cations. *From*: A.L. Page et al. (eds). Methods of Soil Analysis, Part 2. 2nd Ed. Agronomy 9: 159-164.

Tipler, P.A. 1991. Physics for Scientists and Engineers. 3rd ed. Vol. 2. Worth Publishers, New York, NY.

U.S. Geological Survey. 1980. Hickory Valley, TN quadrangle. 7.5 minute series. USGS. Reston, VA.

Vilenskii, D.G. 1957. Soil Science. State Teachers' College Publishing House, Ministry of Culture, Russian Socialist Federated Soviet Republic, Moscow.

Wacsher, H.L., Humbert, R.P., and Cady, J.G., 1947. Loess in the southern Mississippi Valley: Identification and distribution of the loess sheets. Soil Sci. Soc. Am. Proc., 12: 389-399.

West, L.T., E.M. Rutledge, and D.M. Barber. 1980. Sources and properties of loess deposits on Crowleys Ridge in Arkansas. Soil Sci. Soc. Am. J. 44:353-358

Yoder, R.E.; D.C. Yoder; C.R. Mote; M.E. Essington; J.T. Ammons; T.C. Mueller; and D.D. Tyler. 1998. Subsurface Water Movement on an Agricultural Watershed. Paper presented at the A.S.C.E International Water Resources Engineering Conference, August 3-7 1998, Memphis, Tn.

Yoder, R.E., R.S. Freeland, and J.T. Ammons. 1999. Predicting offsite subsurface migration of agrochemicals - noninvasive surveying. Unpublished report. 1-55pp.

Appendicies

Appendix A. Morphology and Laboratory Data for Site One

Field morphology data sheet, texture corrected by lab data.
Site 1.

Landscape position: Upland
Parent Material: Loess/Alluvium/Tertiary Sand
Elevation: 164.85 meters above mean sea level
Slope: 1%
Aspect: 270° NW
Latitude / Longitude: 35.1347, -89.2233

HORIZON	DEPTH (cm)	COLOR	TEXTURE	BOUNDARY	STRUCTURE	CONSISTANCE	NOTES
Ap	0-4	10YR 3/4	SiL	A	WG	VFr	
Bt1	4-18	7.5YR 4/4	SiL	C	WSBK	Fr	Mn conc
Bt2	18-53	7.5YR 4/4	SiCL	C	WSBK	Fr	
BC1	53-105	7.5YR 4/4	SiL	C	WSBK	Fr	
2BC2	105-143	7.5YR 4/4	L	C	WSBK	VFr	
2BC3	143-171	7.5YR 4/3	L	C	WSBK	VFr	
2BC4	171-207	7.5YR 4/4	SL	C	WSBK	VFr	
2BC5	207-247	5YR 5/6	SL	C	WSBK	VFr	stripped
3Bt1	247-290+	2.5YR 4/8	L	C	MoSBK	Fr	stripped

Classification: Fine-silty, mixed, superactive, thermic Ultic Hapludalf

Soil profile description for site one.

Landscape position: Upland
Parent Material: Loess/Alluvium/Tertiary Sand
Elevation: 164.85 meters above mean sea level
Slope: 1%
Aspect: 270° NW
Drainage: well drained
Latitude / Longitude: 35.1347, -89.2233
Classification: Fine-silty, mixed, superactive, thermic Ultic Hapludalf

Ap- 0 to 4 cm; dark yellowish brown (10YR 3/4) silt loam; weak granular structure; very friable; acid; abrupt smooth boundary.

Bt1- 4 to 18 cm; brown (7.5YR 4/4) silt loam; weak subangular blocky structure; friable; nonacid; clear smooth boundary, few manganese concentrations.

Bt2- 18 to 53 cm; brown (7.5YR 4/4) silty clay loam; weak subangular blocky structure; friable, nonacid, clear smooth boundary.

BC1- 53 to 105 cm; brown (7.5YR 4/4) silt loam; weak subanglular blocky structure; friable; acid, clear smooth boundary.

2BC2- 105 to 143 cm; brown (7.5YR 4/4) loam; weak subangular blocky structure; very friable; acid; clear smooth boundary.

2BC3- 143 to 171 cm; brown (7.5YR 4/3) loam; weak subangular blocky structure; very friable; acid; clear smooth boundary.

2BC4- 171 to 207 cm; brown (7.5YR 4/4) sandy loam; weak subangular blocky structure; very friable; acid; clear smooth boundary.

2BC5- 207 to 247 cm; yellowish red (5YR 5/6) sandy loam; weak subangular blocky structure; very friable; acid; few depleted zones, clear smooth boundary.

3Bt1- 247 to 300 cm+; dark red (2.5YR 4/8) loam; moderate subangular blocky structure; friable; acid; depleted zones, clear smooth boundary.

Sodium acetate extractable bases, cation exchange capacity (pH 7) and (pH 8.2), effective cation exchange capacity, KCL extractable aluminum and acidity, BaCl2 acidity, percent base saturation direct measurement and sum of cations.
Site 1.

			cmol(+)/Kg										% Base Saturation	
SAMPLE #	HORIZON	DEPTH (cm)	Ca	Mg	Na	K	Al(KCL)	CEC ph 7	ECEC	KCL Acidity	CEC ph 8.2	BaCl2 Acidity	ph7	Sum of Cations
99108	Ap	0-4	10.50	2.11	1.17	0.45	0.00	19.77	14.23	0.03			72	
99109	Bt1	4-18	8.80	1.56	0.12	0.19	0.00	17.03	10.67	0.03			63	
99110	Bt2	18-53	8.80	3.19	0.13	0.24	0.00	19.93	12.36	0.03			62	
99111	BC1	53-105	1.45	3.58	0.10	0.19	0.99	11.07	6.31	0.44			48	
99112	2BC2	105-143	0.86	2.19	0.09	0.20	0.69	7.42	4.03	0.37	9.68	2.26	45	35
99113	2BC3	143-171	0.63	1.85	0.08	0.17	0.53	5.47	3.26	0.20			50	
99114	2BC4	171-207	0.71	1.85	0.09	0.16	0.50	5.86	3.31	0.27			48	
99115	2BC5	207-247	0.65	1.57	0.10	0.14	0.35	5.35	2.81	0.22			46	
99116	3Bt1	247-290+	1.23	2.29	0.10	0.19	0.59	8.22	4.4	0.28			46	

Particle Size Distribution for Site 1.

		USDA Particle Size Class								
Horizon	LOWER DEPTH (cm)	VCOS %	COS %	MS %	FS %	VFS %	SAND %	SILT %	CLAY %	FINE CLAY % of clay
Ap	4	0.21	0.42	0.95	1.37	1.06	5.07	72.54	22.39	4.48
Bt1	18	0.2	1.38	1.08	0.89	0.79	4.34	68.88	26.79	10.34
Bt2	53	0.2	0.5	0.8	0.50	0.2	2.01	66.11	31.88	10.81
BC1	105	0.1	2.42	3.43	3.63	0.81	10.39	65.15	24.46	7.51
2BC2	143	0.4	8.02	14.13	11.42	1.1	35.07	46.41	18.52	6.33
2BC3	171	1.09	12.88	19.13	17.34	1.49	51.54	31.81	16.65	5.99
2BC4	207	1.1	17.47	24	24.40	1.31	68.37	15.04	16.59	6.83
2BC5	247	1.31	15.68	22.31	24.92	1.61	65.83	19.74	14.43	7.04
3Bt1	290	0.9	9.71	14.81	12.21	1.3	38.94	35.84	25.23	11.77

Total carbon, organic carbon, and pH data.
Site 1.

SAMPLE #	HORIZON	DEPTH (cm)	Total Carbon %	Organic Carbon %	pH 1:1	pH 2:1
99108	Ap	0-4	5.48	2.72	5.3	5
99109	Bt1	4-18	0.91	0.23	6	5.7
99110	Bt2	18-53	0.39	0.08	5.7	5.6
99111	BC1	53-105	0.22	0.04	4.6	4.4
99112	2BC2	105-143	0.29	0.08	4.2	4.3
99113	2BC3	143-171	0.25	0.08	4.8	4.4
99114	2BC4	171-207	0.44	0.08	4.7	4.4
99115	2BC5	207-247	0.19	0.08	4.7	4.4
99116	3Bt1	247-290+	0.15	0.04	4.9	4.5

Dithionite extractable iron, total iron, and hydroxlyamine extractable manganese.
Site 1.

		- - - - - - - - mg kg^-1 - - - - - - - -		
HORIZON	DEPTH (cm)	Free Iron	Total Iron	Ha Mn
Ap	0-4	9756.76	25895.38	290.73
Bt1	4-18	10386.67	29121.73	261.12
Bt2	18-53	12413.33	34689.78	143.24
BC1	53-105	12250.00	28316.85	122.86
2BC2	105-143	8416.11	18809.07	102.35
2BC3	143-171	5865.77	17156.02	128.63
2BC4	171-207	4940.00	15631.66	167.3
2BC5	207-247	5905.41	16438.73	86.14
3Bt1	247-290+	7140.94	19437.31	5.96

Concentration of selected elements for site one.

	mg kg-1																
Horizon	Al	Ba	Ca	Co	Cr	Cu	Fe	K	Mn	Ni	P	Pb	S	Sr	Ti	Zn	Zr
Ap	44673.00	527.07	4111.94	12.33	30.00	31.87	25895.38	15167.36	573.92	11.08	546.94	57.48	729.93	75.39	2094.12	93.29	110.08
Bt1	53442.28	677.23	3194.79	13.28	30.99	22.70	29121.73	16631.80	592.72	22.92	251.62	46.89	399.16	78.98	2348.44	101.32	124.17
Bt2	62767.59	585.91	2403.96	14.06	35.09	16.21	34689.78	16736.40	499.95	25.89	215.07	68.99	94.87	82.94	2536.20	79.90	127.39
BC1	53022.38	544.53	1915.04	11.18	33.28	54.04	28316.85	16422.59	545.03	19.69	181.88	59.22	136.47	84.96	2327.18	65.53	126.94
2BC2	34580.52	382.25	1142.27	12.63	25.41	23.55	18809.07	11087.87	459.79	28.05	58.02	43.60	25.00	55.05	1892.02	49.39	91.66
2BC3	30556.30	302.73	742.02	8.10	25.25	15.61	17156.02	8368.20	444.79	34.79	71.31	32.04	48.43	36.64	1709.47	35.89	76.90
2BC4	24597.20	216.42	577.28	5.94	30.99	27.45	15631.66	4497.91	345.30	40.18	5.00	39.92	25.00	25.00	1375.11	30.24	49.60
2BC5	25488.90	172.46	346.05	8.39	24.92	18.50	16438.73	3765.69	216.98	22.65	5.00	40.81	25.00	25.00	1521.42	60.40	53.93
3Bt1	37396.11	231.13	533.22	6.27	30.33	11.06	19437.31	6066.95	113.63	23.19	5.00	42.05	35.60	25.00	1684.36	80.85	84.44

Saturated hydraulic conductivity data at selected depths for site one.

Site one

Hole depth: 102 cm

Horizon: BC1

Chambers used: 1

Change in water level (cm)	Conversion factor (cm^2)	Elapsed time (min)	Q (cm3/hr)	K (cm/hr)
0	20	0	na	na
0.3	20	10	36	0.017691
0.4	20	5	96	0.047176
0.2	20	5	48	0.023588
0.2	20	5	48	0.023588
			mean K=	0.031451

Site one

Hole depth: 129 cm

Horizon: 2BC1

Chambers used: 1

Change in water level (cm)	Conversion factor (cm^2)	Elapsed time (min)	Q (cm3/hr)	K (cm/hr)
0	20	0	na	na
0.7	20	10	84	0.065152
0.2	20	5	48	0.03723
0.4	20	5	96	0.07446
0.3	20	5	72	0.055845
0.2	20	5	48	0.03723
			mean K=	0.055845

Bulk density, particle density, and total porosity.
Site 1.

Horizon	Lower Depth (cm)	Bulk Density g cm^ -3	Particle Density g cm^ -3	Total Porosity %
Ap	4	ns	ns	ns
Bt1	18	1.64	2.72	39.99
Bt2	53	1.40	2.62	46.56
BC1	105	1.49	2.53	41.11
2BC2	143	1.73	2.63	34.23
2BC3	171	1.98	2.78	28.48
2BC4	207	1.94	2.73	29.18
2BC5	247	2.05	2.75	25.65
3Bt1	290	1.49	2.76	46.01

Appendix B. Morphology and Laboratory Data for Site Two.

Field morphology data sheet, texture corrected by lab data.
Site 2.

Landscape position: Upland
Parent Material: Loess/Alluvium/Tertiary Sand
Elevation: 164.75 meters above mean sea level
Slope: 1%
Aspect: 270° NW
Latitude / Longitude: 35.1346, -89.2233

HORIZON	DEPTH (cm)	COLOR	TEXTURE	BOUNDARY	STRUCTURE	CONSISTANCE	NOTES
Ap	0-5	10YR 4/4	SiL	A	WKG	VF	
Bt1	5-39	7.5YR 4/4	SiCL	C	WKSBK	F	
Bt2	39-74	7.5YR 4/4	SiCL	C	WKSBK	F	
BC1	74-115	7.5YR 4/4	SiL	C	WKSBK	F	
2BC2	115-143	7.5YR 4/4	L	C	WKSBK	F	
2BC3	143-184	7.5YR 4/4	L	C	WKSBK	F	stripped
2BC4	184-219	5YR3/4	SL	C	WKSBK	F	
2BC5	219-244	5YR 4/6	SL	C	WKSBK	VF	
3Bt1	244-300+	2.5YR 4/6	L	C	WKSBK	F	

Classification: Fine-silty, mixed, active, thermic Ultic Hapludalf

Soil profile description for site two.

Landscape position: Upland
Parent Material: Loess/Alluvium/Tertiary Sand
Elevation: 164.75 meters above mean sea level
Slope: 1%
Aspect: 270° NW
Drainage: well drained
Latitude / Longitude: 35.1346, -89.2233
Classification: Fine-silty, mixed, active, thermic Ultic Hapludalf

Ap- 0 to 5 cm; dark yellowish brown (10YR 4/4) silt loam; weak granular structure; very friable; nonacid; abrupt smooth boundary.

Bt1- 5 to 39 cm; brown (7.5YR 4/4) silty clay loam; weak subangular blocky; friable; nonacid; clear smooth boundary.

Bt2- 39 to 74 cm; brown (7.5YR 4/4) silty clay loam; weak subangular blocky structure; friable; acid; clear smooth boundary.

BC1- 74 to 115 cm; brown (7.5YR 4/4) silt loam; weak subangular blocky structure; friable; acid; clear smooth boundary.

2BC2- 115 to 143 cm; brown (7.5YR 4/4) loam; weak subangular blocky structure; friable; acid; clear smooth boundary.

2BC3- 143 to 184 cm; brown (7.5YR 4/4) loam; weak subangular blocky structure; friable; acid; few depleated zones, clear smooth boundary.

2BC4- 184 to 219 cm; dark reddish brown (5YR 3/4) sandy loam; weak subangular blocky structure; friable; acid; clear smooth boundary.

2BC5- 219 to 244 cm; yellowish red (5YR 4/6) sandy loam; weak subangular blocky structure; very friable; acid; clear smooth boundary.

3Bt1- 244 to 300 cm+; dark red (2.5YR 4/8) loam; weak subangular blocky structure; acid; clear smooth boundary.

Sodium acetate extractable bases, cation exchange capacity (pH 7) and (pH 8.2), effective cation exchange capacity, KCL extractable aluminum and acidity, BaCl2 acidity, percent base saturation direct measurement and sum of cations.
Site 2.

			cmol(+)/Kg										% Base Saturation	
SAMPLE #	HORIZON	DEPTH (cm)	Ca	Mg	Na	K	Al(KCL)	CEC ph 7	ECEC	CEC ph 8.2	KCL Acidity	BaCl2 Acidity	ph7	Sum of Cations
99117	Ap	0-5	7.11	2.08	0.05	0.07	0.00	16.41	9.31		0.06		57	
99118	Bt1	5-39	5.75	2.18	0.06	0.25	0.00	13.52	8.24		0.02		61	
99119	Bt2	39-74	2.92	4.15	0.09	0.26	1.18	12.21	8.60		0.46		61	
99120	BC1	74-115	1.03	2.41	0.97	0.28	1.63	9.88	6.32		0.66		47	
99121	2BC2	115-143	0.95	2.22	0.08	0.28	0.90	7.72	4.43	9.99	0.40	2.27	46	35
99122	2BC3	143-184	0.65	1.88	0.09	0.26	0.86	7.60	3.74		0.40		38	
99123	2BC4	184-219	1.52	1.82	0.69	0.24	0.63	8.10	4.90		0.32		53	
99124	2BC5	219-244	1.78	1.92	0.87	0.23	0.51	8.54	5.31		0.32		56	
99125	3Bt1	244-300+	2.58	2.40	0.14	0.24	0.66	10.53	6.02		0.31		51	

Particle Size Distribution for Site 2.

		USDA Particle Size Class								
	LOWER	VCOS	COS	MS	FS	VFS	SAND	SILT	CLAY	FINE CLAY
Horizon	DEPTH (cm)	%	%	%	%	%	%	%	%	% of clay
Ap	5	0.43	1.19	2.16	0.86	0.65	4.75	74	21.25	4.67
Bt1	39	0	0.41	0.62	0.52	0.72	3.1	66.6	30.3	10.40
Bt2	74	0	2.49	4.67	3.98	0.89	12.03	58.55	29.42	9.54
BC1	115	0.1	0.6	0.6	0.7	0.5	2.61	73.37	24.02	7.91
2BC2	143	0.4	6.94	12.98	10.66	1.41	32.39	49.34	18.27	6.44
2BC3	184	0.9	10.47	17.35	15.45	1.4	45.56	38.68	15.75	6.18
2BC4	219	2	14.1	21.2	20.1	1.7	59.1	24.06	16.84	8.01
2BC5	244	1.69	17.53	19.62	21.02	1.59	61.45	19.06	19.48	10.64
3Bt1	300	1.41	10.65	14.57	12.36	1.01	40	33.59	26.41	13.47

Total carbon, organic carbon, and pH data.
Site 2.

SAMPLE #	HORIZON	DEPTH (cm)	Total Carbon	Organic Carbon	pH 1:1	pH 2:1
99117	Ap	0-5	4.38	2.49	5.4	5.2
99118	Bt1	5-39	0.91	0.16	6.1	5.4
99119	Bt2	39-74	0.29	0.04	5.4	4.8
99120	BC1	74-115	0.20	0.04	5	4.4
99121	2BC2	115-143	0.16	0	5.1	4.3
99122	2BC3	143-184	0.15	0	5.1	4.3
99123	2BC4	184-219	0.14	0	5.3	4.4
99124	2BC5	219-244	0.17	0	5.2	4.4
99125	3Bt1	244-300+	0.14	0	5.6	4.6

Dithionite extractable iron, total iron, and hydroxylamine extractable manganese.
Site 2.

		- - - - - - - - -mg kg^-1 - - - - - - -		
HORIZON	DEPTH (cm)	Free Iron	Total Iron	Ha Mn
Ap	0-5	7675.50	22251.92	281.39
Bt1	5-39	10766.67	30323.16	221.3
Bt2	39-74	13644.30	34677.06	88.22
BC1	74-115	10640.00	27227.21	80.73
2BC2	115-143	6966.67	20881.20	67.09
2BC3	143-184	6006.45	17485.07	99.73
2BC4	184-219	6462.59	19135.43	145.11
2BC5	219-244	5913.91	17057.19	71.45
3Bt1	244-300+	8933.77	24295.91	19.72

Concentration of selected elements for site two.

	mg kg-1																
Horizon	Al	Ba	Ca	Co	Cr	Cu	Fe	K	Mn	Ni	P	Pb	S	Sr	Ti	Zn	Zr
Ap	42724.75	531.11	3205.65	15.58	27.71	14.59	22251.92	14539.75	545.03	19.96	375.28	61.95	304.19	75.66	2059.17	57.58	114.96
Bt1	56115.27	603.04	2664.19	13.59	33.94	16.02	30323.16	16736.40	601.68	34.79	260.51	57.40	94.14	78.06	2495.90	83.74	124.50
Bt2	61537.56	572.65	2078.12	15.19	35.74	14.88	34677.06	17468.62	555.11	34.25	259.09	75.72	220.22	82.94	2499.32	81.51	130.16
BC1	49702.20	512.53	1781.67	12.58	28.69	20.81	27227.21	16004.18	468.94	31.28	90.72	64.59	25.00	91.77	2282.17	57.92	143.26
2BC2	38321.79	429.61	1283.40	8.22	26.56	19.35	20881.20	12761.51	360.74	32.63	5.00	52.61	25.00	59.74	1987.69	68.49	107.30
2BC3	30155.92	310.97	839.17	7.65	24.59	31.77	17485.07	8263.60	342.62	29.12	5.00	40.92	25.00	38.66	1656.47	170.34	74.57
2BC4	28273.38	241.47	574.74	7.37	26.40	25.15	19135.43	5857.74	357.13	33.17	40.51	44.01	25.00	29.92	1488.18	46.01	56.26
2BC5	25978.12	247.78	626.09	5.01	23.77	18.36	17057.19	3870.29	196.49	24.00	21.06	45.09	25.00	25.00	1282.58	46.07	47.16
3Bt1	39666.72	233.72	572.44	5.29	38.36	22.81	24295.91	5334.73	142.08	32.36	5.00	55.95	25.00	25.00	1806.42	43.59	83.22

Saturated hydraulic conductivity at selected depths for site two.

Site two

Hole depth: 113 cm

Horizon: BC1

Chambers used: 1

Change in water level (cm)	Conversion factor (cm^2)	Elapsed time (min)	Q (cm3/hr)	K (cm/hr)
0.0	20	0	na	na
0.1	20	17	70.6	0.026134
1.4	20	17	98.8	0.036572
3.2	20	44	87.3	0.032315
2.2	20	33	79.8	0.029539
1.0	20	18	66.7	0.02469
			mean K=	0.032809

Site two

Hole depth: 129 cm

Horizon: 2BC1

Chambers used: 1

Change in water level (cm)	Conversion factor (cm^2)	Elapsed time (min)	Q (cm3/hr)	K (cm/hr)
0	20	0	na	na
0.8	20	19	50.5	0.055999
0.3	20	5	72.0	0.079841
0.2	20	5	48.0	0.053227
0.3	20	5	72.0	0.079841
			mean K=	0.044356

Bulk density, particle density, and total porosity.
Site 2.

Horizon	Lower Depth (cm)	Bulk Density g cm^ -3	Particle Density g cm^ -3	Total Porosity %
Ap	5	ns	ns	ns
Bt1	39	1.64	2.59	36.81
Bt2	74	1.40	2.68	47.94
BC1	115	1.49	2.71	44.92
2BC2	143	1.69	2.75	38.41
2BC3	184	1.76	2.45	27.82
2BC4	219	2.01	2.79	28.14
2BC5	244	1.79	2.55	29.57
3Bt1	300	1.45	2.66	45.49

Appendix C. Morphology and Laboratory Data for Site Three.

Field morphology data sheet, texture corrected by lab data.
Site 3.

Landscape position: Upland
Parent Material: Loess/Alluvium/Tertiary Sand
Elevation: 164.39 meters above mean sea level
Slope 1%
Aspect: 270° NW
Latitude / Longitude: 35.1345, -89.2234

HORIZON	DEPTH (cm)	COLOR	TEXTURE	BOUNDARY	STRUCTURE	CONSISTANCE	NOTES
Ap	0-5	10YR 4/4	SiL	A	WKG	VFr	
Bt1	5-36	7.5YR 4/6	SiCL	C	WSBK	Fr	
Bt2	36-75	7.5YR 4/4	SiCL	C	WSBK	Fr	
BC1	75-109	7.5YR 4/6	SiL	C	WSBK	Fr	
2BC2	109-156	7.5YR 4/6	SiL	C	WSBK	Fr	
2BC3	156-186	7.5YR 4/4	L	C	WSBK	Fr	
2BC4	186-208	2.5YR 4/8	SCL	C	WSBK	Fr	
2BC5	208-234	2.5YR 4/6	SCL	C	WSBK	Fr	stripped
3Bt1	234-274	2.5YR 4/8	L	C	MoSBK	Fr	
3Bt2	274-300+	2.5YR 4/8	SCL	C	MoSBK	Fr	stripped

Classification: Fine-silty, mixed, active, thermic Ultic Hapludalf

Soil profile description for site three.

Landscape position: Upland
Parent Material: Loess/Alluvium/Tertiary Sand
Elevation: 164.39 meters above mean sea level
Slope 1%
Aspect: 270° NW
Drainage: well drained
Latitude / Longitude: 35.1345, -89.2234
Classification: Fine-silty, mixed, active, thermic Ultic Hapludalf

Ap- 0 to 5 cm; dark yellowish brown (10YR 4/4) silt loam; weak granular structure; very friable; nonacid; abrupt smooth boundary.

Bt1- 5 to 36 cm; strong brown (7.5YR 4/6) silty clay loam; weak subangular blocky structure; friable; nonacid; clear smooth bloundary.

Bt2- 36 to 75 cm; brown (7.5YR 4/4) silty clay loam; weak subangular blocky structure; friable; acid; clear smooth boundary.

BC1- 75 to 109 cm; strong brown (7.5YR 4/6) silt loam; weak subangular blocky structure; friable; acid; clear smooth boundary.

2BC2- 109 to 156 cm; strong brown (7.5YR 4/6) silt loam; weak subangular blocky structure; friable; acid; clear smooth boundary.

2BC3- 156 to 186 cm; brown (7.5YR 4/4) loam; weak subangular blocky structure; friable; acid; clear smooth boundary.

2BC4- 186 to 208 cm; dark red (2.5YR 4/8) sandy clay loam; weak subangular blocky structure; friable; acid; clear smooth boundary.

2BC5- 208 to 234 cm; dark red (2.5YR 4/6) sandy clay loam; weak subangular blocky structure; friable; acid; depleted zone; clear smooth boundary.

3Bt1- 234 to 274 cm; dark red (2.5YR 4/8) loam; moderate subangular blocky structure; friable; acid; clear smooth boundary.

3Bt2- 274 to 300 cm+; dark red (2.5YR 4/8) sandy clay loam; moderate subangular blocky; friable; acid; depleted zones; clear smooth boundary.

Sodium acetate exchangeable bases, cation exchange capacity (pH 7) and (pH 8.2), effective cation exchange capacity, KCL extractable aluminum and acidity, BaCl2 acidity, percent base saturation direct measurement and sum of cations.
Site 3.

			cmol(+)/Kg										% Base Saturation	
SAMPLE #	HORIZON	DEPTH (cm)	Ca	Mg	Na	K	Al(KCL)	CEC ph 7	ECEC	CEC ph 8.2	KCL Acidity	BaCl2 Acidity	ph7	Sum of Cations
99126	Ap	0-5	11.02	2.74	0.09	0.69	0.00	25.30	14.54		0.07		57	
99127	Bt1	5-36	6.85	3.20	0.17	0.27	0.00	18.35	10.49		0.05		57	
99128	Bt2	36-75	4.22	3.72	0.12	0.25	0.71	16.83	9.02		0.41		49	
99129	BC1	75-109	2.88	3.12	0.13	0.20	0.31	12.56	6.64		0.30		50	
99130	2BC2	109-156	2.02	2.36	0.13	0.16	0.24	9.14	4.91	12.37	0.25	3.23	51	38
99131	2BC3	156-186	1.99	2.45	0.14	0.13	0.32	9.10	5.03		0.26		52	
99132	2BC4	186-208	1.77	2.34	0.13	0.14	0.31	8.69	4.69		0.26		50	
99133	2BC5	208-234	1.60	2.16	0.17	0.13	0.24	8.89	4.30		0.27		46	
99134	3Bt1	234-274	2.27	2.34	0.14	0.15	0.35	8.16	5.25		0.31		60	
99135	3Bt2	274-300+	2.15	3.99	0.14	0.21	0.51	14.23	4.85		0.37		46	

Particle Size Distribution for Site 3.

		USDA Particle Size Class								
	LOWER	VCOS	COS	MS	FS	VFS	SAND	SILT	CLAY	FINE CLAY
Horizon	DEPTH (cm)	%	%	%	%	%	%	%	%	% total clay
Ap	5	0.37	1.1	1.1	0.73	0.73	3.66	72.29	24.06	3.88
Bt1	36	0	0.1	0.41	0.51	0.41	1.42	66.22	32.36	24.35
Bt2	75	0	0.59	0.59	0.49	0.39	2.06	70.32	27.61	9.99
BC1	109	0	2.81	3.62	4.22	0.9	11.56	66.37	22.07	6.87
2BC2	156	0.3	5.63	10.76	10.36	1.21	28.27	54.31	17.42	6.16
2BC3	186	0.69	9.4	15.87	14.59	1.67	42.12	39.51	18.37	7.76
2BC4	208	1.21	11.32	20.53	18.5	1.72	53.19	25.54	21.27	10.31
2BC5	234	1.01	12.96	20.2	19.5	1.61	55.18	24.81	20.02	9.37
3Bt1	274	0.9	7.38	8.77	8.08	1.3	26.32	49.59	24.09	14.00
3Bt2	300+	1.51	12.66	14.17	15.38	1.41	44.92	22.11	32.96	15.76

Total carbon, organic carbon, and pH data.
Site 3.

SAMPLE#	HORIZON	DEPTH (cm)	Total Carbon	Organic Carbon	pH 1:1	pH 2:1
99126	Ap	0-5	6.35	3.5	5.4	5
99127	Bt1	5-36	0.57	0.31	5.8	5.2
99128	Bt2	36-75	0.24	0.03	5.4	4.6
99129	BC1	75-109	0.18	0.08	5.4	4.5
99130	2BC2	109-156	0.18	0.03	5.4	4.6
99131	2BC3	156-186	0.17	0.03	5.4	4.5
99132	2BC4	186-208	0.17	0.12	5.2	4.4
99133	2BC5	208-234	0.20	0.08	5.1	4.5
99134	3Bt1	234-274	0.17	0.08	5.5	4.5
99135	3Bt2	274-300+	0.17	0.08	5.4	4.6

Dithionite extractable iron, total iron, and hydroxylamine extractable manganese.
Site 3.

		mg kg^-1		
HORIZON	DEPTH (cm)	Free Iron	Total Iron	Ha Mn
Ap	0-5	11040.54	22844.45	278.06
Bt1	5-36	16449.66	32569.69	135.54
Bt2	36-75	10081.63	33102.21	70.43
BC1	75-109	8948.39	26466.50	89.43
2BC2	109-156	7343.56	20059.34	76.94
2BC3	156-186	7093.33	18824.41	147.77
2BC4	186-208	6675.68	18206.95	192.29
2BC5	208-234	5557.82	20974.25	145.36
3Bt1	234-274	7445.95	21026.15	32.25
3Bt2	274-300+	11476.51	29729.77	10.59

Concentration of selected elements for site three.

	mg kg-1																
Horizon	Al	Ba	Ca	Co	Cr	Cu	Fe	K	Mn	Ni	P	Pb	S	Sr	Ti	Zn	Zr
Ap	41968.75	484.24	3421.42	13.02	30.00	14.99	22844.45	13389.12	605.73	32.63	557.72	61.33	325.41	68.21	1968.69	93.40	104.53
Bt1	60242.96	674.68	2384.16	13.00	33.95	17.44	32569.69	16700.61	483.44	36.73	262.03	61.30	25.00	86.94	2468.11	80.25	117.97
Bt2	60519.06	584.07	1902.42	13.87	31.23	15.38	33102.21	17107.94	523.43	32.48	253.37	67.83	69.10	86.20	2382.10	96.68	123.65
BC1	51167.40	558.16	2070.29	11.34	26.10	14.83	26466.50	16802.44	490.59	24.74	22.88	51.94	25.00	89.81	2267.11	131.53	128.13
2BC2	37939.13	441.32	1446.85	7.85	23.84	13.95	20059.34	12525.46	348.50	26.74	69.38	39.26	25.00	63.33	1973.42	101.21	98.31
2BC3	34232.44	349.73	892.25	8.33	21.27	16.06	18824.41	9368.64	475.19	10.00	92.53	36.48	25.00	71.48	1816.13	39.52	83.02
2BC4	30818.13	258.63	500.28	9.59	25.80	20.06	18206.95	6313.65	404.94	35.73	5.00	32.13	25.00	27.87	1630.70	32.42	63.03
2BC5	33392.51	255.21	607.59	8.45	31.08	26.67	20974.25	6211.81	349.97	32.73	5.00	38.54	25.00	47.87	1576.40	45.21	64.34
3Bt1	38421.13	305.24	626.05	4.89	30.03	17.41	21026.15	5600.81	160.82	17.49	60.16	28.94	25.00	26.02	1655.25	101.69	81.05
3Bt2	53080.76	306.87	683.99	9.38	41.19	25.63	29729.77	7535.64	162.57	23.24	5.00	48.01	25.00	119.34	2097.25	54.09	97.77

Saturated hydraulic conductivity at selected depths for site three.

Site three

Hole depth: 102 cm

Horizon: BC1

Chambers used: 1

Change in water level (cm)	Conversion factor (cm^2)	Elapsed time (min)	Q (cm3/hr)	K (cm/hr)
0.0	20	0	na	na
0.4	20	5	84	0.103152
0.1	20	5	12	0.014736
0.1	20	5	12	0.014736
0.1	20	5	12	0.014736
			mean K=	0.014736

Site three

Hole depth: 135 cm

Horizon: 2BC1

Chambers used: 1

Change in water level (cm)	Conversion factor (cm^2)	Elapsed time (min)	Q (cm3/hr)	K (cm/hr)
0	20	0	na	na
0.1	20	5	24.0	0.031123
0.1	20	5	24.0	0.031123
0.05	20	5	12.0	0.015562
0.35	20	5	72.0	0.09337
0.15	20	3	60	0.077808
0.15	20	3	60	0.077808
			mean K=	0.062246

Bulk density, particle density, and total porosity.
Site 3.

Horizon	Lower Depth (cm)	Bulk Density g cm^ -3	Particle Density g cm^ -3	Total Porosity %
Ap	5	ns	ns	ns
Bt1	36	1.72	2.64	34.96
Bt2	75	1.57	2.60	39.56
BC1	109	1.52	2.72	44.19
2BC2	156	1.69	2.74	38.5
2BC3	186	1.68	2.68	37.36
2BC4	208	1.83	2.56	28.52
2BC5	234	1.94	2.77	30.09
3Bt1	274	1.61	2.52	36.33
3Bt2	300+	1.54	2.66	41.97

Appendix D. Morphology and Laboratory Data for Site Four.

Field morphology data sheet, texture corrected by lab data.
Site 4.

Landscape position: Upland
Parent Material: Loess/Alluvium/Tertiary Sand
Elevation: 165.76 meters above mean sea level
Slope: 1%
Aspect: 270° NW
Latitude / Longitude: 35.1346, -89.2231

HORIZON	DEPTH (cm)	COLOR	TEXTURE	BOUNDARY	STRUCTURE	CONSISTANCE	NOTES
Ap	0-8	10YR 4/3	SiL	A	WG	VFR	
Bt1	8-26	7.5YR 4/6	SiCL	C	WSBK	FR	
Bt2	26-60	7.5YR 4/6	SiCL	C	WSBK	FR	Mn conc
BC1	60-87	7.5YR 4/6	SiL	C	MoSBK	FR	Mn conc
BC2	87-114	7.5YR 4/4	SiL	C	MoSBK	FR	stripped
2BC3	114-147	7.5YR 4/4	L	C	WSBK	FR	Mn conc
2BC4	147-191	5YR 4/4	L	C	MoSBK	FR	Fe Mn conc
2BC5	191-217	2.5YR 4/6	SL	C	WSBK	FR	blind pores, stripped
2BC6	217-247+	2.5YR 4/6	SL	C	SG	VFR	

Classification: Fine-silty, mixed, active, thermic Ultic Hapludalf

Soil profile description for site four.

Landscape position: Upland
Parent Material: Loess/Alluvium/Tertiary Sand
Elevation: 165.76 meters above mean sea level
Slope: 1%
Aspect: 270° NW
Drainage: well drained
Latitude / Longitude: 35.1346, -89.2231
Classification: Fine-silty, mixed, active, thermic Ultic Hapludalf

Ap- 0 to 8 cm; brown (10YR 4/3) silt loam; weak granular structure; very friable; nonacid; abrupt smooth boundary.

Bt1- 8 to 26 cm; strong brown (7.5YR 4/6) silty clay loam; weak subangular blocky structure; friable; nonacid; clear smooth boundary.

Bt2- 26 to 60 cm; strong brown (7.5YR 4/6) silty clay loam; weak subangular blocky structure; friable; acid; few manganese concentrations; clear smooth boundary.

BC1- 60 to 87 cm; strong brown (7.5YR 4/6) silt loam; moderate subangular blocky structure; friable; acid; manganese concentrations; clear smooth boundary.

BC2- 87 to 114 cm; brown (7.5YR 4/4) silt loam; moderate subangular blocky structure; friable; acid; few depleted zones present; clear smooth boundary.

2BC3- 114 to 147 cm; brown (7.5YR 4/4) loam; weak subangular blocky structure; friable; acid; many manganese concentrations; clear smooth boundary.

2BC4- 147 to 191 cm; reddish brown (5YR 4/4) loam; moderate subangular blocky structure; friable; acid; iron and manganese concentrations; clear smooth boundary.

2BC5- 191 to 217 cm; dark red (2.5YR 4/6) sandy loam; weak subangular blocky; friable; acid; few blind pores; few depleted zones; clear smooth boundary.

2BC6- 217 to 247 cm+; dark red (2.5YR 4/6) sandy loam; single grain structure; very friable; acid; clear smooth boundary.

Sodium acetate extractable bases, cation exchange capacity (pH 7) and (pH 8.2), effective cation exchange capacity, KCL extractable aluminum and acidity, BaCl2 acidity, percent base saturation; direct measurement and sum of cations.
Site 4.

			cmol(+)/Kg										Base Saturation	
SAMPLE #	HORIZON	DEPTH (cm)	Ca	Mg	Na	K	Al(KCL)	CEC ph 7	ECEC	KCL Acidity	CEC ph 8.2	BaCl2 Acidity	ph7	Sum of Cations
99136	Ap	0-8	6.42	2.06	0.06	0.26	0.00	18.37	8.80	0.07			48	
99137	Bt1	8-26	4.53	2.35	0.12	0.24	0.00	16.76	7.24	0.03			43	
99138	Bt2	26-60	3.95	4.11	0.13	0.27	0.40	17.10	8.46	0.32			50	
99139	BC1	60-87	2.56	3.84	0.13	0.26	0.57	14.59	7.36	0.40			47	
99140	BC2	87-114	1.31	3.07	0.13	0.27	0.37	10.56	5.15	0.26			45	
99141	2BC3	114-147	1.15	2.71	0.13	0.28	0.21	10.08	4.48	0.26	12.16	2.08	42	35
99142	2BC4	147-191	1.12	3.21	0.13	0.24	0.24	10.42	4.94	0.22			45	
99143	2BC5	191-217	1.01	1.72	0.13	0.28	0.00	8.18	3.14	0.11			38	
99144	2BC6	217-247+	0.83	1.63	0.08	0.24	0.00	6.44	2.78	0.13			43	

Particle Size Distribution for Site 4.

		USDA Particle Size Class								
	LOWER	VCOS	COS	MS	FS	VFS	SAND	SILT	CLAY	FINE CLAY
Horizon	DEPTH (cm)	%	%	%	%	%	%	%	%	% of clay
Ap	8	0.1	1.56	1.66	1.24	1.14	6.54	73.26	20.21	4.65
Bt1	26	0	0.61	0.91	0.61	0.61	2.73	68.91	28.36	10.83
Bt2	60	0.1	0.4	0.5	0.6	0.2	1.81	67.16	31.04	13.43
BC1	87	0.1	1.1	2.21	1.81	0.6	5.92	69.29	24.79	8.79
BC2	114	0.3	5.37	8.56	6.87	1.29	22.59	57.71	19.7	7.08
2BC3	147	0.4	9.59	10.69	9.69	1	31.67	48.31	20.02	8.19
2BC4	191	0.2	11.3	17.34	13.18	1.29	43.31	36.47	20.22	9.63
2BC5	217	1.51	16.88	24.72	17.99	1.41	62.51	20.84	16.64	8.44
2BC6	247	1.41	17.15	25.53	22.6	2.32	74.97	11.83	13.2	6.94

Total carbon, organic carbon, and pH data.
Site 4.

SAMPLE#	HORIZON	DEPTH (cm)	Total Carbon	Organic Carbon	pH 1:1	pH 2:1
99136	Ap	0-8	4.17	2.18	5.5	5
99137	Bt1	8-26	0.74	0.31	6.1	5.7
99138	Bt2	26-60	0.35	0.03	5.4	4.6
99139	BC1	60-87	0.22	0.08	5.4	4.4
99140	BC2	87-114	0.20	0.08	5.4	4.5
99141	2BC3	114-147	0.17	0.08	5.6	4.5
99142	2BC4	147-191	0.19	0	5.2	4.4
99143	2BC5	191-217	0.21	0.11	5.2	4.6
99144	2BC6	217-247+	0.18	0	5.3	4.5

Dithionite extractable iron, total iron, and hydroxylamine extractable manganese.
Site 4.

		mg kg ^-1		
HORIZON	DEPTH (cm)	Free Iron	Total Iron	Ha Mn
Ap	0-8	9628.38	22244.79	275.01
Bt1	8-26	8866.67	24173.52	154.31
Bt2	26-60	10340.14	34625.27	92.81
BC1	60-87	9311.26	30427.77	128.00
BC2	87-114	7574.32	22322.53	339.57
2BC3	114-147	6503.36	22410.04	382.22
2BC4	147-191	6291.39	20684.49	290.51
2BC5	191-217	5215.69	16335.00	332.93
2BC6	217-247+	5006.76	12761.01	261.90

Concentration of selected elements for site four.

	mg kg-1																
Horizon	Al	Ba	Ca	Co	Cr	Cu	Fe	K	Mn	Ni	P	Pb	S	Sr	Ti	Zn	Zr
Ap	44332.38	742.15	2539.58	11.59	26.40	14.46	22244.79	14562.12	501.12	25.49	280.64	55.66	247.91	83.33	2262.55	77.26	115.68
Bt1	47083.40	560.93	2059.46	11.92	24.90	12.43	24173.52	14663.95	437.49	13.49	196.01	48.73	25.00	71.11	2041.27	73.34	98.42
Bt2	62236.72	587.33	2011.15	14.74	32.29	18.00	34625.27	17617.11	503.52	30.23	315.88	61.56	25.00	91.57	2454.08	86.35	117.10
BC1	56597.86	551.16	1974.01	13.60	31.69	16.32	30427.77	17515.28	570.38	38.73	186.65	56.14	25.00	93.79	2397.39	113.42	125.18
BC2	43317.97	482.38	1675.91	12.74	24.44	23.16	22322.53	14562.12	588.94	17.74	145.07	39.43	25.00	94.07	2154.78	54.67	106.83
2BC3	41986.48	462.01	1397.41	9.51	26.10	20.92	22410.04	13238.29	627.75	21.74	56.26	39.61	25.00	82.40	2012.15	48.77	99.95
2BC4	37428.83	364.07	947.71	6.67	22.48	23.05	20684.49	9164.97	525.30	15.24	146.23	40.02	25.00	51.57	1775.72	60.57	81.27
2BC5	25897.48	222.94	465.68	5.57	19.92	19.92	16335.00	5091.65	505.40	10.00	148.71	33.37	25.00	85.55	1365.43	39.89	48.83
2BC6	19241.50	158.89	325.83	4.30	18.86	16.96	12761.01	3665.99	317.48	14.49	114.32	28.40	25.00	25.00	1064.66	65.76	39.98

Site four

Hole depth: 101 cm

Horizon: BC1

Chambers used: 1

Change in water level (cm)	Conversion factor (cm^2)	Elapsed time (min)	Q (cm3/hr)	K (cm/hr)
0.0	20	0	na	na
1.2	20	15	105.6	0.092842
0.2	20	11	21.8	0.019166
0.1	20	5	24	0.0211
0.1	20	5	24	0.0211
			mean K=	0.020456

Site four

Hole depth: 116 cm

Horizon: 2BC1

Chambers used: 1

Change in water level (cm)	Conversion factor (cm^2)	Elapsed time (min)	Q (cm3/hr)	K (cm/hr)
0	20	0	na	na
0.5	20	5	120.0	0.126698
0.3	20	5	72.0	0.076019
0.4	20	5	96.0	0.101359
0.4	20	5	96.0	0.101359
			mean K=	0.092912

Bulk density, particle density, and total porosity.
Site 4.

Horizon	Lower Depth (cm)	Bulk Density g cm^ -3	Particle Density g cm^ -3	Total Porosity %
Ap	8	ns	ns	ns
Bt1	26	1.64	2.68	38.77
Bt2	60	1.41	2.73	48.44
BC1	87	1.36	2.63	48.21
BC2	114	1.55	2.64	41.52
2BC3	147	1.80	2.73	34.1
2BC4	191	1.84	2.63	30.23
2BC5	217	1.71	2.68	36.26
2BC6	247	ns	ns	ns

Appendix E. Morphology and Laboratory Data for Site Five.

Field morphology data sheet, texture corrected by lab data.
Site 5.

Landscape position: Upland
Parent Material: Loess/Alluvium/Tertiary Sand
Elevation: 164.98 meters above mean sea level
Slope: 1%
Aspect: 270° NW
Longitude / Latitude: 35.1344, -89.2233

HORIZON	DEPTH (cm)	COLOR	TEXTURE	BOUNDARY	STRUCTURE	CONSISTANCE	NOTES
Ap	0-6	10YR 4/4	SiL	A	WKG	FR	
Bt1	6-22	10YR 4/3	SiL	C	WSBK	FR	
Bt2	22-60	7.5YR 4/3	SiL	C	WSBK	FR	Mn conc, stripped
Bt3	60-109	7.5YR 4/4	SiL	C	WSBK	FR	
2BC1	109-137	7.5YR 4/4	SiL	C	WSBK	FR	
2BC2	137-176	7.5YR 4/6	L	C	MoSBK	FR	bind pores
2BC3	176-204	5YR 4/4	L	C	MoSBK	FR	blind pores, Mn conc
2BC4	204-260	2.5YR 4/6	SL	C	WSBK	FR	stripped
3BC5	260-300+	2.5YR 4/8	SL	C	WSBK	VFR	stripped

Classification: Fine-silty, mixed, superactive, thermic Ultic Hapludalf

Soil profile description for site five.

Landscape position: Upland
Parent Material: Loess/Alluvium/Tertiary Sand
Elevation: 164.98 meters above mean sea level
Slope: 1%
Aspect: 270° NW
Drainage: well drained
Longitude / Latitude: 35.1344, -89.2233
Classification: Fine-silty, mixed, superactive, thermic Ultic Hapludalf

Ap- 0 to 6 cm; dark yellowish brown (10YR 4/4) silt loam; weak granular structure; very friable; nonacid; abrupt smooth boundary.

Bt1- 6 to 22 cm; brown (10YR 4/3) silt loam; weak subangular blocky structure; friable; nonacid; clear smooth boundary.

Bt2- 22 to 60 cm; brown (7.5YR 4/3) silt loam; weak subangular blocky structure; friable; acid; few manganese concentrations; clear smooth boundary.

Bt3- 60 to 109 cm; brown (7.5YR 4/4) silt loam; weak subangular blocky structure; friable; acid; clear smooth boundary.

2BC1- 109 to 137 cm; brown (7.5YR 4/4) silt loam; weak subangular blocky structure; friable; acid; clear smooth boundary.

2BC2- 137 to 176 cm; strong brown (7.5YR 4/6) loam; moderate subangular blocky structure; friable; acid; few blind pores present; clear smooth boundary.

2BC3- 176 to 204 cm; reddish brown (5YR 4/4) loam; moderate subangular blocky structure; friable; acid; few blind pores present; manganese concentrations; few depleted zones; clear smooth boundary.

2BC4- 204 to 260 cm; dark red (2.5YR 4/6) sandy loam; weak subangular blocky structure; friable; acid; depleted zones present; clear smooth boundary.

3BC5- 260 to 300 cm+; dark red (2.5YR 4/8) sandy loam; weak subangular blocky structure; friable; acid; depleted zones; clear smooth boundary.

Sodium acetate extractable bases, cation exchange capacity (pH 7) and (pH 8.2), effective cation exchange capacity, KCL extractable aluminum and acidity, BaCl2 acidity, percent base saturation; direct measurement and sum of cations.
Site 5.

				cmol(+)/Kg										Base Saturation	
SAMPLE #	HORIZON	DEPTH (cm)	Ca	Mg	Na	K	Al(KCL)	CEC ph 7	ECEC	KCL Acidity	CEC ph 8.2	BaCl2 Acidity	ph7	Sum of Cations
99145	Ap	0-6	7.43	1.65	0.12	0.30	0.00	12.47	9.50	0.05			76	
99146	Bt1	6-22	3.95	1.13	0.07	0.19	0.00	10.67	5.34	0.05			50	
99147	Bt2	22-60	4.23	4.75	0.21	0.26	0.13	15.35	9.58	0.22			62	
99148	Bt3	60-109	1.58	3.14	0.22	0.24	1.54	13.22	6.72	0.66			39	
99149	2BC1	109-137	1.14	1.87	0.21	0.23	1.26	7.43	4.71	0.57	9.61	2.18	46	36
99150	2BC2	137-176	0.73	1.93	0.10	0.21	1.04	6.88	4.01	0.55			43	
99151	2BC3	176-204	0.71	1.99	0.14	0.19	0.90	6.40	3.93	0.54			47	
99152	2BC4	204-260	0.69	1.82	0.11	0.15	0.37	5.08	3.14	0.31			54	
99153	3BC5	260-300+	0.76	1.44	0.10	0.13	0.10	4.70	2.53	0.24			52	

Particle Size Distribution for Site 5.

		USDA Particle Size Class								
	LOWER	VCOS	COS	MS	FS	VFS	SAND	SILT	CLAY	FINE CLAY
Horizon	DEPTH (cm)	%	%	%	%	%	%	%	%	% of clay
Ap	6	0.29	1.05	1.15	0.76	1.15	5.54	76.02	18.43	4.28
Bt1	22	0.19	0.65	1.48	0.83	1.11	4.63	73.26	22.11	6.44
Bt2	60	0	0.2	0	0.3	0.4	1.09	77.86	21.05	13.58
Bt3	109	0	1.41	1.72	1.31	0.71	5.05	73.08	21.88	10.25
2BC1	137	0.2	5.95	9.88	7.96	1.11	25.3	57.64	17.06	7.26
2BC2	176	0.6	9.36	14.39	9.66	1.11	35.21	48.81	15.98	7.57
2BC3	204	0.99	12.69	18.43	14.47	1.29	47.97	35.3	16.73	10.07
2BC4	260	1.9	17.43	22.75	21.84	1.1	65.13	21.44	13.43	8.66
3BC5	300	1.98	14.19	20.44	18.35	1.19	56.15	30.79	13.06	8.17

Total carbon, organic carbon, and pH data.
Site 5.

SAMPLE#	HORIZON	DEPTH (cm)	Total Carbon	Organic Carbon	pH 1:1	pH 2:1
99145	Ap	0-6	3.32	1.82	5.6	5
99146	Bt1	6-22	0.84	0.31	5.9	5.2
99147	Bt2	22-60	0.42	0.06	5.5	4.7
99148	Bt3	60-109	0.26	0.06	5.2	4.4
99149	2BC1	109-137	0.24	0	5.2	4.2
99150	2BC2	137-176	0.18	0.05	5	4.2
99151	2BC3	176-204	0.18	0	5.1	4.2
99152	2BC4	204-260	0.12	0.06	5.2	4.3
99153	3BC5	260-300+	0.09	0.06	5.1	4.4

Dithionite extractable iron, total iron, and hydroxylamine extractable manganese.
Site 5.

		mg kg^-1		
HORIZON	DEPTH (cm)	Free Iron	Total Iron	Ha Mn
Ap	0-6	4335.57	19145.60	378.11
Bt1	6-22	5006.76	20551.13	369.33
Bt2	22-60	9844.30	33911.22	285.27
Bt3	60-109	10821.19	29440.94	297.17
2BC1	109-137	5896.55	21579.15	305.24
2BC2	137-176	8884.09	19467.48	293.70
2BC3	176-204	7677.55	18563.04	284.95
2BC4	204-260	6002.21	15239.48	242.39
3BC5	260-300+	7293.18	16544.47	84.28

Concentration of selected elements for site five.

	mg kg-1																
Horizon	Al	Ba	Ca	Co	Cr	Cu	Fe	K	Mn	Ni	P	Pb	S	Sr	Ti	Zn	Zr
Ap	40009.15	572.99	2500.46	11.19	23.99	14.09	19145.60	14765.79	571.43	27.24	232.44	47.59	140.81	90.55	2203.05	79.93	112.18
Bt1	43046.22	673.22	2367.75	11.53	23.54	21.09	20551.13	16191.45	589.70	22.49	140.19	49.54	67.08	112.31	2139.00	77.24	108.36
Bt2	62285.21	647.31	2086.84	15.35	31.38	18.02	33911.22	17515.28	622.19	31.48	272.36	55.39	25.00	123.05	2376.91	111.04	113.49
Bt3	55035.00	619.28	1884.03	13.65	31.69	14.44	29440.94	17413.44	568.86	35.23	139.17	63.55	25.00	94.34	2363.09	68.75	123.65
2BC1	43485.15	488.90	1552.96	11.28	23.54	16.93	21579.15	14969.45	535.61	29.74	81.59	51.33	25.00	76.01	2140.61	98.43	113.49
2BC2	37321.46	431.37	1078.65	10.19	22.48	15.66	19467.48	11608.96	510.14	24.99	27.10	38.21	25.00	95.36	1889.51	61.22	92.41
2BC3	32496.21	307.68	641.97	7.06	24.44	17.81	18563.04	8452.14	449.02	31.98	36.75	31.05	25.00	85.09	1515.85	64.14	68.27
2BC4	23613.95	192.14	311.47	6.31	22.33	18.63	15239.48	4480.65	363.55	24.24	26.45	36.33	25.00	28.15	1199.15	34.03	44.57
3BC5	26309.53	210.88	326.33	6.28	28.97	21.80	16544.47	5091.65	178.14	25.74	5.00	26.27	25.00	88.33	1382.20	33.92	61.28

Saturated hydraulic conductivity at selected depths for site five.

Site five
Hole depth: 104 cm
Horizon: BC1
Chambers used: 1

Change in water level (cm)	Conversion factor (cm^2)	Elapsed time (min)	Q (cm3/hr)	K (cm/hr)
0.0	20	0	na	na
1.3	20	16	97.5	0.058256
1.0	20	22	54.5	0.032564
0.8	20	19	50.5	0.030174
0.6	20	15	48	0.02868
			mean K=	0.030473

Site five
Hole depth: 122 cm
Horizon: 2BC1
Chambers used: 1

Change in water level (cm)	Conversion factor (cm^2)	Elapsed time (min)	Q (cm3/hr)	K (cm/hr)
0	20	0	na	na
0.4	20	15	32.0	0.04128
0.1	20	5	24.0	0.03096
0.1	20	5	24.0	0.03096
0.1	20	5	24.0	0.03096
			mean K=	0.03096

Bulk density, particle density, and total porosity.
Site 5.

Horizon	Lower Depth (cm)	Bulk Density g cm^ -3	Particle Density g cm^ -3	Total Porosity %
Ap	6	ns	ns	ns
Bt1	22	1.74	2.72	35.92
Bt2	60	1.45	2.70	46.28
Bt3	109	1.55	2.65	41.31
2BC1	137	1.71	2.70	36.85
2BC2	176	1.8	2.74	34.44
2BC3	204	1.93	2.77	30.51
2BC4	260	1.81	2.54	28.65
3BC5	300+	1.98	2.67	26.01

Appendix F. Morphology and Laboratory Data for Site 6.

Field morphology data sheet, texture corrected by lab data.
Site 6.

Landscape position: Upland
Parent Material: Loess/Alluvium/Tertiary Sand
Elevation: 164.98 meters above mean sea level
Slope: 1%
Aspect: 270° NW
Longitude / Latitude: 35.1344, -89.2233

HORIZON	DEPTH (cm)	COLOR	TEXTURE	BOUNDARY	STRUCTURE	CONSISTANCE	NOTES
Ap	0-4	10YR 4/4	SiL	A	WGR	FR	
Bt1	4-28	10YR 4/4	SiL	C	WSBK	FR	Mn conc
Bt2	28-55	7.5YR 4/4	SiL	C	WSBK	FR	
BC1	55-89	7.5 YR 4/4	SiL	C	WSBK	FR	Mn conc
BC2	89-138	7.5YR 4/4	SiL	C	WSBK	FR	
2BC3	138-178	7.5YR 4/4	L	C	WSBK	FR	blind pores, stripped
2BC4	178-214	5YR 4/6	L	C	WSBK	FR	blind pores, stripped
2BC5	214-244	5YR 4/4	SL	C	SG	FR	stripped
3BC6	244-300+	2.5YR 4/6	SL	C	SG	FR	stripped

Classification: Fine-silty, mixed, active, thermic Ultic Hapludalf

Soil profile description for site six.

Landscape position: Upland
Parent Material: Loess/Alluvium/Tertiary Sand
Elevation: 164.98 meters above mean sea level
Slope: 1%
Aspect: 270° NW
Drainage: well drained
Longitude / Latitude: 35.1344, -89.2233
Classification: Fine-silty, mixed, active, thermic Ultic Hapludalf

Ap- 0 to 4 cm; dark yellowish brown (10YR 4/4) silt loam; weak granular structure; friable; nonacid; abrupt smooth boundary.

Bt1- 4 to 28 cm; dark yellowish brown (10YR 4/4) silt loam; weak subangular blocky structure; friable; acid; manganese concentrations; clear smooth boundary.

Bt2- 28 to 55 cm; brown (7.5YR 4/4) silt loam; weak subangular blocky structure; friable; acid; clear smooth boundary.

BC1- 55 to 89 cm; brown (7.5YR 4/4) silt loam; weak subangular blocky structure; friable; acid; few manganese concentrations; clear smooth boundary.

BC2- 89 to 138 cm; brown (7.5YR 4/4) silt loam; weak subangular blocky structure; friable; acid; clear smooth boundary.

2BC3- 138 to 178 cm; brown (7.5YR 4/4) loam; weak subangular blocky structure; friable; acid; few blind pores; few depleted zoned; clear smooth boundary.

2BC4- 178 to 214 cm; yellowish red (5YR 4/6) loam; weak subangular blocky structure; friable; acid; few blind pores; few depleted zones; clear smooth boundary.

2BC5- 214 to 244 cm; reddish brown (5YR 4/4) sandy loam; single grain structure; friable; acid; depleted zones; clear smooth boundary.

3BC6- 244 to 300 cm+; dark red (2.5YR 4/8) sandy loam; single grain structure; friable; acid; few depleted zones; clear smooth boundary.

Sodium acetate extractable bases, cation exchange capacity (pH 7) and (pH 8.2), effective cation exchange capacity, KCL extractable aluminum and acidity, BaCl2 acidity, percent base saturation; direct measurement and sum of cations.
Site 6.

				cmol(+)/Kg									% Base Saturation	
SAMPLE #	HORIZON	DEPTH (cm)	Ca	Mg	Na	K	Al(KCL)	CEC ph 7	ECEC	KCL Acidity	CEC ph 8.2	BaCl2 Acidity	ph7	Sum of Cations
99154	Ap	0-4	5.96	1.63	0.09	0.26	0.00	13.62	7.94	0.07			58	
99155	Bt1	4-28	4.48	1.95	0.13	0.20	0.00	10.65	6.76	0.10			63	
99156	Bt2	28-55	2.95	3.37	0.21	0.22	1.49	13.08	8.24	0.67			52	
99157	BC1	55-89	2.29	3.84	0.21	0.17	0.60	11.06	7.11	0.41			59	
99158	BC2	89-138	2.16	2.44	0.22	0.16	0.01	7.33	4.99	0.22	11.98	4.65	68	42
99159	2BC3	138-178	1.51	2.29	0.09	0.14	0.09	5.23	4.12	0.22			77	
99160	2BC4	178-214	1.58	2.51	0.10	0.16	0.15	8.32	4.50	0.22			52	
99161	2BC5	214-244	1.09	1.89	0.11	0.13	0.10	6.11	3.32	0.20			53	
99162	3BC6	244-300+	0.83	1.34	0.15	0.09	0.00	4.25	2.41	0.12			57	

Particle Size Distribution for Site 6.

		USDA Particle Size Class								
	LOWER	VCOS	COS	MS	FS	VFS	SAND	SILT	CLAY	FINE CLAY
Horizon	DEPTH (cm)	%	%	%	%	%	%	%	%	% of clay
Ap	4	0.2	1.31	1.2	0.8	0.9	4.62	77.27	18.11	4.26
Bt1	28	0	0.57	0.48	1.05	0.67	3.16	70.63	26.21	10.19
Bt2	55	0	0.4	0.5	0.4	0.3	1.61	70.94	27.45	10.17
BC1	89	0	1.39	1.89	1.49	0.6	5.58	73.15	21.27	1.16
BC2	138	0.5	7.49	9.69	8.69	1.1	27.47	56.22	16.3	7.87
2BC3	178	1.1	12.35	17.27	13.45	1.31	45.48	40.38	14.14	4.90
2BC4	214	0.5	12.28	18.91	17.62	1.39	50.69	32.59	16.71	7.41
2BC5	244	1.58	15.15	28.12	23.86	1.88	70.5	17.7	11.8	6.77
3BC6	300+	1.52	14.95	29.8	27.58	1.82	74.75	17.33	7.92	4.24

Total carbon, organic carbon, and pH data.
Site 6.

Sample #	HORIZON	DEPTH (cm)	Total Carbon %	Organic Carbon %	pH 1:1	pH 2:1
99154	Ap	0-4	3.62	1.01	5.5	5
99155	Bt1	4-28	0.72	0.15	5.6	4.8
99156	Bt2	28-55	0.28	0.03	5.3	4.4
99157	BC1	55-89	0.20	0.06	5.4	4.5
99158	BC2	89-138	0.17	0.06	5.5	4.6
99159	2BC3	138-178	0.16	0	5.5	4.5
99160	2BC4	178-214	0.16	0	5.4	4.4
99161	2BC5	214-244	0.17	0	5.3	4.5
99162	3BC6	244-300+	0.19	0.05	5.1	4.5

Dithionite extractable irons, total iron, and hydroxylamine extractable manganese.
Site 6.

		mg kg ^-1		
HORIZON	DEPTH (cm)	Free Iron	Total Iron	Ha Mn
Ap	0-4	7521.99	20025.52	350.99
Bt1	4-28	10694.47	26808.99	344.06
Bt2	28-55	12964.55	33121.54	248.33
BC1	55-89	10934.56	28500.50	268.14
BC2	89-138	7015.97	19679.67	251.72
2BC3	138-178	6714.63	15279.38	227.67
2BC4	178-214	5711.55	15570.04	302.90
2BC5	214-244	6010.46	13516.37	210.68
3BC6	244-300+	4891.22	10230.63	90.38

Concentration of selected elements for site six.

	mg kg-1																
Horizon	Al	Ba	Ca	Co	Cr	Cu	Fe	K	Mn	Ni	P	Pb	S	Sr	Ti	Zn	Zr
Ap	40679.93	598.72	2729.57	12.24	27.32	12.37	20025.52	14489.80	587.58	18.21	356.60	51.65	350.54	71.12	2110.75	84.86	105.97
Bt1	52740.98	611.67	2178.94	15.52	31.69	16.02	26808.99	16326.53	640.90	16.30	305.84	50.89	354.80	78.13	2282.01	77.54	113.53
Bt2	61428.91	581.09	1827.13	14.70	34.19	17.57	33121.54	17142.86	562.43	23.97	287.53	57.85	287.20	84.40	2323.16	140.74	113.96
BC1	54831.05	573.97	2014.64	12.54	27.32	12.67	28500.50	17244.90	556.83	18.45	159.89	53.96	235.44	92.43	2586.15	69.19	123.97
BC2	40047.62	468.62	1650.56	15.18	23.11	18.95	19679.67	13265.31	523.05	17.98	83.26	54.05	119.04	74.63	2176.57	74.10	101.81
2BC3	30034.65	325.09	909.00	7.96	17.17	10.93	15279.38	8367.35	414.93	10.00	167.81	34.34	112.08	58.11	1600.07	33.63	76.79
2BC4	28358.58	242.40	540.10	7.05	19.52	14.23	15570.04	6122.45	465.95	10.00	152.15	35.63	178.59	34.78	1534.25	33.43	56.34
2BC5	20836.81	156.64	337.24	4.54	18.74	18.57	13516.37	3469.39	332.20	10.00	146.49	25.00	186.44	25.00	1184.49	47.10	54.21
3BC6	16004.22	121.52	215.27	4.65	15.93	13.16	10230.63	2653.06	180.32	10.00	118.54	25.00	177.16	25.00	1108.27	14.17	34.93

Saturated hydraulic conductivity data at selected depths for site six.

Site six

Hole depth: 116 cm

Horizon: BC1

Chambers used: 1

Change in water level (cm)	Conversion factor (cm^2)	Elapsed time (min)	Q (cm3/hr)	K (cm/hr)
0.0	20	0	na	na
0.5	20	5	120	0.11024
0.4	20	5	96	0.088192
0.3	20	5	72	0.066144
0.3	20	5	72	0.066144
			mean K=	0.073494

Site six

Hole depth: 142 cm

Horizon: 2BC1

Chambers used: 1

Change in water level (cm)	Conversion factor (cm^2)	Elapsed time (min)	Q (cm3/hr)	K (cm/hr)
0	20	0	na	na
0.2	20	5	48.0	0.07399
0.3	20	5	72.0	0.110985
0.3	20	5	72.0	0.110985
0.2	20	5	48.0	0.07399
			mean K=	0.098653

Bulk density, particle density, and total porosity.
Site 6.

Horizon	Lower Depth (cm)	Bulk Density g cm^ -3	Particle Density g cm^ -3	Total Porosity %
Ap	4	ns	ns	ns
Bt1	28	1.65	2.58	35.86
Bt2	55	1.43	2.73	47.55
BC1	89	1.44	2.67	45.99
BC2	138	1.72	2.60	34.10
2BC3	178	1.91	2.65	27.91
2BC4	214	1.93	2.71	28.86
2BC5	244	ns	ns	ns
3BC6	300	1.99	2.74	27.42

Appendix G. Morphology and Laboratory Data for Site 7.

Field morphology data sheet, textures corrected by lab data
Site 7.

Landscape position: Upland
Parent Material: Loess/Alluvium/Tertiary Sand
Elevation: 165.06 meters above mean sea level
Slope: 1%
Aspect: 270° NW
Longitude / Latitude: 35.1343, -89.2231

HORIZON	DEPTH (cm)	COLOR	TEXTURE	BOUNDARY	STRUCTURE	CONSISTANCE	NOTES
Ap	0-4	10YR 4/3	SiL	A	WGR	FR	
Bt1	4-31	10YR 4/4	SiL	C	WSBK	FR	
Bt2	31-60	7.5YR 4/4	SiL	C	MoSBK	FR	Mn conc
BC1	60-106	7.5YR 4/4	SiL	C	MoSBK	FR	Mn conc, bind pores
2BC2	106-144	7.5YR 4/4	SiL	C	MoSBK	FR	Mn conc
2BC3	144-172	5YR 4/4	SiL	C	MoSBK	FR	Mn conc, bind pores
2BC4	172-188	5YR 4/4	SC	C	MoSBK	FR	bind pores
2BC5	188-238+	5YR 4/4	SCL	C	WSBK	FR	bind pores

Classification: Fine-silty, mixed, active, thermic Ultic Hapludalf

Soil profile description for site seven.

Landscape position: Upland
Parent Material: Loess/Alluvium/Tertiary Sand
Elevation: 165.06 meters above mean sea level
Slope: 1%
Aspect: 270° NW
Drainage: well drained
Longitude / Latitude: 35.1343, -89.2231
Classification: Fine-silty, mixed, active, thermic Ultic Hapludalf

Ap- 0 to 4 cm; brown (10YR 4/3) silt loam; weak granular structure; friable; nonacid; abrupt smooth boundary.

Bt1- 4 to 31 cm; dark yellowish brown (10YR 4/4) silt loam; weak subangular blocky structure; friable; nonacid; clear smooth boundary.

Bt2- 31 to 60 cm; brown (7.5YR 4/4) silt loam; moderate subangular blocky structure; friable; acid; few manganese concentrations; clear smooth boundary.

BC1- 60 to 106 cm; brown (7.5YR 4/4) silt loam; moderate subangular blocky structure; friable; acid; few blind pores; many manganese concentrations; clear smooth boundary.

2BC2- 106 to 144 cm; brown (7.5YR 4/4) silt loam; moderate subangular blocky structure; friable; acid; many manganese concentrations; clear smooth boundary.

2BC3- 144 to 172 cm; reddish brown (5YR 4/4) silt loam; moderate subangular blocky structure; friable; acid; few blind pores; few manganese concentrations; clear smooth boundary.

2BC4- 172 to 188 cm; reddish brown (5YR 4/4) sandy clay; moderate subangular blocky structure; friable; acid; few blind pores; clear smooth boundary.

2BC5- 188 to 238 cm+; reddish brown (5YR 4/4) sandy clay loam; weak subangular blocky structure; friable; acid; few blind pores; clear smooth boundary.

Sodium acetate extractable bases, cation exchange capacity (pH 7) and (pH 8.2), effective cation exchange capacity, KCL extractable aluminum and acidity, BaCl2 acidity, percent base saturation; direct measurement and sum of cations.
Site 7.

			cmol(+)/Kg										% Base Saturation	
SAMPLE #	HORIZON	DEPTH (cm)	Ca	Mg	Na	K	Al(KCL)	CEC ph 7	ECEC	KCL Acidity	CEC ph 8.2	BaCl2 Acidity	ph7	Sum of Cations
99163	Ap	0-4	11.91	2.26	0.06	0.26	0.00	19.25	14.49	0.03			75	
99164	Bt1	4-31	7.22	2.92	0.06	0.22	0.00	14.87	10.44	0.05			70	
99165	Bt2	31-60	3.02	4.06	0.09	0.22	1.25	15.23	8.66	0.55			49	
99166	BC1	60-106	2.21	3.55	0.09	0.24	1.57	13.24	7.66	0.53			46	
99167	2BC2	106-144	1.54	2.85	0.09	0.24	1.03	8.45	5.75	0.41	12.69	4.24	55	37
99168	2BC3	144-172	1.55	3.34	0.10	0.22	0.00	8.28	5.21	0.34			63	
99169	2BC4	172-188	1.45	3.12	0.11	0.20	0.75	7.53	5.63	0.28			55	
99170	2BC5	188-238+	1.18	2.16	0.09	0.17	0.58	7.46	4.18	0.25			48	

Particle Size Distribution for Site 7.

		USDA Particle Size Class								
	LOWER	VCOS	COS	MS	FS	VFS	SAND	SILT	CLAY	FINE CLAY
Horizon	DEPTH (cm)	%	%	%	%	%	%	%	%	% of clay
Ap	4	0.1	0.9	1.39	1.1	0.9	4.48	74.44	21.08	5.06
Bt1	31	0	0.71	1.06	0.98	0.62	3.07	71.28	25.65	10.94
Bt2	60	0.2	0.6	0.6	0.5	0.4	2.3	68.12	28.51	12.06
BC1	106	0	1	1.3	1.2	0.5	4.19	74.57	21.24	9.82
2BC2	144	0.3	5.09	8.59	6.99	1.3	22.38	60.08	17.54	7.07
2BC3	172	0.3	8.7	14.4	10	1.1	34.3	46.06	19.64	9.80
2BC4	188	0.9	11.76	16.75	13.66	1.4	44.17	37.97	17.87	10.61
2BC5	238	1	14.86	21.89	18.37	1.31	57.93	27.05	15.02	10.16

Total carbon, organic carbon, and pH data.
Site 7.

Sample #	HORIZON	DEPTH (cm)	Total Carbon	Organic Carbon	pH 1:1	pH 2:1
99163	Ap	0-4	3.31	1.91	6.4	5.8
99164	Bt1	4-31	0.65	0.31	6.2	5.4
99165	Bt2	31-60	0.23	0	5.4	4.4
99166	BC1	60-106	0.20	0	5.5	4.3
99167	2BC2	106-144	0.17	0	5.5	4.4
99168	2BC2	144-172	0.23	0	5.3	4.4
99169	2BC3	172-188	0.21	0	5.6	4.4
99170	2BC4	188-238+	0.18	0.08	5.6	4.3

Dithionite extractable iron, total iron, and hydroxylamine extractable manganese.
Site 7.

HORIZON	DEPTH (cm)	Free Iron	Total Iron	Ha Mn
Ap	0-4	9756.31	23927.74	253.00
Bt1	4-31	12122.00	28743.78	225.89
Bt2	31-60	13060.93	31433.49	213.61
BC1	60-106	11995.68	31181.75	239.89
2BC2	106-144	9103.53	22362.66	322.14
2BC3	144-172	7534.57	21388.19	328.46
2BC4	172-188	7011.13	20609.00	333.42
2BC5	188-238+	6521.72	18245.20	341.93

Concentration of selected elements for site seven.

	mg kg-1																
Horizon	Al	Ba	Ca	Co	Cr	Cu	Fe	K	Mn	Ni	P	Pb	S	Sr	Ti	Zn	Zr
Ap	46689.70	550.67	3515.06	17.93	27.32	16.98	23927.74	14897.96	488.77	27.80	346.78	61.94	258.65	74.16	2360.10	126.96	119.39
Bt1	54855.42	587.40	2275.04	14.75	29.35	14.63	28743.78	16632.65	532.30	10.00	394.02	59.16	222.75	73.43	2459.20	67.98	117.36
Bt2	57862.19	573.16	1548.12	13.68	29.51	13.27	31433.49	17448.98	547.03	12.46	277.76	68.10	284.90	81.54	2501.03	92.28	120.88
BC1	57877.74	568.56	1914.68	13.78	39.77	11.18	31181.75	18656.72	582.21	11.17	387.74	53.14	203.81	92.02	2536.62	72.89	127.71
BC2	44693.88	488.15	1647.30	15.43	25.56	14.60	22362.66	14712.15	673.71	12.13	242.96	38.84	203.30	80.68	2273.90	77.50	110.89
2BC3	41553.58	419.89	1157.69	16.80	19.98	20.36	21388.19	11833.69	687.52	10.00	343.61	38.51	254.15	61.57	2196.38	75.06	93.34
2BC4	38665.95	350.13	885.49	9.72	22.29	12.69	20609.00	9808.10	654.02	26.48	141.35	42.41	25.00	42.84	1890.75	55.24	79.69
2BC5	32028.79	291.86	602.32	9.24	21.33	15.73	18245.20	6503.20	678.51	21.38	208.85	39.97	62.22	27.85	1584.87	35.28	58.00

Saturated hydraulic conductivity data at selected depths for site seven.

Site seven

Hole depth: 101 cm

Horizon: BC1

Chambers used: 1

Change in water level (cm)	Conversion factor (cm^2)	Elapsed time (min)	Q (cm3/hr)	K (cm/hr)
0.0	20	0	na	na
0.5	20	6	100	0.074536
0.2	20	5	48	0.035777
0.3	20	5	72	0.053666
0.2	20	5	48	0.035777
0.2	20	5	48	0.035777
			mean K=	0.04174

Site seven

Hole depth: 127 cm

Horizon: 2BC1

Chambers used: 1

Change in water level (cm)	Conversion factor (cm^2)	Elapsed time (min)	Q (cm3/hr)	K (cm/hr)
0	20	0	na	na
0.6	20	6	120.0	0.058971
0.3	20	5	72.0	0.035383
0.6	20	5	144.0	0.070765
0.4	20	5	96.0	0.047177
0.5	20	5	120	0.058971
			mean K=	0.058971

Bulk density, particle density, and total porosity.
Site 7.

Horizon	Lower Depth (cm)	Bulk Density g cm^ -3	Particle Density g cm^ -3	Total Porosity %
Ap	4	ns	ns	ns
Bt1	31	1.53	2.69	43.06
Bt2	60	1.41	2.76	48.86
BC1	106	1.42	2.68	47.23
2BC2	144	1.66	2.74	39.61
2BC3	172	1.69	2.61	35.25
2BC4	188	1.89	2.74	31.04
2BC5	238+	1.85	2.66	30.67

Appendix H. Morphology and Laboratory Data for Site 8.

Field morphology data sheet, texture corrected by lab data.
Site 8.

Landscape position: Upland
Parent Material: Loess/Alluvium/Tertiary Sand
Elevation: 165.41 meters above mean sea level
Slope: 1%
Aspect: 270° NW
Latitude / Longitude: 35.1344, -89.2230

HORIZON	DEPTH (cm)	COLOR	TEXTURE	BOUNDARY	STRUCTURE	CONSISTANCE	NOTES
Ap	0-4	10YR 4/4	SiL	A	WGR	FR	
Bt1	4-22	7.5YR 4/4	SiL	C	WSBK	FR	
Bt2	22-46	7.5YR 4/4	SiL	C	WSBK	FR	Mn conc
BC1	46-82	7.5YR 4/4	SiL	C	MoSBK	FR	Mn conc
BC2	82-123	7.5YR 4/4	SiCL	C	MoSBK	FR	Mn conc
2BC3	123-166	5YR 4/4	SiCL	C	MoSBK	FR	Mn conc, stripped
2BC4	166-224	5YR 4/4	SCL	C	WSBK	FR	Mn conc, stripped
3BC5	224-260	2.5YR 4/4	SL	G	WSBK	FR	1/2cm pore, stripped, Mn conc
3BC6	260-293+	2.5YR 4/4	LS	G	SG	VFR	stripped

Classification: Fine-silty, mixed, active, thermic Ultic Hapludalf

Soil profile description for site eight.

Landscape position: Upland
Parent Material: Loess/Alluvium/Tertiary Sand
Elevation: 165.41 meters above mean sea level
Slope: 1%
Aspect: 270° NW
Drainage: well drained
Latitude / Longitude: 35.1344, -89.2230
Classification: Fine-silty, mixed, active, thermic Ultic Hapludalf

Ap- 0 to 4 cm; dark yellowish brown (10YR 4/4) silt loam; weak granular structure; friable; acid; abrupt smooth boundary.

Bt1- 4 to 22 cm; brown (7.5YR 4/4) silt loam; weak subangular blocky structure; friable; acid; clear smooth boundary

Bt2- 22 to 46 cm; brown (7.5YR 4/4) silt loam; weak subangular blocky structure; friable; acid; few manganese concentrations; clear smooth bondary.

BC1- 46 to 82 cm; brown (7.5YR 4/4) silt loam; moderate subangular blocky structure; friable; acid; few manganese concentrations; clear smooth boundary.

BC2- 82 to 123 cm; brown (7.5YR 4/4) silty clay loam; moderate subangular blocky structure; friable; acid; manganese concentrations common; clear smooth boundary.

2BC3- 123 to 166 cm; reddish brown (5YR 4/4) silty clay loam; moderate subangular blocky structure; friable; acid; manganese concentrations common; few depleted zones; clear smooth boundary.

2BC4- 166 to 224 cm; reddish brown (5YR 4/4) sandy clay loam; weak subangular blocky stucture; friable; acid; manganese concentrations common; few depleted zones; clear smooth boundary.

3BC5- 224 to 260 cm; dusky red (2.5YR 4/4) sandy loam; weak subangular blocky structure; friable; acid; large pore present (.5cm dia.); manganese concentrations common; few depleted zones; clear smooth boundary.

3BC6- 260to 293 cm+; dusky red (2.5YR 4/4) loamy sand; single grain structure; very friable; acid; few depleted zones present; clear smooth boundary.

Sodium acetate extractable bases, cation exchange capacity (pH 7) and (pH 8.2), effective cation exchange capacity, KCL extractable aluminum and acidity, BaCl2 acidity, percent base saturation; direct measurement and sum of cations.
Site 8.

			cmol(+)/Kg										% Base Saturation	
SAMPLE #	HORIZON	DEPTH (cm)	Ca	Mg	Na	K	Al(KCL)	CEC ph 7	ECEC	KCL Acidity	CEC ph 8.2	BaCl2 Acidity	ph7	Sum of Cations
99171	Ap	0-4	3.61	3.47	0.11	0.19	0.03	14.04	7.41	0.06			52	
99172	Bt1	4-22	5.46	1.98	0.23	0.15	0.10	11.68	7.92	0.10			67	
99173	Bt2	22-46	5.34	1.90	0.10	0.15	1.64	14.69	9.13	0.63			51	
99174	BC1	46-82	2.07	2.37	0.30	0.19	2.74	13.62	7.67	0.97			36	
99175	BC2	82-123	1.29	3.97	0.11	0.17	1.75	10.96	7.29	0.67			51	
99176	2BC3	123-166	1.22	3.31	0.22	0.16	1.08	10.18	6.02	0.45	11.23	1.05	48	44
99177	2BC4	166-224	1.30	2.74	0.20	0.13	0.85	8.64	5.22	0.38			51	
99178	3BC5	224-260	1.10	2.23	0.11	0.12	0.63	7.00	4.19	0.31			51	
99179	3BC6	260-293+	0.67	1.52	0.11	0.09	0.33	4.78	2.72	0.19			50	

Particle Size Distribution for Site 8.

		USDA Particle Size Class								
	LOWER	VCOS	COS	MS	FS	VFS	SAND	SILT	CLAY	FINE CLAY
Horizon	DEPTH (cm)	%	%	%	%	%	%	%	%	% of clay
Ap	4	0.11	0.42	1.16	0.84	0.84	3.46	78.73	17.78	5.41
Bt1	22	0	0.61	1.05	0.79	0.79	3.32	73.79	22.89	9.41
Bt2	46	0	0.2	0.3	0.1	0.3	1.5	69.46	29.04	15.4
BC1	82	0	1.09	0.99	0.1	0.1	2.38	74.85	22.77	11.88
BC2	123	0	0.4	0.5	0.59	0.1	1.59	78.47	19.94	9.75
2BC3	166	0	4.37	8.16	6.32	1.26	20.21	61.83	17.96	8.86
2BC4	224	0	11.12	12.5	12.3	1.08	37.01	45.31	17.68	11.02
3BC5	260	1.11	13.93	20.79	19.88	1.61	58.12	26.26	15.62	10.74
3BC6	293+	1.41	19.05	26.51	20.77	1.71	71.17	19.64	9.19	6.69

Total carbon, organic carbon, and pH data.
Site 8.

Sample #	HORIZON	DEPTH (cm)	Total Carbon	Organic Carbon	pH 1:1	pH 2:1
99171	Ap	0-4	2.76	1.21	5.6	4.8
99172	Bt1	4-22	0.83	0.46	5.8	4.9
99173	Bt2	22-46	0.28	0.23	5.4	4.5
99174	BC1	46-82	0.31	0.08	5.3	4.3
99175	BC2	82-123	0.20	0.08	5.4	4.4
99176	2BC3	123-166	0.20	0.06	6.1	4.3
99177	2BC4	166-224	0.22	0	6	4.3
99178	3BC5	224-260	0.18	0.04	5.7	4.4
99179	3BC6	260-293+	0.14	0.04	5.6	4.4

Dithionite extractable iron, total iron, and hydroxylamine extractable manganese.
Site 8.

		mg kg^-1		
HORIZON	DEPTH (cm)	Free Iron	Total Iron	Ha Mn
Ap	0-4	7419.05	22768.95	258.27
Bt1	4-22	8759.13	26831.31	234.04
Bt2	22-46	13855.78	35260.67	208.92
BC1	46-82	11683.80	34733.32	163.62
BC2	82-123	10179.66	32073.72	151.44
2BC3	123-166	7871.43	26017.58	162.69
2BC4	166-224	8734.03	19641.90	293.47
3BC5	224-260	8240.78	16623.55	396.70
3BC6	260-293+	8285.00	16593.40	383.62

Concentration of selected elements for site eight.

	mg kg-1																
Horizon	Al	Ba	Ca	Co	Cr	Cu	Fe	K	Mn	Ni	P	Pb	S	Sr	Ti	Zn	Zr
Ap	46323.54	592.87	2471.66	13.64	24.79	8.23	22768.95	15778.25	627.63	35.42	411.01	49.47	221.80	74.15	2420.94	64.15	118.44
Bt1	52953.37	712.91	2393.23	15.12	31.13	11.54	26831.31	17164.18	590.79	32.87	247.24	61.44	59.12	80.30	2687.78	59.75	125.76
Bt2	64858.89	634.32	1759.73	17.36	33.43	14.48	35260.67	17377.40	704.45	28.72	390.26	58.77	25.00	78.57	2874.09	82.68	120.88
BC1	62808.21	610.02	1671.30	16.87	34.20	14.65	34733.32	18017.06	721.02	51.69	281.37	52.99	35.26	84.04	2988.58	89.15	130.63
BC2	59969.21	615.84	2007.28	15.39	30.17	11.54	32073.72	18550.10	734.03	25.85	307.67	57.34	183.32	104.31	2722.46	64.16	133.19
2BC3	49539.54	547.58	1789.59	13.62	25.75	11.79	26017.58	16417.91	732.58	21.06	269.47	61.63	104.81	82.03	2432.97	51.94	115.89
2BC4	40185.35	404.05	1025.10	11.80	25.67	10.07	19641.90	10794.30	735.80	39.38	137.64	39.90	25.00	49.51	1988.14	36.99	89.72
3BC5	30662.54	255.22	476.18	9.42	19.91	10.55	16623.55	6008.15	708.73	27.24	136.43	36.11	25.00	26.47	1490.60	30.01	57.95
3BC6	18890.21	144.49	324.89	6.87	30.04	35.00	16593.40	3462.32	474.39	39.38	41.98	26.38	25.00	25.00	1105.41	24.35	35.26

Saturated hydraulic conductivity data at selected depths for site eight.

Site eight

Hole depth: 102 cm

Horizon: BC1

Chambers used: 1

Change in water level (cm)	Conversion factor (cm^2)	Elapsed time (min)	Q (cm3/hr)	K (cm/hr)
0	20	0	na	na
0.2	20	7	34.3	0.036215
0.4	20	10	48.0	0.050679
0.4	20	10	48.0	0.050679
0.3	20	10	36.0	0.03801
0.3	20	10	36	0.03801
			mean K=	0.042233

Site eight

Hole depth: 122 cm

Horizon: 2BC1

Chambers used: 1

Change in water level (cm)	Conversion factor (cm^2)	Elapsed time (min)	Q (cm3/hr)	K (cm/hr)
0.0	20	0	na	na
0.4	20	8	96	0.124493
0.2	20	4	48	0.062246
0.2	20	4	48	0.062246
0.2	20	4	48	0.062246
			mean K=	0.062246

Bulk density, particle density, and total porosity.
Site 8.

Horizon	Lower Depth (cm)	Bulk Density g cm^ -3	Particle Density g cm^ -3	Total Porosity %
Ap	4	ns	ns	ns
Bt1	22	1.59	2.51	36.53
Bt2	46	1.45	2.66	45.39
BC1	82	1.47	2.7	45.58
BC2	123	1.56	2.76	43.47
2BC3	166	1.64	2.7	38.99
2BC4	224	1.86	2.72	31.7
3BC5	260	1.79	2.59	30.89
3BC6	293+	1.85	2.53	27.09

Appendix I. Morphology and Laboratory Data for Site 9.

Field morphology data sheet, texture corrected by lab data.
Site 9.

Landscape position: Upland
Parent Material: Loess/Alluvium/Tertiary Sand
Elevation: 165.91 meters above mean sea level
Slope: 1%
Aspect: 270° NW
Latitude / Longitude: 35.1345, -89.2230

HORIZON	DEPTH (cm)	COLOR	TEXTURE	BOUNDARY	STRUCTURE	CONSISTANCE	NOTES
Ap	0-5	10YR 4/4	SiL	A	WGR	FR	
Bt1	5-25	10YR 4/3	SiL	C	WSBK	FR	
Bt2	25-57	7.5YR 4/4	SiL	C	WSBK	FR	
BC1	57-90	7.5YR 4/4	SiL	C	WSBK	FR	Mn conc
BC2	90-117	7.5YR 4/4	SiL	C	MoSBK	FR	Mn conc, blind pores
2BC3	117-160	5YR 4/4	SiCL	C	MoSBK	FR	Mn conc, blind pores, stripped
2BC4	160-199	5YR 4/4	SC	C	MoSBK	FR	blind pores, stripped
3Bt1	199-246+	2.5YR 4/4	SCL	C	WSBK	FR	stripped

Classification: Fine-silty, mixed, active, thermic Ultic Hapludalf

Soil profile description for site nine.

Landscape position: Upland
Parent Material: Loess/Alluvium/Tertiary Sand
Elevation: 165.91 meters above mean sea level
Slope: 1%
Aspect: 270° NW
Drainage: well drained
Latitude / Longitude: 35.1345, -89.2230
Classification: Fine-silty, mixed, active, thermic Ultic Hapludalf

Ap- 0 to 5 cm; dark yellowish brown (10YR 4/4) silt loam; weak granular structure; friable; nonacid; clear smooth boundary.

Bt1- 5 to 25 cm; brown (10YR 4/3) silt loam; weak subangular structure; friable; nonacid; clear smooth boundary.

Bt2- 25 to 57 cm; brown (7.5YR 4/4) silt loam; weak subangular blocky structure; friable; acid; clear smooth boundary.

BC1- 57 to 90 cm; brown (7.5YR 4/4) silt loam; weak subangular blocky structure; friable; acid; few manganese concentrations; clear smooth boundary.

2BC2- 90 to 117 cm; brown (7.5YR 4/4) silt loam; moderate subangular blocky structure; friable; acid; few manganese concentrations; few blind pores; clear smooth boundary.

2BC3- 117 to 160 cm; reddish brown (5YR 4/4) silty clay loam; moderate subangular blocky structure; acid; few blind pores; depleted zones present; clear smooth boundary.

2BC4- 160 to 199 cm; dusky red (2.5YR 4/4) sandy clay; moderate subangular blocky structure; acid; friable; few blind pores; few depleted zones; clear smooth boundary.

3Bt1- 199 to 246 cm+; dusky red (2.5YR 4/4) sandy clay; weak subangular blocky structure; acid; friable; depleted zones; clear smooth boundary.

Sodium acetate extractable bases, cation exchange capacity (pH 7) and (pH 8.2), effective cation exchange capacity, KCL extractable aluminum and acidity, percent base saturation; direct measurement and sum of cations.
Site 9.

			cmol(+)/Kg										Base Saturation	
SAMPLE #	HORIZON	DEPTH (cm)	Ca	Mg	Na	K	Al(KCL)	CEC ph 7	ECEC	KCL Acidity	CEC ph 8.2	BaCl2 Acidity	ph7	Sum of Cations
99180	Ap	0-5	5.12	1.22	0.35	0.26	0.00	11.45	6.95	0.08			61	
99181	Bt1	5-25	4.48	1.17	0.17	0.16	0.00	8.59	5.98	0.06			70	
99182	Bt2	25-57	4.14	4.79	0.29	0.21	0.91	14.82	10.34	0.39			64	
99183	BC1	57-90	3.93	2.51	0.06	0.23	1.08	13.84	9.81	0.47			49	
99184	2BC2	90-117	3.42	2.42	0.08	0.27	0.60	11.06	8.79	0.25			56	
99185	2BC3	117-160	3.02	2.38	0.09	0.21	0.23	9.64	5.93	0.18	11.45	1.81	59	49
99186	2BC4	160-199	1.98	2.35	0.08	0.26	0.22	8.37	4.89	0.18			55	
99187	3Bt1	199-246+	1.78	2.33	0.06	0.20	0.20	7.01	4.57	0.17			34	

Particle Size Distribution for Site 9.

		USDA Particle Size Class								
	LOWER	VCOS	COS	MS	FS	VFS	SAND	SILT	CLAY	FINE CLAY
Horizon	DEPTH (cm)	%	%	%	%	%	%	%	%	% of clay
Ap	5	0.1	0.72	1.03	0.83	0.93	4.44	80.29	15.27	4.38
Bt1	25	0	0.6	0.7	0.6	0.7	2.89	78.77	18.35	5.65
Bt2	57	0	0.4	0.49	0.49	0.59	1.88	70.35	27.77	14.80
BC1	90	0	0.19	0.58	0.48	0.48	2.13	75.12	22.75	9.92
2BC2	117	0	0.88	2.63	2.05	0.58	7.21	72.48	20.31	9.71
2BC3	160	0	3.43	8.89	5.96	0.51	21.01	60.61	18.38	5.01
2BC4	199	0.1	8.52	12.63	10.87	1.57	34.28	62.9	2.82	9.56
3Bt1	246	0.88	15.03	18.57	18.66	1.38	56.39	25.03	18.59	12.57

Total carbon, organic carbon, and pH data.
Site 9.

Sample #	HORIZON	DEPTH (cm)	Total Carbon	Organic Carbon	pH 1:1	pH 2:1
99180	Ap	0-5cm	2.47	1.34	5.6	4.9
99181	Bt1	5-25cm	0.65	0.37	6	5
99182	Bt2	25-57cm	0.39	0.08	5.5	4.5
99183	BC1	57-90cm	0.27	0.05	5.5	4.4
99184	2BC2	90-117cm	0.21	0	5.6	4.4
99185	2BC3	117-160cm	0.22	0	5.7	4.6
99186	2BC4	160-199cm	0.23	0.05	5.8	4.6
99187	3Bt1	199-246+cm	0.21	0	5.6	4.5

Dithionite extractable iron, total iron, and hydroxlyamine extractable manganese.
Site 9.

HORIZON	DEPTH (cm)	Free Iron	Total Iron	Ha Mn
Ap	0-5	9114.43	19658.83	440
Bt1	5-25	7221.28	21562.72	385.5
Bt2	25-57	11986.92	34148.14	299.8
BC1	57-90	10808.18	32133.71	214.4
2BC2	90-117	5339.39	27916.26	141.1
2BC3	117-160	4591.25	22055.43	202.2
2BC4	160-199	4444.73	19910.07	210.9
3Bt1	199-246+	4261.43	15828.18	339.8

Concentration of selected elements for site nine.

	mg kg-1																
Horizon	Al	Ba	Ca	Co	Cr	Cu	Fe	K	Mn	Ni	P	Pb	S	Sr	Ti	Zn	Zr
Ap	41889.47	596.11	2153.05	12.50	28.64	9.98	19658.83	15580.45	729.03	39.97	358.26	41.86	71.84	73.94	2472.49	48.65	112.99
Bt1	47315.61	662.81	2085.37	17.21	29.51	15.64	21562.72	17311.61	782.69	32.86	312.39	45.21	25.00	85.41	2738.73	140.99	125.44
Bt2	64439.13	764.87	2121.28	16.37	37.20	18.53	34148.14	17718.94	786.34	19.24	517.46	45.50	135.44	87.17	2542.65	162.95	117.76
BC1	60208.75	591.13	1859.84	15.03	35.45	18.73	32133.71	17820.77	677.76	39.97	250.77	51.97	25.00	91.33	2486.51	98.19	125.67
2BC2	54962.94	588.72	2205.38	12.98	34.58	10.77	27916.26	18024.44	584.36	40.56	207.28	54.19	25.00	99.75	2336.68	78.35	129.05
2BC3	45871.18	527.16	1853.70	9.94	26.02	10.59	22055.43	15173.12	711.32	32.27	176.09	31.68	25.00	80.78	2284.13	43.71	116.25
2BC4	40190.26	445.52	1391.79	15.58	42.61	17.09	19910.07	12321.79	735.66	34.64	125.68	41.33	25.00	64.50	2123.88	50.37	95.30
3Bt1	30486.45	323.98	728.83	10.65	51.52	18.67	15828.18	6781.38	663.28	82.85	5.00	53.92	25.00	31.70	1506.60	60.90	68.11

Site nine

Hole depth: 111 cm

Horizon: BC1

Chambers used: 1

Change in water level (cm)	Conversion factor (cm^2)	Elapsed time (min)	Q (cm3/hr)	K (cm/hr)
0.0	20	0	na	na
0.2	20	5	48	0.048317
0.2	20	5	48	0.048317
0.1	20	5	24	0.024158
0.1	20	5	24	0.024158
0.2	20	5	48	0.048317
			mean K=	0.032211

Site nine

Hole depth: 125 cm

Horizon: 2BC1

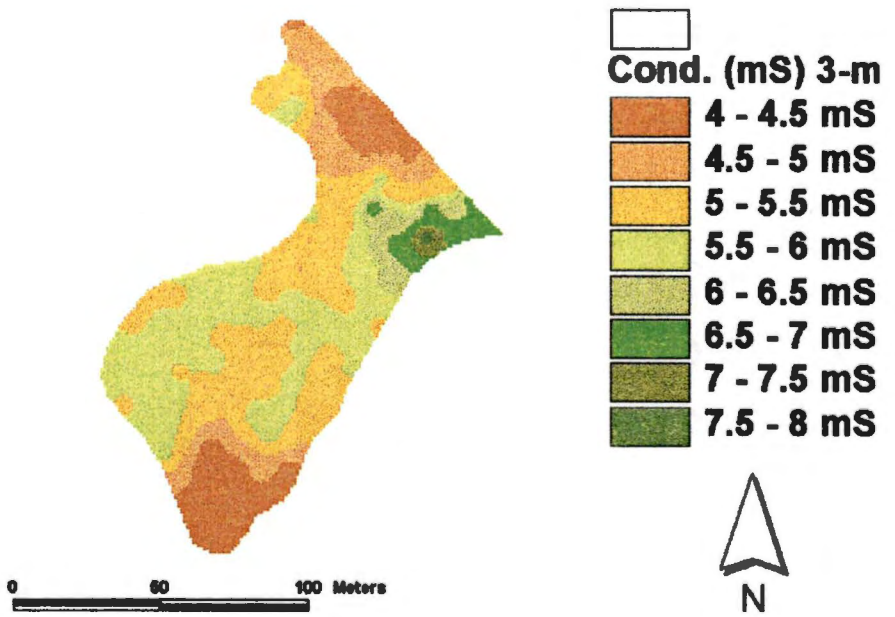
Chambers used: 1

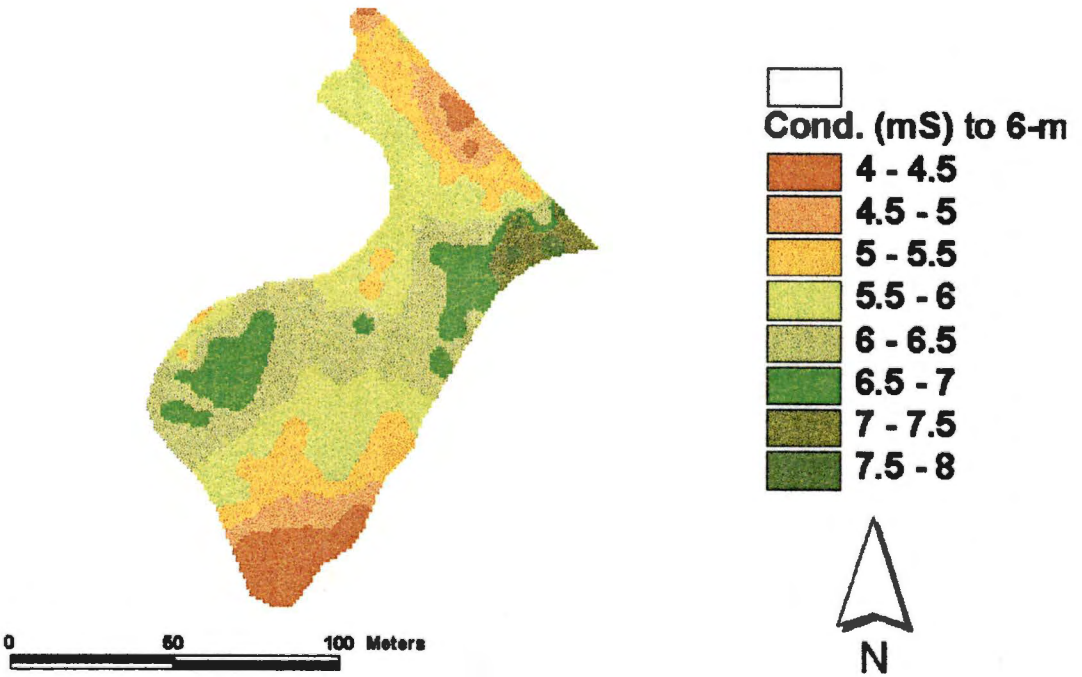
Change in water level (cm)	Conversion factor (cm^2)	Elapsed time (min)	Q (cm3/hr)	K (cm/hr)
0	20	0	na	na
0.4	20	5	96.0	0.124493
0.2	20	5	48.0	0.062246
0.2	20	5	48.0	0.062246
0.2	20	5	48.0	0.062246
			mean K=	0.062246

Bulk density, particle density, and total porosity.
Site 9.

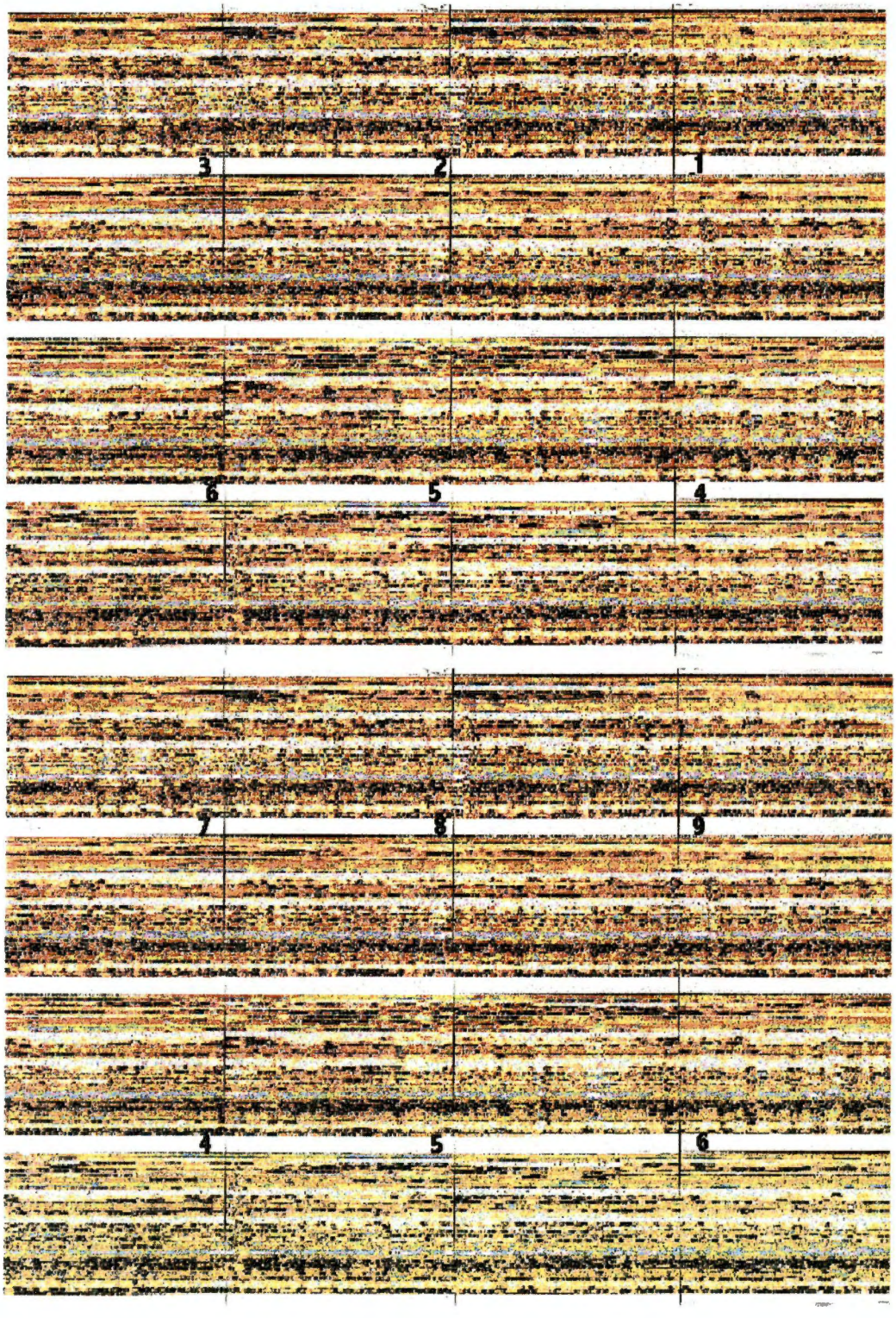
Horizon	Lower Depth (cm)	Bulk Density g cm^ -3	Particle Density g cm^ -3	Total Porosity %
Ap	5	ns	ns	ns
Bt1	25	1.62	2.64	38.88
Bt2	57	1.43	2.75	47.85
BC1	90	1.52	2.62	41.9
BC2	117	1.55	2.71	42.8
2BC3	160	1.67	2.51	33.46
2BC4	199	1.92	2.72	29.51
3Bt1	246+	1.45	2.79	48.05

Appendix J. EM-31 Maps of Field 75


Cond. (mS) 3-m
4 - 4.5 mS
4.5 - 5 mS
5 - 5.5 mS
5.5 - 6 mS
6 - 6.5 mS
6.5 - 7 mS
7 - 7.5 mS
7.5 - 8 mS
N
0
50
100 Meters


Cond. (mS) to 6-m
4 - 4.5
4.5 - 5
5 - 5.5
5.5 - 6
6 - 6.5
6.5 - 7
7 - 7.5
7.5 - 8
N
0
50
100 Meters

Appendix K. GPR Scans of Field 75


3
2
1
6
5
4
7
8
9
4
5
6

VITA

Daniel Inman was born on August 16, 1974, in Oak Ridge, Tennessee. He attended Oak Ridge High school, were he graduated in 1992. He entered the University of Tennessee at Knoxville in August of 1994, and graduated with a Bachelor's of Science in Agriculture in December, 1997. In August of the following year he entered graduate school and began work on a master of science degree with an emphasis on soil genesis and classification. He received his degree in August, 2000.

8108 1217 4
10•11•00 MAB
ICI INFORMATION CONSERVATION, INC